Novel activity-based probes for functional analysis of deubiquitinating enzymes

Von der Fakultät für Lebenswissenschaften

der Technischen Universität Carolo-Wilhelmina

zu Braunschweig

zur Erlangung des Grades eines

Doktors der Naturwissenschaften

(Dr. rer. nat.)

genehmigte

D i s s e r t a t i o n

von Alexander Iphöfer
aus Dshetysaj / Kasachstan

1. Referent: Professor Dr. Lothar Jänsch
2. Referent: Professor Dr. Michael Steinert
eingereicht am: 11.01.2012
mündliche Prüfung (Disputation) am 27.03.2012

Druckjahr 2012

Vorveröffentlichungen der Dissertation

Teilergebnisse aus dieser Arbeit wurden mit Genehmigung der Fakultät für Lebenswissenschaften, vertreten durch den Mentor der Arbeit, in folgenden Beiträgen vorab veröffentlicht:

Patent

Alexander Iphöfer, Raimo Franke, Antje Ritter, Tatjana Arnold, Lothar Jänsch, Novel Ubiquitin-Isopeptide Probes, Europäische Patentanmeldung: Patent Nr. EP 11 000 351.4 (18.1.2011), US-Anmeldung: Patent Nr. US 13/213 647 (19.8.2011).

Tagungsbeiträge

Alexander Iphöfer, Raimo Franke, Kathrin Goltz, Antje Ritter, Ronald Frank and Lothar Jänsch, Active-site directed probes for the Identification and Mechanistic Study of Deubiquitinating Enzymes, 2nd Annual Ubiquitin Drug Discovery & Diagnostics Conference 2010, Philadelphia (PA).

Alexander Iphöfer, Raimo Franke, Kathrin Goltz, Anne Kummer, Antje Ritter, Ronald Frank and Lothar Jänsch, Novel active-site directed probes for Profiling and Characterization of Deubiquitinating Enzymes, 3rd Annual Ubiquitin Drug Discovery & Diagnostics Conference 2011, Philadelphia (PA).

“The future belongs to those who believe in the beauty of their dreams.”

Eleanore Roosevelt

Content

1 Abbreviations

Note the following abbreviations are used throughout this study:

AA	Amino acids
Ab	Antibody
ABP	Activity-based probe
ABPP	Activity-based protein profiling
ACN	Acetonitrile
APS	Ammonium persulfate
BSA	Bovine serum albumin
CIEX	Cation exchange
Da	Dalton
DNA	Deoxyribonucleic acid
DTT	Dithiothreitol
DUB	Deubiquitinating enzyme
E1	Ubiquitin activating enzyme
E2	Ubiquitin conjugating enzyme
E3	Ubiquitin ligase
ECL	Enhanced chemoluminescence
EDTA	Ethylenediaminetetraacetic acid
FA	Formic acid
FBS	Fetal bovine serum
E-cadherin	Epithelial cadherin
HA	*Hemagglutinin*
HA-Ub	Ubiquitin tagged with YPYDVPDYA (HA-tag)
HAUbMF	HA-ubiquitin glycine vinylmonofluorethylamide probe
HAUbVME	HA-ubiquitin glycine vinylmethylester probe
HEPES	4-(2-hydroxyethyl)-1-piperazineethanesulfonic acid
HPA	The Human Protein Atlas
HZI	Helmholtz Zentrum für Infektionsforschung
IGEPAL	Octylphenoxypolyethoxyethanol
IP	Immunoprecipitation
JAMM	JAB1/MPN/Mov34 metalloenzyme domain
K	Lysine (Lys)
MALDI	Matrix-assisted laser desorption/ionization
MESNa	2-Mercapto*e*thane *s*ulfonate with coordinated sodium

MJD	Machado-Josephin disease domain
mRNA	Messenger RNA
MW	Molecular weight [Da]
NY	Nylon
OTU	Ovarian tumor domain
PBS	Phosphate buffered saline
PEG	Polyethylene glycol
ppm	Parts per million
RNA	Ribonucleic acid
rpm	Rounds per minute
RT	Room temperature
SDS	Sodium dodecyl sulfate
SDS-PAGE	Sodium dodecyl sulfate polyacrylamide gel electrophoresis
S-NHS	Sulfo-N-hydroxysulfosuccinimide
TEMED	N, N, N', N' -tetramethylethylenediamide
TFA	Trifluoroacetic Acid
TOF	Time of flight
Tris	N-tris(Hydroxymethyl)-methylglycine
Tween20	Polyethylene glycol sorbitan monolaurate (connectivity 20)
Ub	Ubiquitin
UBL	Ubiquitin-like protein
UCH	Ubiquitin C-terminal hydrolase
UIPP	Ubiquitin isopeptide probe
USP	Ubiquitin-specific protease
UV	Ultra violet
v/v	Volume per volume
VME	Vinyl methyl ester
VS	Vinyl methyl sulfone
w/v	Weight per volume

Aims

The posttranslational modification of proteins by ubiquitin (Ub) is a reversible process and coordinates the stability, turn-over and localization of protein substrates and also alters important protein-protein interactions. Deubiquitinating proteases (DUBs) remove specifically the conjugated ubiquitin from modified proteins and thus are able to direct the fate of the protein. Their catalytic mechanism and the ability to regulate various cellular events render this enzyme class to an attractive drug target.
In contrast to their general importance, their distribution in different cell types and tissues as well as the question of how they achieve substrate specificity is poorly understood at this time. Functional proteomics utilizing activity based probes (ABPs) has shown great potential in the annotation of DUB function and to obtain access to previously uncharacterized members of this enzyme class. Novel ABPs could serve as targeted research tools to assign biochemical and physiological functions of known and poorly characterized DUBs.

The aim of this study was the improvement of current activity based probes (ABPs) to increase specificity towards DUBs. The first intent was the improvement of ubiquitin derived ABPs by systematic modulation of HAUb-VME as the gold standard probe, while providing information on significant parameters determining its reactivity towards DUB proteases. The second aim of this thesis was the development of a completely new approach for the generation of a novel class of ubiquitin probes, which are able to dissect ubiquitin-linkage specificity and substrate preference of targeted DUBs.

2 Introduction

Regulation of protein function is often mediated by the reversible attachment of chemical modifiers, such as phosphate or acetyl groups. Ubiquitin can also modify other proteins and influence their function and half-life in several ways.

The posttranslational modification of proteins by ubiquitin (Ub) and ubiquitin-like (Ubl) modifiers is a reversible process and is involved in many signal transduction pathways[1,2]. Deubiquitinating enzymes (DUBs) remove covalently bound Ub and Ubl moieties from modified proteins. Apart from mono- and multi-ubiquitination, further ubiquitination diversity is achieved by the assembly of poly-Ub chains, such as Lys_{48} (K_{48})- and Lys_{63} (K_{63})-linked Ub chains.

Many detailed reviews on DUBs have been published in recent years, describing their implication in various cellular functions like proteasome-dependent protein degradation[3], cell cycle regulation[4], gene expression[5] and in regulating kinase activity[6]. Thereby, because of their potential to regulate important cellular processes, malfunction of many DUBs have been implicated in several diseases including inflammatory diseases[7], Fanconi anemia, neurodegenerative diseases and cancer[8,9]. In addition to these highly regulated cellular processes, a number of studies reported pathogenic microorganisms with genes encoding DUBs, which very likely provide an advantage for certain viruses like HSV-1[10] or bacteria such *Chlamydia* or *Salmonella*[11]. Thus, recent studies identified a protease in *Chlamydia trachomatis* which was detected with an activity-based probe (ABP) and indeed represents the first known bacterial DUB that possesses both deubiquitinating and deneddylating activities[12]. Deubiquitination also occurs in virus infections[13] like Epstein-Barr virus and is executed by three *bona fide* ubiquitin-specific proteases[14].

Thus, the activities of deubiquitinating enzymes have to be precisely regulated to prevent missing or inappropriate Ub cleavages and to ensure the equilibrium in the ubiquitin system. In order to recognize this regulation, more studies are needed to understand the unexplored mechanisms of specificity of DUBs towards their substrates and ubiquitin or ubiquitin-like proteins. In the last decades it was shown that DUBs contain not only catalytic domains but also various ubiquitin-binding and protein-protein interaction domains. These domains assist in the selective binding of Ub-linkages and the assembly of multi-functional protein complexes, which also contribute to their localization and substrate specificity[15]. The investigation of DUB specificity is clearly focused, but still poorly understood due to the complex multiple

mode of actions and the restrictions to *in vitro* assays. In spite of the paucity of knowledge about DUB mechanisms and regulations, some drugs have already been successfully tested in clinical trials. However, novel DUB characterization tools will certainly provide significant information to advance the drug discovery with greater strides.

Most of the current tools are *in vitro* assays that aim to capture a wide range of DUBs or to test the deubiquitinating activity, rather than investigating their catalytic mechanism and Ub-linkage specificity *in vivo*.

Considering DUBs multiple actions as described above, the comparison of absolute activities in a biological environment can shed light on DUB regulation and its substrate specificity. This is especially important when a DUB shows preference for multiple substrates with different efficiencies. For example, an *in vitro* cleavage assay with K48- and K63-linked Ub chains subjected to USP5 would show the cleavage of both chains[16], due to the multiple substrate specificity of this DUB. Information about its relative substrate preferences and the course of reaction in a more natural environment could not be determined with this *in vitro* strategy. To understand the mode of action in more detail, the development of activity-based selective and quantitative binding assays *in vivo* is required. This present study will introduce DUBs functionality in more detail and will discuss how chemical tools, such as activity based site-directed probes, can facilitate the discovery of further deubiquitinating enzymes, their functional profiling, advances in crystallography and understanding of catalytic mechanisms.

After the introduction of these powerful tools, the new generation of ABPs developed in this study and their upgrading possibility will be presented.

Finally, in order to address the complex selectivity of DUBs novel selective Ubiquitin Isopeptide Activity-Based Probe (UIPPs) were engineered to characterize the molecular basis of DUB target specificities for the first time.

Briefly, the novel UIPPs described here can be used as a tool to characterize previously unknown target specificities of DUBs, enable their detailed mechanistic characterization and deduce their importance in various infectious diseases.

2.1 Ubiquitin

Ubiquitin (Ub) is a small 76 amino acid (AA) protein which is named according to its extraordinarily ubiquitous distribution and high conservation in eukaryotes.

Ubiquitin is translated as a linear fusion construct containing multiple ubiquitins or is fused to ribosomal proteins. Ub is resistant and stable at extreme temperatures and pH values as well as high salt concentrations[17]. However, ubiquitin has a finite half-life and is removed by ATP-dependent proteasomal degradation (see Ubiquitin-Proteasome-System section). In a posttranslational enzyme-catalyzed process it is able to form covalent bonds with a variety of cellular proteins. Ubiquitin is expressed as an inactive precursor and consists either of head-to-tail repeats of the ubiquitin or is expressed as a fusion protein, like small ribosomal subunits[18,19]. Monomeric ubiquitin is released through the activity of ubiquitin-specific proteases, which cleave after the C-terminal di-glycine motif. This resulting free C-terminal is then able to form an isopeptide bond with the ε-amino group of lysine residues of a target protein, a process termed ubiquitination. In distinct cases the ubiquitination also occurs at the N-terminus of the substrate[20]. The ubiquitin sequence contains seven lysine (K) residues (**Figure 1**) and is thus capable to be ubiquitinated itself [21]. Although ubiquitin abundance varies in different conditions and within different tissues, the ratio of monoubiquitin to conjugated ubiquitin is approximately 1/1.

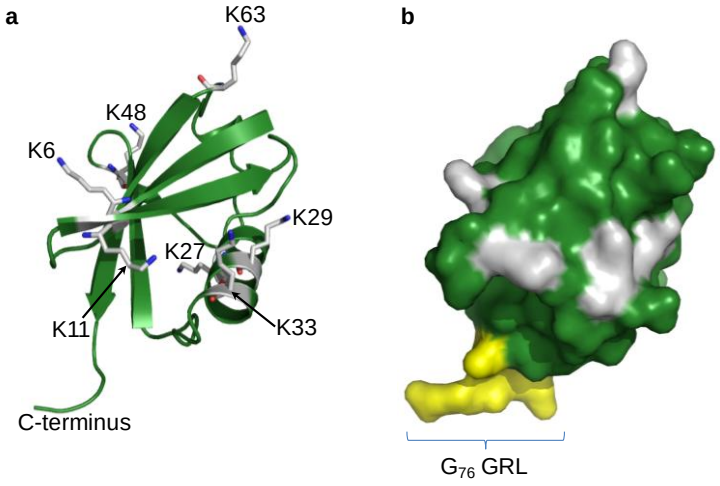

Figure 1. Ribbon and surface illustration of functionally relevant features of the Ub structure. (a) Ubiquitin structure with seven internal lysine residues (shown in grey as sticks) used to build up Ub-linkages. (b) The same ubiquitin molecule is shown as surface representation with additional labeling of the C-terminus (LRGG-motif in yellow). The pictures were generated using *The PyMOL Molecular Graphics System,* DeLano Scientific LLC, Palo Alto, CA, 2008, PDB-ID: 1UBQ).

2.1.1 Ubiquitin Linkages

It is important to underline that a target protein can be modified by ubiquitin in several ways, by mono-, di-, multi-, or polyubiquitination (**Figure 2**). However, a combination of these types cannot be excluded. Monoubiquitination is the conjugation of one single ubiquitin with its target protein and is involved in processes like signal transduction, endocytosis and by modulation of protein activity. Di- and multi-ubiquitination is the modification of one protein with several single ubiquitins on separate lysine residues and is implicated for instance in the formation of multivesicular bodies, protein localization and modulation of protein activities. Polyubiquitination is the result of sequential attachment of ubiquitin moieties to the proximal ubiquitin through their lysine residues as described above. The basic process for ubiquitination and polyubiquitination is carried out by an enzyme cascade and will be described in chapter 2.2.1.

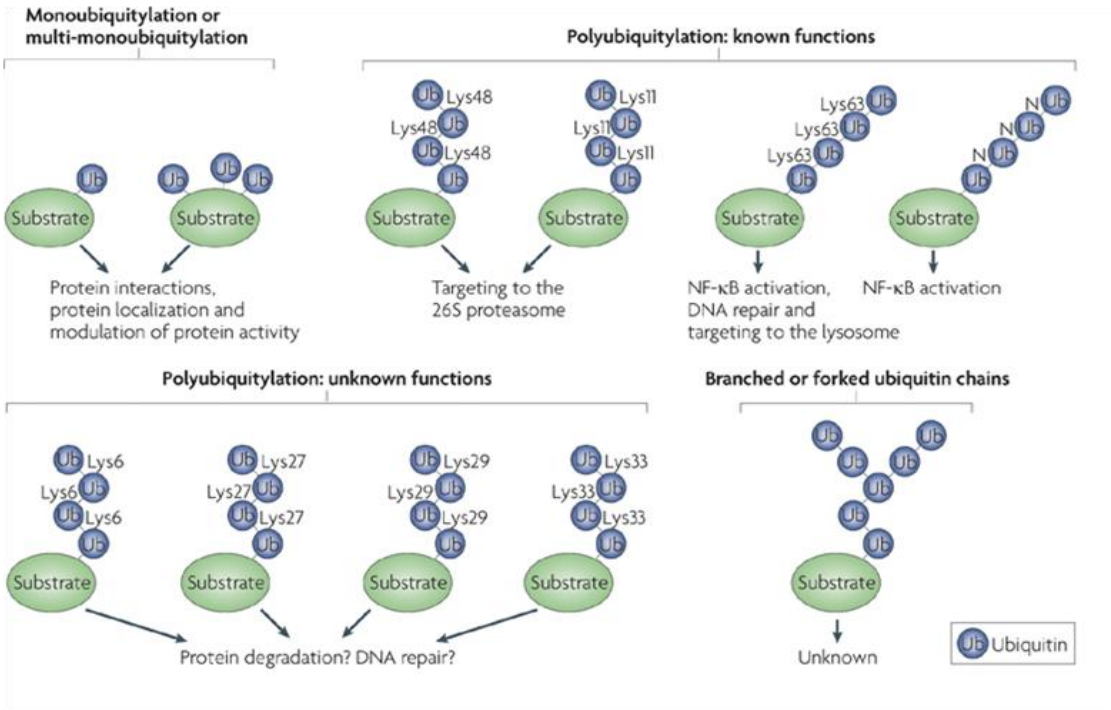

Figure 2. Possible ubiquitin modifications and their effect on the fate and function of the modified proteins. Monoubiquitination is the conjugation of one ubiquitin to a single lysine -and multiubiquitination the modification of various lysine residues on the target protein. These modifications have been implicated in cellular processes such as transcription regulation, membrane trafficking, DNA repair and DNA replication. Repeated ubiquitination of the first ubiquitin on the target protein results in polyubiquitin chains, which differ in their topology depending on the lysine residue chosen on the proximal ubiquitin. The topology of the polyubiquitin chains define the fate of the target

protein in different cellular processes like degradation, cellular localization, protein activation and diverse interactions in signaling (Ye & Rape 2009).

Since ubiquitin itself contains seven lysine residues (K6, K11, K27, K29, K33, K48 and K63) at least seven different topologically different polyubiquitin chains are possible and contribute to diverse functional effects (**Figure 2**).

Recently, mass spectrometry analysis revealed the relative abundance of polyubiquitin chains as following: Lys_{48} > Lys_{11} > Lys_{63}>> Lys_6, Lys_{27}, Lys_{29} and Lys_{33} [22]. In addition to these homotypic polyubiquitin chains, also heterogeneously forked chains containing two different Ub-linkage types are possible and were observed for Lys_6+Lys_{11}, Lys_{27}+Lys_{29}, Lys_{29}+Lys_{33} [23]. Considering that polyubiquitin chains can split and form branches, even more topologies and functions of polyubiquitin chains can be expected[24]. Furthermore, the combination of other Ubl modifiers with ubiquitin chains results in even more heterogeneous chains and was recently observed for SUMO-Ub combinations[25,26].

However, Lys_{48} - and Lys_{63} - linked polyubiquitin chains are well studied and have been shown to affect many cellular functions. While Lys_{48}-linked chains with more than four ubiquitin moieties in length target the substrate for proteasomal proteolysis, the Lys_{63}-linkages serve for non-proteolytical functions including cellular signaling, DNA repair and lysosomal targeting[27,28]. Furthermore, recent studies refer to K_{63}–polyubiquitin modifications as docking sites for adapter proteins in the NF-kappaB signaling pathway[29]. From the structural point of view, the linear polyubiquitin chains are similar to the K_{63} –polyubiquitin[30] and are also interestingly found in the NF-kappaB pathway[28]. Concerning the K_{11}-linked chains, recent observations showed surprising similarities to K_{48}-polyubiquitin chains by targeting proteins to proteasomal and endoplasmatic reticulum-associated proteolysis [31,32].

In respect of another polyubiquitin chains formed through Lys_6, Lys_{27}, Lys_{29} and Lys_{33}, there is not much known which demonstrates the discovery need and the potential of further putative unique regulatory insights.

Although scientists are working intensively on the structural characterization of these different Ub-linkages, only three Ub-linkages (K11, K48, K63) have been described well to date. It is importantly to note that, beside the crystal structures also NMR studies were performed, however, they were not always consistent[33]. For example, concerning different pH conditions, the polyubiquitin structures differ extremely[34] as

demonstrated for K_{48}- di-ubiquitin in **Figure 3**. In addition to different structural conformations between *in vitro* and *in vivo* studies it is also important to know the localization of certain polyubiquitin chains in the cell.

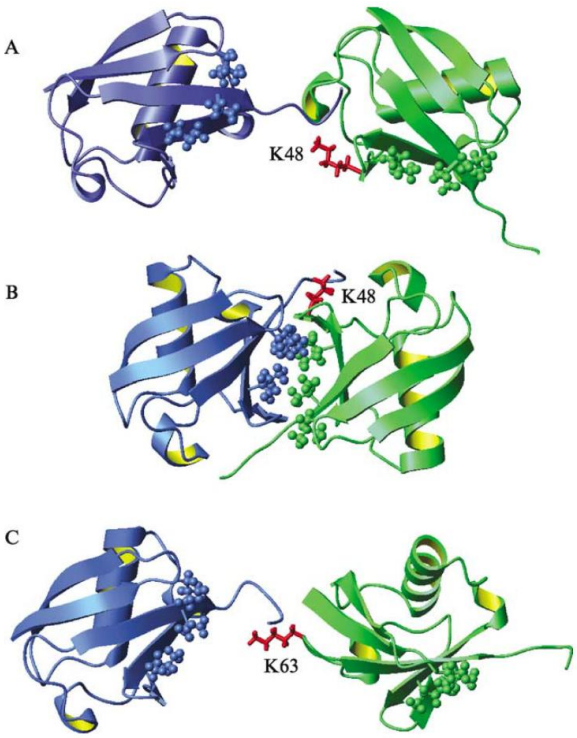

Figure 3. NMR spectroscopy of solution conformations of K_{48}- and K_{63} -linked di-ubiquitin at different pH conditions. Solution conformation of Lys48 –linked di-ubiquitin at pH 4.5 (A), at ph 6.8 (B) and of K_{63} –linked di-ubiquitin at pH 6.8 (C). The distal and proximal ubiquitin domains are depicted as cartoons in blue and green, respectively. Balls and sticks represent the hydrophobic patch. The side residues responsible for the corresponding ubiquitin linkages are shown in red. Structures were generated using experimental data of Varadan R. *et al*. 2005, PDB: 2BGF.

2.2 The Ubiquitin System

The posttranslational modification by ubiquitin conjugation is termed as ubiquitination or ubiquitilation and is executed step for step by an enzyme cascade[35,36] (**Figure 4**). The responsible members of these are belong to three primary enzyme families; ubiquitin-activating enzyme (E1), ubiquitin- conjugating protein (E2) and ubiquitin-protein ligase (E3). Firstly, Ub is activated by a ubiquitin-activating enzyme, which uses ATP to form a highenergy, labile E1- thiolester intermediate between the C-terminal ubiquitin glycine (G76) and its own catalytical cysteine[37] . The activated ubiquitin is then transferred from E1 to a cysteine residue of an E2[38] to create a

further thiolester intermediate. This activated ubiquitin can now undergo different ubiquitination possibilities. It can be passed from E2 to a HECT (homologous to E6-AP carboxyl terminus) domain containing E3, generate a third thiol ester intermediate and then be transferred to a substrate by forming a stable isopeptide bond. The final catalyzed isopeptide formation is then between the activated C-terminus of ubiquitin and ε-amino groups of internal lysine residues of target proteins[39] . The sequential addition of further ubiquitin moieties constitutes a polyubiquitin chain. Alternatively, the ubiquitination of the activated Ub can be preformed directly from E2 to the Lys residue of the substrate which is supplied from the RING finger containing E3s. In cases where the polyubiquitin chain is linked through Lys_{48} of ubiquitin, the substrates undergo 26S proteasomal degradation. Nevertheless, beside the ubiquitin conjugation on the internal Lys from substrate, the observation of ubiquitin conjugation on other substrate internal residues such as Thr, Ser or Cys [40,41,42] is remarkable.

2.2.1 Ubiquitin Proteasomal System

The proteasome is a 2.4 mDa multicatalytic central protease complex and responsible for the degradation of abnormal and damaged proteins that are labeled with K^{48}-polyubiquitin chains (polyubiquitin chains are described in the next section). The so-called 26S proteasome complex is comprised of at least 32 different subunits, which are arranged in two subcomplexes: two 19S regulatory lid-particles -and one 20S proteolytic core complex (CP) (**Figure 4**). The hydrolysis of proteins by 20 CP does not require ATP, thus the degradation of ubiquitinated substrates by the 26S proteasome is an ATP-independent process[43].

The 19S assembly regulates mainly the capturing and entry of ubiquitinated substrates into the 20S proteasome and has no proteolytic activity. Functionally, this cap structure contains embedded deubiquitinating enzymes, recognizes K_{48}-polyubiquitinated proteins, unfolds protein substrates and introduces these into the 20S proteolytic core[44]. However, recent studies observed the proteasomal degradation of substrates which also are labeled by other polyubiquitin chains[45,46].

Importantly, in order to control cell-cycle regulators, oncogenes, and tumor suppressors, correctly folded proteins such as transcription factors or antigens are degraded as well[47,48]. Despite the degradation of proteins labeled by ubiquitin,

ubiquitin itself can be degraded by three different 26S proteasomal degradation processes. Firstly, the ubiquitin from the most proximal part of the polyubiquitin chain is degraded together with its conjugated substrate. Secondly, ubiquitin with a C-terminal peptide extension longer than 20 amino acids is degraded effectively by the 26S proteasome. Thirdly, since monomeric ubiquitin has the ability to bind the proteasome but does not contain a long enough tail to be delivered into the 20S catalytic core, it has to be ubiquitinated also. These kinds of ubiquitination is E3-independent and specifically performed by an E2 (UBE2K), which catalyses the proteasomal degradation of typical Lys_{48}–linked polyubiquitin chains[49].

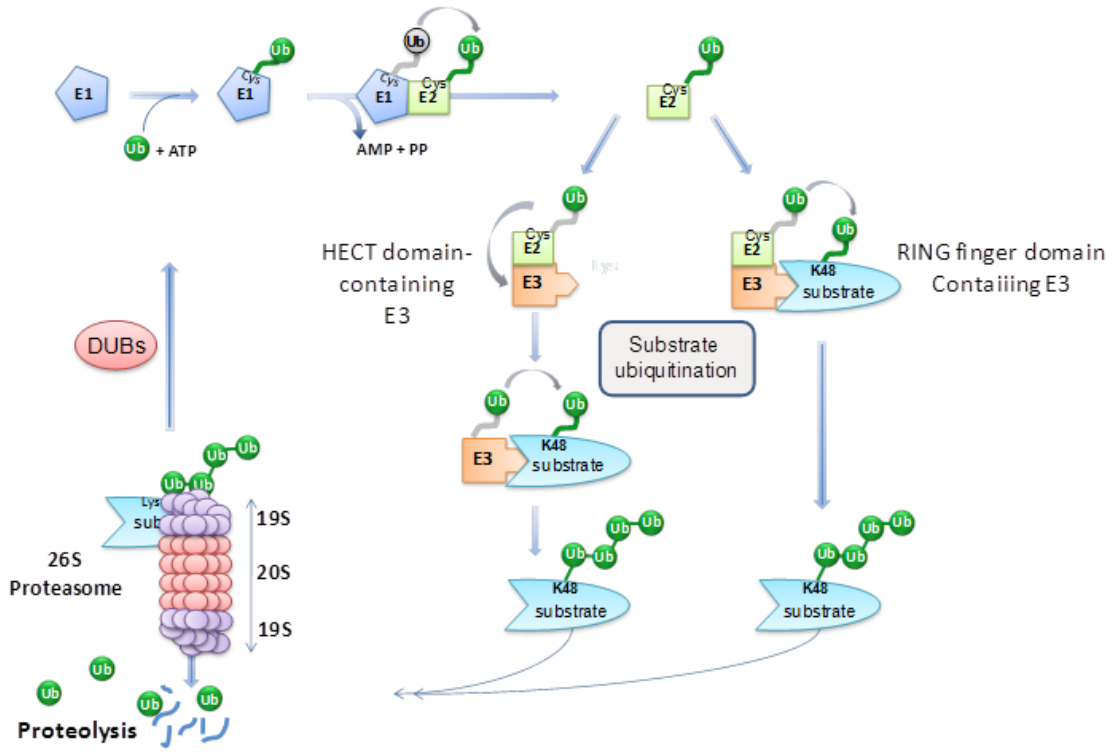

Figure 4. Schematic overview of the ubiquitin-proteasome system.

During the ubiquitination cascade, ubiquitin is firstly bound and activated by the ubiquitin-activating enzyme (E1) via a thiol ester in an ATP–dependent process. The activated ubiquitin is then transferred by a *trans*-thiolation reaction to ubiquitin-conjugating enzymes (E2) that create a second thiol ester intermediate. Afterwards, the ubiquitin can be conjugated to the substrate by two strikingly different pathways. i) The E2 enzyme interacts with a HECT domain containing E3 ligase and delivers the ubiquitin by generating a third homogenous thiol ester intermediate. This E3 enzyme binds its substrate and transfers the ubiquitin to the substrate by forming an isopeptide bond between the C-terminus of ubiquitin and an εNH_2 group of an internal Lysine of the substrate. ii) Alternatively, the conjugation can be performed directly from E2 to the Lysine residue of the substrate while both are bound to a RING domain containing E3 enzyme. In case the polyubiquitin chain was formed through the Lys_{48} of ubiquitin, the ubiquitinated protein is directed to the proteasomal degradation.

2.2.2 The Roles of ubiquitination in proteasome-independent pathways

Despite the involvement in degradation, ubiquitination is also implicated in various pathways depending on the respective topology of polyubiquitin chains.

In addition to the effects described before, the modification of proteins with ubiquitin can influence transcriptional activity[47,50] and may regulate the sorting into lysosomes[51] as well. Moreover, monoubiquitin and Lys63-linked di-ubiquitin chains can trigger the regulated endocytosis of plasma membrane proteins into primary endocytic vesicles[52] or into multivesicular bodies (MVBs)[53]. Furthermore, the internalization of receptor tyrosine kinases (RTKs) and G-protein coupled receptors (GPCRs) towards the endosomal compartment has been observed and validated[54]. The involvement of monoubiquitination was also described for the assembling of vesicels with opposite direction to that during endocytosis, as known for virus budding[55]. These are definitely not the final ubiquitin functions of this wide spread and multilateral posttranslational modification and it remains to be seen if further sophisticated analysis methods shed light on more cellular functions.

2.3 Ubiquitin like proteins

Beside the ubiquitin introduced above, various ubiquitin like proteins (UBL) that form 9 phylogenetically distinct classes (NEDD8, ISG15, SUMO, FAT10, FUB1, Atg8, Atg12, Urm1, and UFM1) and share the characteristic three-dimensional fold have been discovered. Concerning the conjugation to a target protein, these Ubls are conjugated by the same enzyme cascade which is described below for ubiquitin, and are covalently attached through the c–terminal glycine to the selected substrate. To represent the diversity of these UBLs, the four best-studied ubiquitin like modifiers are introduced shortly and summarized with remaining UBLs in **Table 1**.

2.3.1 NEDD8

The neural cell-expressed developmentally down regulated (NEDD8) genes was shown to share 60 % sequence similarity with ubiquitin [56]. Analog to ubiquitin, NEDD8 is expressed as a precursor that is processed at the conserved c-terminal Gly76 by deneddylating enzymes such as Senp8. Mass spectrometry analysis recently demonstrated that Lys11, Lys22, Lys48 and Lys60 residues of NEDD8 can

be used to form poly-NEDD8-chains[57]. Interestingly, the conjugation to already existing polyubiquitin chains is also possible but their function is unknown[58].

2.3.2 ISG15

The first identified member of the UBL-family was the Interferon stimulated gene 15 (ISG15), which is also known as Ubiquitin Cross-Reactive Protein (UCRP)[59]. The expression of ISG15 is mainly induced by type I interferon (IFN-α and IFB-β) together with viral and bacterial infections[60,61]. In comparison to ubiquitin there is no evidence for a role in the proteasome degradation system[61] . Instead, because of the type I interferon inducible expression of ISG15 and its conjugation to cellular proteins during viral and bacterial infections, it was implicated to play an important role in the immune response.

2.3.3 SUMO

One of the best-studied UBLs is the Small-Ubiquitin-related Modifier (SUMO). Mammalian cells express four major SUMO paralogues (SUMO1,2,3,4), however, only the first three forms can be covalently conjugated to the target protein. These paralogues are classified in subgroups as SUMO-1 and SUMO-2/3 because of the sequence similarity of 95% between SUMO-2 and SUMO-3, in comparison to SUMO-1 (45%). Those two families differ in their cellular concentration, cellular localization and their ability to modify distinct proteins[62]. In recent years more than 1000 proteins have been identified as SUMO conjugation targets (SUMOylation)[63] and have been implicated in transcription, DNA-replication, cell cycling, intracellular transport and DNA repair[64].

2.3.4 FAT10

Another ubiquitin like protein is the TNF-alpha-inducible human leukocyte antigen F-Adjacent-Transcript 10 (FAT10). FAT10 is composed of two consecutive ubiquitin-related domains and possesses a C-terminal di-glycine motif which is required for the conjugation to proteins. The functional role of FAT10 is still not fully understood but it was shown to have the ability to act as a proteasomal degradation signal[65] and to be up-regulated in activated dendritic cells and several epithelial tumors[66].

Although Ub and Ubl share structural and biochemical properties, this study will focus on the well-studied ubiquitin.

Table 1. Ubiquitin-like Modifier and their functions

Ubiquitin-like protein	Sequence coverage to ubiquitin (%)	Function
NEDD8 (Rub1)	60	Positive regulation of E3s
ISG15/UCRP	29, 37	Immune response, interferone signal transduction, potentiall involved in cell growth and differentiation
FUB1	37	T-cell activation, negative regulator of proliferation
FAT10 (2 ubiquitins)	29	Apoptosis, cell cycle
UBL5	22	Pre-mRNA splicing
SUMO1 (Smt3)	18	Control of protein stabilization, Transiption regulation, neclear localizationcr
ATG12	17	Autophagy, cytoplasm - vacuole targeting
SUMO-2 / SUMO-3	16	Cell cycle progression, Transiption regulation, mitosis
URM1	12	Oxidative stress response
ATG8	10	Autophagy, cytoplasm - vacuole targeting

(Modified and extended from Herrmann et al., 2007)

2.4 Deubiquitinating Enzymes

Deubiquitinating enzymes (DUBs) are isopeptidases and remove ubiquitin moieties from conjugated substrates and they play regulatory roles in a variety of cellular processes such as trafficking, endocytosis and in various signaling pathways[67]. Alterations in these processes contribute to disease pathologies such as Parkinson's disease[68], autoimmune diseases[69] and cancer[70]. Deubiquitination might be highly regulated and functional as important as ubiquitination but is more poorly understood than ubiquitination.

Humans encodes approximately 95 putative DUBs that have been predicted by bioinfotrmatic studies to date, whereas five of these are probably missing the transcription[67]. These proteases have different overall structures, myriad of distinct mechanisms and a low sequence similarity, but the overall arrangement of the catalytic triad is conserved. Nevertheless, DUBs can be divided in five subclasses, classified by their internal domains and the sequence similarity, while four families belong to papain-like cysteine proteases and one to zinc-dependent metalloprotease[71]. These subfamilies can be separated in to 58 Ubiquitin-Specific Proteases (USP), 4 Ubiquitin C-terminal Hydrolases (UCH), 5 Machado-Josephin Disease domain containing proteases (MJD), 14 Ovarian Tumor domain containing DUBs (OTU) and 14 metalloenzyme domain containing DUBs (JAMM).

2.5 DUB Function

The investigations of DUBs function have demonstrated their implication in different cellular key processes and their importance will be still continuously discovered. The best studied function of DUBs is the generation of free mono ubiquitin by processing the ubiquitin-linear-fusion product consisting of multiple ubiquitins, the ribosomally synthesized ubiquitin precursors or cytoplasmatic polyubiquitin chains (**Figure 5a,e**). Another well characterized role is the deubiquitination process of K_{48}- linked polyubiquitin chains, to rescue the ubiquitinated proteins form proteasomal degradation (**Figure 5b**). DUBs act not only beyond the 26S proteasom machinery but also integrat into the proteasome complex itself and couples protein deubiquitination, unfolding and translocation into the proteasom. POH1(Rpn11) has emerged as the main functional DUB in the proteasome complex, attributed to its deletion which cause lethality[72,73,74]. To maintain the homeostasis of free ubiquitin, DUBs recycle ubiquitin by preventing the 26S proteasomal degradation of ubiquitin itself (**Figure 5d**). More recent studies have demonstrated that DUB is involved in the removal of non degradative ubiquitin signals (**Figure 5c**). Such observations were done in the regulation of transcription[75], intracellular trafficking and sorting of proteins[76]. Alternatively, the contribution in non degradative pathways can be supported by DUBs with editing function, and they trim the ubiquitin chain and generate another signal at the same time (e.g. trimming from poly- to di-ubiquitin) (**Figure 5f**). Furthermore, due to the fact that branched and forked polyubiquitin chains[77] exist, the trimming of these chains could generate an exclusively ubiquitin

signal. However, high throughput protein-protein interaction experiments suggest other potential roles for DUBs including synapse function[78] and further signaling cascades[79].

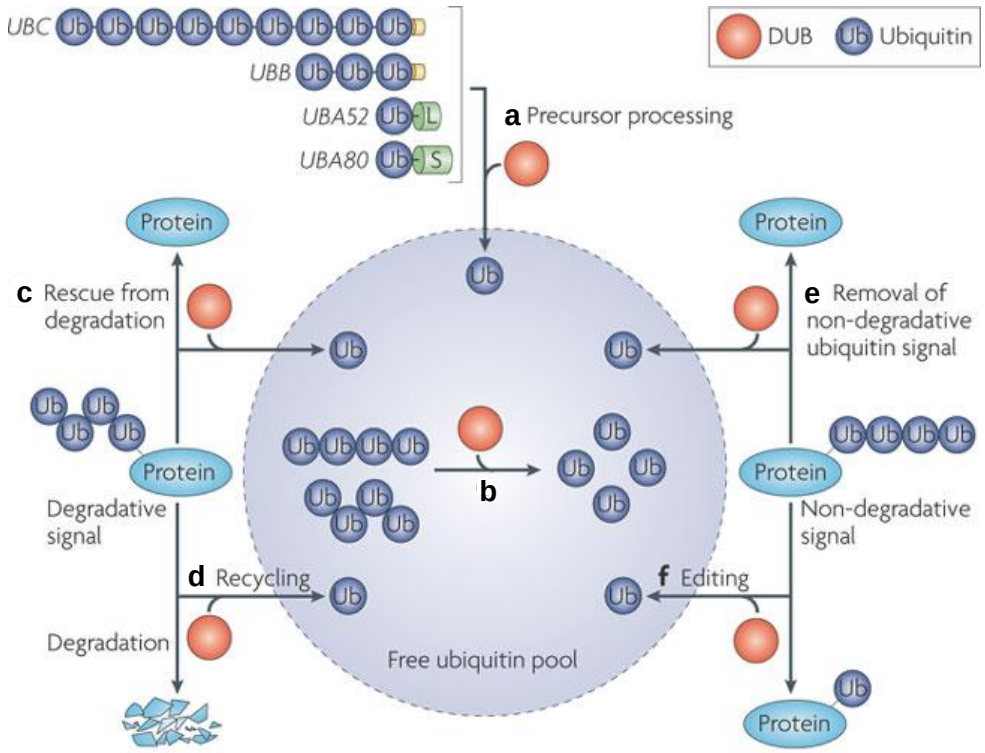

Figure 5. Functions of Deubiquitinating enzymes.

Deubiquitinating enzymes are indicated with red- and ubiquitin with blue balls. DUBs generate free mono ubiquitin by processing the ribosomally synthesized ubiquitin precursors (a) or by disassembling of unanchored polyubiquitin chains (b & d). One important task is the removing of ubiquitin from ubiquitinated proteins and rescue these preoteins from the proteasomal degradation (c). Alternatively, DUBs are involved in non degradation pathways by removing distinct ubiquitin signals or edit certain polyubiquitin chains. The Scheme is adapted from Komander, et al. 2009.

To conclude, we have just began to scratch on the surface to understand the biological function of DUBs, which is increasing daily with every publication. To highlight the importance of this enzyme class, some selected DUBs functions are briefly summarized below (**Table 2**).

Table 2. Survey of deubiquitinating enzymes and their associated biological functions.

DUB	Biological functions	References
USP8, AMSH, USP9X	Endocytosis	80,81, 82
UCHL1, UCHL3, USP5	Ubiquitin processing	83, 84, 85
USP7, USP6, USP28	Cell proliferation	86, 87, 88
USP1, USP3, USP28	DNA damage response	89, 90, 91
USP14, USP15, PSMD14	Proteasomal degradation	92,93, 94
CYLD	NF-kB signaling	95
USP11, USP15	Regulation of substrate degradation during viral replication	96, 97

2.6 Regulation of Deubiquitinating Enzymes

The activity of DUBs is carefully controlled to prevent an inappropriate ubiquitin processing, which is also represented by their low abundance. Thus the enzyme activity is not always present directly after the translocation. For some DUBs, such as UCHs and USPs, it could be shown that their catalytic triad adopt the active conformation while binding to ubiquitin[67], thereby avoiding the false protease activity. The active conformation can be achieved in different ways, for example by shifting the occlusion loops from the active site, by active site domain motion or by rearrangement of catalytic residues (**Figure 6**). Another level of controlling is the appropriate cellular localization. Good examples are USP14, UCH37 and POH1, which achieve their activity after binding to the proteasome[98,99]. DUB activity can also be regulated by transcription, whose transcription is rapidly induced or rapidly degraded as an answer to certain cellular processes[100].

Most proteins are regulated by phosphorylation, ubiquitination or ubiquitin like modifications and DUBs are not an exception. Thereby recent phosphorylation

examples are USP15, USP19, USP28 and USP34, which were phosphorylated by ATR/ATM in response to DNA damage[101]. The ubiquitination of DUBs may directly enhances the activity of deubiquitinating enzymes and was recently reported for Ataxin-3[102]. Otherwise, it could be shown that the sumolation of USP25 inhibits its activity[103].

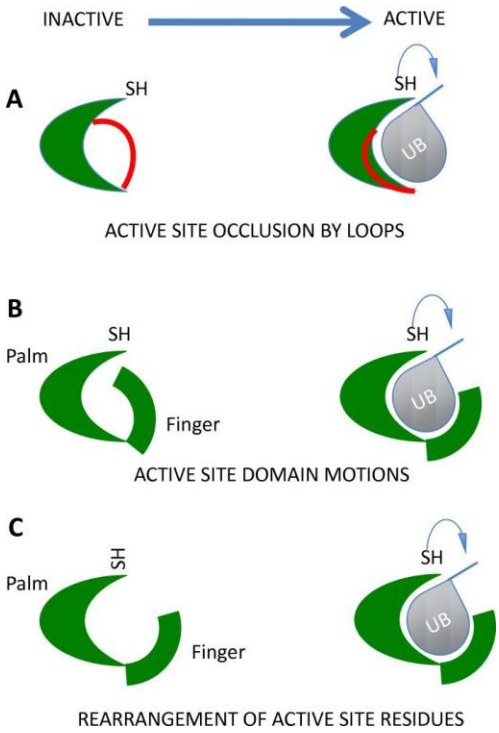

Figure 6. DUBs regulation upon conformational changes.
A) The accessibility of the active site is regulated by occluding loops which must be displaced to allow the substrate binding. B) The active site is occupied by certain domains which must be displaced for an appropriate substrate binding. C) The substrate binding cause a conformational change which reorients the catalytic residues and therefore allow an active processing (F. Reyes-Turcu *et al.* 2009)

2.7 DUB Specificity

DUBs specificity can be displayed at multiple levels and may be referred to as the specificity towards different ubqiuitin linkages or to the ubiquitinated proteins. The different DUB specificity layers are summarized in **Figure 7** and described below. The polyubiquitin chains differ in their topology and the sequence context around the isopeptide bond between two ubiquitin moieties. These features contribute to DUB cleavage specificity and are not restricted to a certain DUB family. The disassembly of polyubiquitin chains can be carried out from the chain ends (exo) or may started directly within a chain (endo). Comparing to exo-DUBs, the endo-DUBs recognize

larger surface patches of two Ub moieties and cover thereby more the polyubiquitin specified DUBs. Deubiquitinating enzymes can also recognize and bind directly to the ubqiuitinated target protein. For instance, these DUBs are able to cleave off the whole polyubiquitin chain, rescue the protein from degradation or amputate the Ub chain till monoubiquitin, which gives the possibility to build up a new Ub chain. More target specific DUBs may be those whose specifically recognize a monoubiquitinated substrate and remove Ub from mono- or multiple sites. Last but not least, the mono ubiquitin pool will be mostly generated from DUBs whose process just unanchored polyubiquitin chains or ubiquitin with small remained tails. This kind of processing is mostly carried out by DUBs from the UCH family.

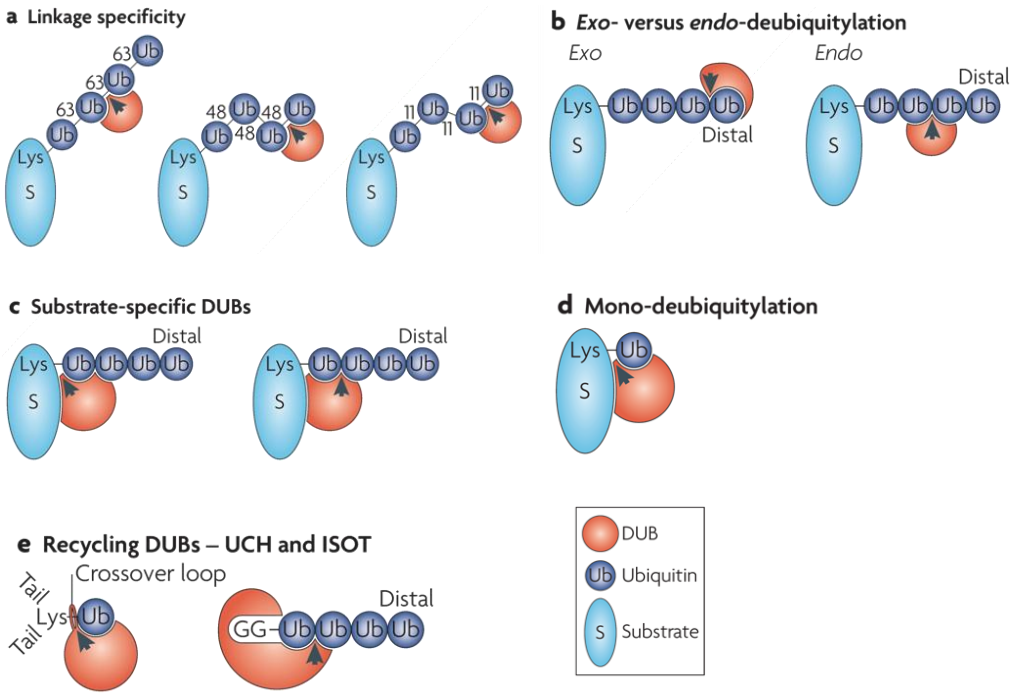

Figure 7. DUB specificity at multiple levels. a) DUBs which recognize and process distinct ubiquitin linkages. b) DUBs with the preference to disassemble the polyubiquitin chains from the ends (exo) or starting to cleave directly within the ubiquitin chain. c) DUBs with certain substrate specificity which are able to amputate directly the whole ubiquitin chain (right scheme) or remove ubiquitin moieties in one step till monoubiquitination. d) DUBs with substrate specificity which recognize the protein and remove the mono- or multi-ubiquitin. e) DUBs which are specialized to remove small peptide fragments (< 8 AA) from the C-terminus
of ubiquitin, such as products after the proteasomel degradation (Komander, et al. 2009).

2.7.1 Enzymatic reaction mechanism of DUBs

Although DUBs display distinct substrate specificities and are involved in different functional roles, the important regulatory mechanism within the cysteine proteases and metalloproteases show certain similarities.

The papain-like cysteine protease DUB subclasses (USP, UCHs, OTUs and MJDs) rely on the catalytic conserved diad (cysteine (Cys) and histidine (His)) or constituting a triad through additional amino acids such as asparagine (Asn), aspartate (Asp), glutamine (Gln) or glutamate (Glu). Remarkably, all cysteine protease derived DUBs present divergent structural folds, but superpose only small differences in catalytic rearrangement after binding the C-terminus of ubiquitin.

The catalytic mechanism of these subclasses will be briefly described below.

Within the catalytical triad the thiol group of cysteine is deprotonated by an neighbouring histidine which itself is polarized by asparagine or aspartate, although this is not always essential for activity[104]. The final deprotonation is accomplished during the nucleophilic attack of cysteines thiol group onto the crucial peptide linkage bond (**Figure 8**). In terms of DUBs this reaction occurs at the Ub-linkage dependent isopeptide bond, consisting through the covalent bond the carboxy-terminal glycine of one ubiquitin to an internal lysine of another.

In terms of DUBs this reaction occurs at the isopeptide bond, consisting of the covalent bond of the carboxy-terminal glycine of one ubiquitin and an internal lysine of another ubiquitin or substrate. The thiol-ester intermediate consisting of Ub-carboxy-terminus and the cysteine thiol, is stabilized in the “oxyanion hole”, which is spatial composed above catalytic backbone of the cysteine and the residues Gln, Glu or Asn. The next catalytic steps are performed through the formation of an acyl-enzyme intermediate, generation of the second tetrahedral intermediate and its hydrolysis via a water molecule. Finally, the ubiquitin carboxylic acid product diffuse from the active site and the catalytical triad rearranges for the next cleaving process.

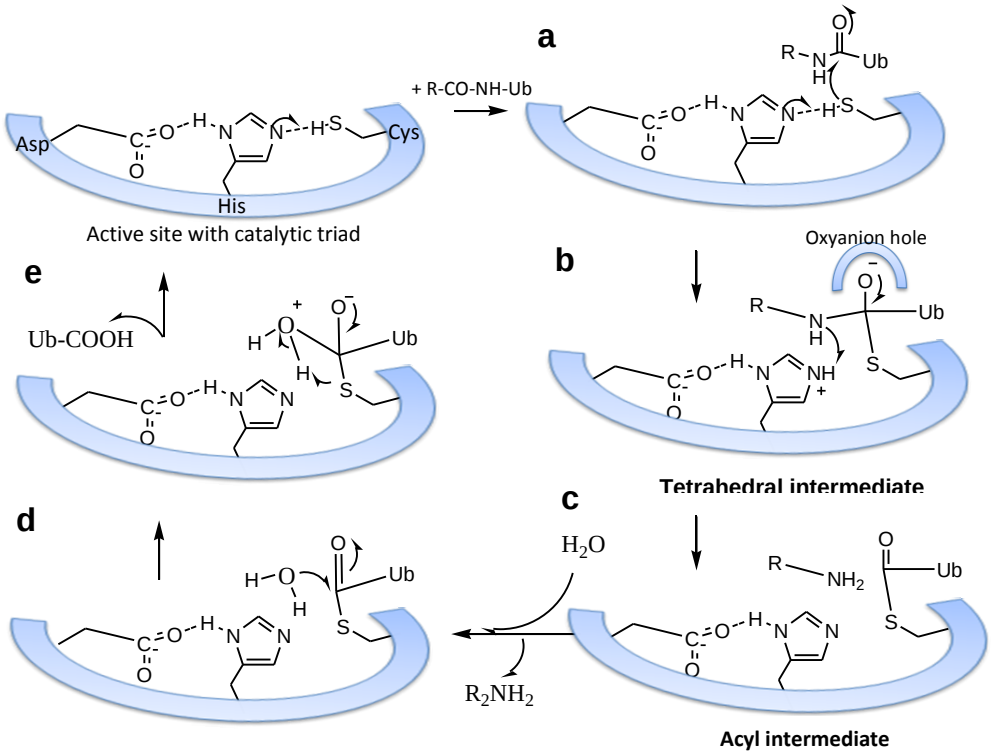

Figure 8. Schematic reaction mechanism of substrate hydrolysis by papain-like cysteine proteases. **a**) FORMATION OF ES COMPLEX:The active site Cys-SH is activated by His (imidazole ring N:) in catalytic triad. Afterwards Cys-S becomes a reactive nucleophile and undergo a nucleophilic attack on carbonyl C of substrate and forms a covalent bond. **b**) TRANSITION STATE STABILIZATION by movement of substrate oxyanion of intermediate into the oxyanion hole. **c**) FORMATION OF ACYL-ENZYME INTERMEDIATE: The amide bond breaks and that amine product (RNH2) dissociates.The oxyanion is accomplished back into C=O by forming the acyl-enzyme-intermediate which represents a covalent ester linkage.**d**) FORMATION OF THE SECOND TETRAHEDRAL INTERMEDIATE: His activates the O from the water molecule (H_2O), makes it nucleophile potent which than attack the carbonyl C of acyl-enzyme intermediate. **e**) DISSOCIATION OF SUBSTRATE:The ester bond cleaves and generate the carboxylic acid component (R'COOH) which than dissociates from the active site.

In contrast to cysteine proteases, metalloproteases generally coordinate a metal ion (Zn^{2+}) with two His and an Asp in order to polarize a water molecule and create a noncovalent intermediate of substrate/enzyme intermediate. Further residues such as Glu and Ser contribute to the coordination of the water molecule and the substrate. After the substrate was conformational detected, the spatial orientation towards the catalytic site is coordinated by Ser, Asp and Glu while a water molecule is activated by a zinc ion. Similar to the reaction mechanism described for cysteine proteases above, the “activated” water molecule undergoes a nucleophilic attack on carboxylate

of the isopeptide bond (**Figure 9a**) and generate the tetrahedral intermediate. Just before the proteolytic step occurs, the glutamic acid serves as a proton acceptor (**Figure 9b**) and transfer than the proton to the amide nitrogen which is followed by tetrahedral intermediate collapse and causing the substrate release (**Figure 9c**)[105].
The following section will introduce the five individual DUB subclasses.

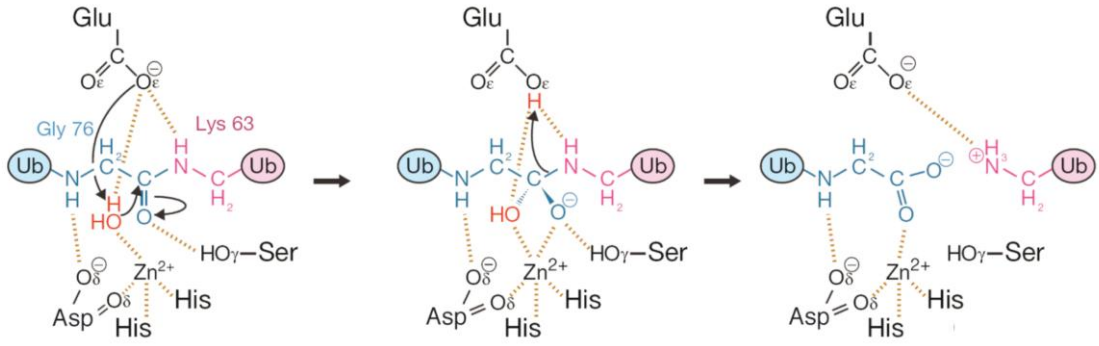

Figure 9. Schematic representation of the catalytic mechanism of metalloproteases derived from the structure of AMSH-LP bound to diubiquitin[106]. Distal ubiquitin is labeled in blue, the proximal ubiqiutin highlighted in pink and Zn coordinated water is depicted in red. **a**) Nucleophilic attack of water molecule on the carbonyl carbon of the isopeptide bond. **b**) Glu 292 conduce as proton acceptor and is in the final step **c**) -responsible for the intermediate collapse by transferring the proton on the amide nitrogen from the distal ubiquitin, (modified from Urbé et *al.,* 2009).

2.7.2 Five Subclasses of Deubiquitinating Enzymes

In spite of the paucity of the knowledge concerning the DUB specificity, some of the structures and internal domains are investigated and display various features. Despite these large presented differences all cysteine protease DUB families (UCHs, USPs, OTUs and MJDs) belong to papain-like cysteine proteases and rely on a catalytic diad or triad[30]. In contrast to cysteine proteases, metalloproteases (JAMMs) uses a metal ion oriented water molecule which acts as a nucleophile and enables the catalytic reaction[105]. To further shed light on the important differences, the subclasses will be briefly introduced separately.

2.7.3 Ubiquitin carboxy-terminal hydrolases (UCHs)

The human encodes four UCH domain containing DUBs with highly conserved 230 amino acids catalytic domoain (Reyes-Turcu et al., 2009). Those were discovered as enzymes which preferentially cleave newly synthesized polyubiquitin precursors or

ubiquitin fused to ribosomal protein precursors. This process can be carried out cotranslationally[107] and represents the extreme fast catalytically activity of these enzymes. It was long believed that these enzymes hydrolyze only small fragments from the C-terminus of ubiquitin which attributes to a plugging loop directly in the catalytic groove. However, recent structural analysis show that the ubiquitin binding orients the misaligned active site into productive conformation[108] and thus explains the observed disassemble ability of polyubiquitin chains and ubiquitin-conjugates[67,15].

2.7.4 Ubiquitin – Specific Proteases (USPs)

The USP family is the largest and most diverse subclass of DUBs and is represented with more than 50 USPs. These cysteine proteases poses a conserved catalytic motif, the Cys box and the His box, but the size of the domains varies from 300 to 800 AAs. Structural analysis showed that the sequence similarity is low but the USP domain fold is highly conserved[15] and is constellated of three sub-domains termed finger, palm and thumb[109]. The USP sequences also contain several specificity dependent domains like, ubiquitin binding domains (UBDs), ubiquitin interacting motifs (UIMs), different zinc finger (ZnF) motifs and various enormously in their size. Not surprisingly, the cleavage activity of USPs is involved in several cellular key processes (e.g. signal transduction[110], endocytosis[111] and DNA repair[27]) and thus is not restricted for one specific Ub-constelation or Ub-linkage type[112,15].

2.7.5 Machado-Joseph Disease (MJDs) Protein Domain Proteases

Applying bioinformatic approaches, Ataxin 3 was the first identified member of MJD proteases and is the best studied one. The name derived from a gene mutation which results in a spinocerebellar ataxia type-3 disease or also known as Machado-Joseph Disease[15]. The sequence similarity to other classes is low but the overall fold is similar to UCH DUBs. Recently, Stephen Weeks and his colleges solved the first crystal structure[113] for a Josephin-substrate complex and Brett Winborn showed the specificity of Ataxin 3 towards K_{63}- linked ubiquitin chains[113]. However, both the biological function as well as Ub-linkage preference of the other class members still have not been discovered[67].

2.7.6 3.7.4. The JAMM Motif Metalloproteases

The JAMM subclass is represented by 14 metalloproteases which contain the conserved Zn^{2+} ion stabilization assemble. This motif coordinates two zinc ions for the activation of a watermolecule which then attack the internal isopeptide bond within the ubiquitin linkage. To note are the seven JAMM members which have at least one amino acid exchange in the catalytically Zn motif and thus are most likely not deubiquitinating enzymes[67] Interestingly, most of the JAMM DUBs were commonly found within large complexes, for instance POH1 (Rpn11) in the core structural component of the 19S proteasome complex[114] or AMSH as an associated DUB in the ESCRT machinery (also known as STAMBP)[115]. The crystal structure of AMSH-LP bound to K_{63}- linked di-ubiquitin revealed for the first time the mechanism for the preference of JAMM DUBs towards K_{63} linked ubiquitin chains[106].

JAMM members exhibits different functions and were described to precipitate for instance in vesicle trafficking[106], in DNA repair[116] or in endocytosis[117].

2.7.7 Ovarian Tumor Proteases (OTUs)

The first Ovarian Tumor (OTU) family members were discovered by bioinformatics homology[118] with the ovarian tumor genes which regulate the translation of RNA transcripts[119].

The OTU subclass members serve the OTU domain and contain the typical cysteine protease catalytic triad formed of His, Cys and Asn/Asp. One interesting member is A20, that contains the OTU as well the as the zinc finger domain and can act as an ubiquitin-protein ligase[69] as well. Furthermore, the multifunctional aspect was shown by OTUB1 which is able to interact with an enteropathogen Yersinia encoded virulence factor[120], and is assembled in a complex encompassed by USP8 and GRAIL[121]. However, the functional role of further members remains to be investigated.

2.8 Active site directed probes

Various sequencing efforts and proteomics approaches, such as analysis of protein expression level and protein modification by LC-MS, have shed light on the proteome. However, their detection does not directly imply the functional state of the

protein, whose activity often relies on post-translational modifications or subcellular localization. To address this issue, a powerful technique termed activity-based protein profiling (ABPP) can be applied to analyze the protein expression and directly their function in complex proteome mixtures (**Figure 11**). ABPP utilizes chemical- and protein-based probes, also called as active-site directed probes (ABP). These probes are designed to address the substrate specificity of certain target enzymes and are able to bind covalently a subset of proteome with similar catalytically features. Several enzyme classes, such as proteases, kinases and phosphotases have been characterized by utilizing ABPs[122]. The generation of high potential ABPs has emerged either through the knowledge of enzymes or by careful selection of irreversible and reversible inhibitors[123]. The constellation of ABPs is based on three components (**Figure 10**): (i) a chemical reactive group (trap) which is designed to interact covalently with the catalytic residues of the enzyme of choice, (ii) a binding group which is responsible for the specific interaction with the target enzyme, (iii) and an analytical tag.

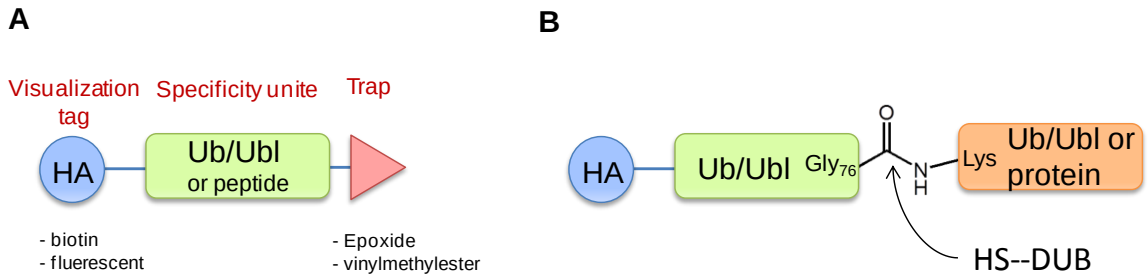

Figure 10. Building blocks of an ubiquitin derived activity-based probe (ABP).
A) The general constellation of ubiquitin derived probe, consisting of a reactive chemical group (trap), ubiquitin as the specificity unit and the tag for detection, immunoprecipitation and visualization purposes. **B)** Deubiquitination of ubiquitin conjugated proteins. The catalytic active cysteine residue of DUBs performs a nucleophilic attack on the isopeptide bond of the C-terminus of ubiquitin and the lysine of the substrate.

The internal trap, such as an epoxide or Michael acceptor, is designed to address the catalytic chemistry of enzymes. The reactivity of probe towards the enzyme (DUB) active-site depends partially also on chemical properties of the traps, including their affinity and native chemical reactivity. The fine-tuning of probes in respect to the variation of traps provides a suitable handle to control their enzyme selectivity.

The integration of specific elements, e.g. ubiquitin in this study, alters the probe from their broad reactivity to more selective labeling of enzymes.

The possibility to vary the tag; for instance in a suitable fluorescence or FRET based tag would allow the monitoring of active-enzyme formation in a more real-time way. Nevertheless, the choice of tag type should be considered accurately to avoid the negative interference with other probe elements, such specificity unit or the trap. To address this challenge, good performance was observed by using click chemistry based probes[124,125]. A further possibility is the introduction of a “delivering element”, for example a cell penetrating peptide, which targets the probe to a certain cell type and also enables *in vivo* experiments. The design of DUB specific probes was pioneered by development of intein-based protein-expression systems[126], which enables the modification of the C-terminus of Ubiquitin with a additional chemical reactive group[127]. The ubiquitin-vinylmethylester probe (HAUB-VME) is a well studied and promising active-site directed probe with broad reactivity towards DUBs[128]. This probe binds covalently to the active-site (Cys) of DUBs, with the exception of the few metalloproteases. The N-terminal epitope tag hemagglutinin (HA tag, YPYDVPDYA) of ABPs helps to detect the modified DUBs after the separation of a protein mixture by SDS-PAGE or immunoprecipitation, followed by immunobloting or mass spectrometry analysis (**Figure 11**). The wide range of possibilities to design the probes are very promising for the development of powerful tools which would allow to characterization of enzymes in their biological environment in more detail.

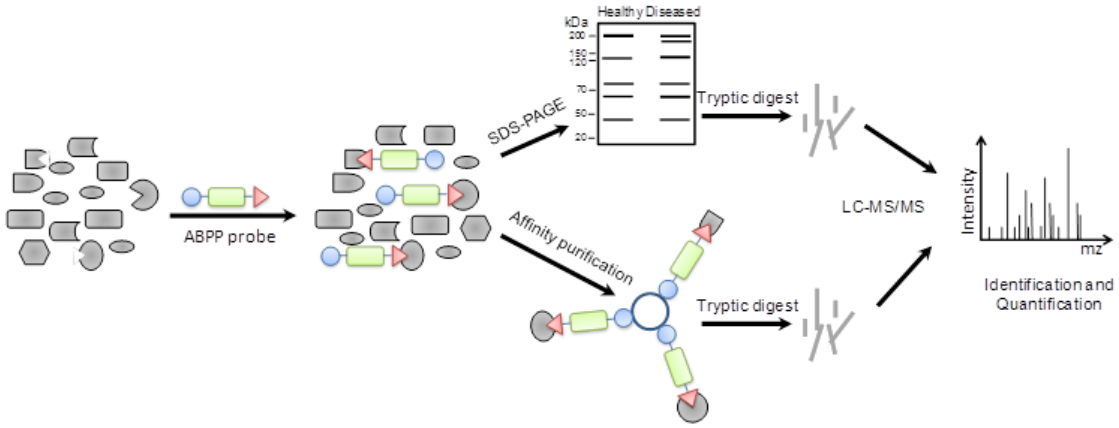

Figure 11. Workflow of activity-based protein profiling (ABPP).

Target proteins of the complex proteome mixture are modified (labeled) with activity-based probes. Shown are two possible ABBP workflows: (i) Gel-based activity-based protein profiling and (ii) enriched by affinity purification, followed by identified using mass spectrometry.

3 Materials and Methods

All Chemicals and organic solvents used were reagent and HPLC grade, respectively. The materials were purchased from Sigma-Aldrich (Taufkirchen, Germany) unless indicated otherwise.

Table 3. Material and reagents supplied from distinct companies.

Material	Company
1,4-Dithiothreitol ≥99% (DTT)	Serva
Amersham ECL+ Western Blotting Detection Reagent	GE Healthcare
Ammoniumphosphat (APS)	Serva
Benzonase	Merck
Complete Protease Inhibitor Cocktail	Roche
Coomassie Brillant Blue G250	Serva
EDTA	Merck
HEPES Pufferan® ≥99.5%	Roth
Glycin ≥99% p.A.	Roth
Glycerin ~86% p.A.	Roth
LiChroprep RP-18	Merck
Natrium-Chlorid ≥99.5% p.A. (NaCl)	Roth
Rotiphorese® Gel 30 (37.5:1)	Roth
TEMED 99% p.A.	Roth
Triethylammonium Bicarbonat Puffer p.A. for HPLC (TEAB)	Fluka
Trifluor-Essigsäure ≥99.5% (TFA)	Fluka
Material	**Company**

Tween® 20	Roth
Zip-Tip-C18µ	Millipore
Chitin Beads (S6651L)	BioLabs

3.1 Peptides

Peptides were kindly provided by the Dept. Chemical Biology and analyzed by RP-HPLC (Agilent 1200 Infinity HPLC, column: Phenomenex Gemini 50 × 2mm, C18, 3µm, 110Å; gradient: 5–95% 0.1% TFA/acetonitrile in 0.1% TFA/water in 7 min, flow rate: 0.4 mL min^{-1}, detection: 214 nm) with online ESI-mass spectrometry detection (Applied Biosystems API2000 triple quadrupole MS).

3.2 Antibodies

The following antibodies were used in this study:

Table 4. Antibodies used in this study.

	AB species	**Dilution**	**Company**
α-HA	Mouse, monoclonal	1:1000	Roche, Switzerland,
α-HIS	Mouse, monoclonal	1:2000	Merck, Germany
α-mouse IgG+IgM	Goat	1:3000	Jackson ImmunoResearch
α-HA agarosa beds	Mouse, monoclnal	50-100 µl suspension	Sigma-Aldrich, Germany

3.3 Cell lines and culture conditions

All cells (**Table 5**) were cultured at 37°C and 7.5% stable carbon dioxide (CO_2) using Innova (Germany) incubators.

Table 5. Cell lines and culture conditions used in this study.

Cell Line	Origin	Culter Conditions
EL-4	mouse, lymphoma	Dulbecco's modified Eagle's Medium (DMEM), 10% FBS, 1X Pen/Strep, 2mM glutamine
Jurkat E6-1	human,T cell leukemia	RPMI1640, 10% FBS, 1X Pen/Strep, 2mM glutamine
HeLa S3	human, cervix, adenocarcinoma	DMEM, 10% FBS, 1X Pen/Strep, 2mM glutamine
MCF-7	human, breast-adenocarcinoma	Modified Eagle's Medium (MEM-α), 10 % FBS, 1X Pen/Strep, 2mM glutamine, 10 µg/ml of bovine insulin
A549	adenocarcinomic human alveolar basal epithelial	F-12K, 10% FBS, 1X Pen/Strep, 2mM glutamine

3.4 Fermenter parameters

The following fermenter parameters were used for the Fermenter Labfors 5L in this study:

	Composition	Amount		
Selection factor	**Ampicillin, chloramphenicol**			
Run time	24h			
Medium:	Tryptone	60g	4.5L	5L
	Glycerin	20ml		
	Yeast Extract	120g		

Composition	Amount	
add after autoclaving (10 min 121°C):		
KH2PO4	11.5g	0.5L
K2HPO4	62.7g	
Harvesting 5L by centrifuge 15 min at 6000 x g (4°C)		

3.5 Protein expression in *E. coli*

The HA-Ub-intein-chitin fusion construct was expressed in BL-21star *E. coli*. For this purpose 15 ml LB-medium containing 100µl/ml chloramphenicol (cmp) and ampicillin (amp) were inoculated with the glycerol stock *E. coli* cells containing the "pTyb2-HAUb" plasmid. The culture was incubated over night at 180 rpm and 37 °C in a Multitron (INFROS HT) incubator. Following, the 15 ml culture was transferred to a 2L shaking flask with 500ml LB-medium (cmp/amp) and incubated by shaking at 130 rpm and 37 °C for 1-3 h, until the optical density (OD) value of 0.9-1.0. The protein expression was induced by 0.5 mM IPTG and the continued culturing at 180 rpm, 20 °C over night. After the cultivation the cells were pelletized at 3500 x g.

3.6 Buffer and reagents used in this study

Buffer	Composition	Concentration
Lysis buffer (pH 7.5)	4-(2-hydroxyethyl)-1-piperazineethanesulfonic acid (HEPES)	50 mM
	sucrose	250 mM
	$MgCl_2$	50mM
	IGEPAL	1% (v/v)

Buffer	Composition	Concentration
4x sample buffer	N-tris(hydroxymethyl)-methylglycine (Tris) pH 6.8	25mM
	SDS	8% (w/v)
	dithiothreitol (DTT)	3 mM
	glycerol	80% (v/v)
	bromphenol blue	0.02% (v/v)
NET-buffer (pH 7.5)	TRIS	50 mM
	NaCl	150 mM
	ethylenediaminetetraacetic acid (EDTA)	5 mM
	IGEPAL	0.5% (v/v)
RP buffer A	TFA	0.1% (v/v) in MQ
RP buffer B	TFA	0.1% (v/v) in MQ
	acetonitrile (ACN)	60% (v/v) in MQ
DUB-reaction-buffer (pH8.0)	TRIS	50 mM
	NaCl	50 mM
	DTT	1 mM
	ATP	1mM

Buffer	Composition	Concentration
Buffer-CIEX A (pH 4.5)	HEPES	10 mM
Buffer-CIEX B (pH 4.5	HEPES	10 mM
	NaCl	1M
1xSDS running buffer	TRIS	24 mM
	glycine	199 mM
	SDS	0.2% (v/v)
Gel fixing solution	EtOH	30% /v/v)
	Acetic acid	10% (v/v)
Coomassie Silver (according to Candiano)	H_3PO_4 (85%)	10% (v/v)
	$(NH_4)_2SO_4$	10% (w/v)
	MeOH	20% (v/v)
	Coomassie BB-G250	0.12% (w/v)
10x Blot buffer	TRIS, pH 8.3 (HCl)	0.25 M
	Glycine	1.92 M
	SDS	35 mM
1x Blot buffe	10x Blot buffe	10% (v/v)
	MeOH	20% (v/v)

Buffer	Composition	Concentration
PBS (pH 7.4)	NaCl	137 mM
	KCl	2.7mM
	Na_2HPO_4	10mM
	KH_2PO_4	2mM
LB-Medium	Luria Broth powder	15 g
autoclaved at 121 °C	MiliQ	600 ml
	amp(x 1000; 100 mg/ml)	5ooµl

3.7 Intein-based chemical ligation

3.7.1 Synthesis of $HAUb_{75}$ – MESNa thioester

In order to get the starting material $HAUb_{75}$, the HA-Ub-intein-chitin fusion construct (containing the chitin binding domain, CBD) was expressed in BL-21star *E. coli* and induced with 0.5 mM IPTG at 20°C O/N using 2L shaking flask or fermented in 2 or 5L Labfors (Swizerland) fermenter.

Detailed information according fermenter parameters are supplied in the supplement section. For harvesting, cells were pelleted at 3000 x g, resuspended in 100ml lysis buffer (+ protease inhibitor cocktail (Roche), 4°C) and homogenized by one French press passage at 20000 psi followed by sonication for 10min at 4°C. The suspension was then clarified at 36000 x g (RC6 centrifuge, Thermo Fisher Scientific, USA) for 30 min and the supernatant filtered with 0.45 µm nylon (NY) membrane filter (Millipore, France).

The clarified cell lysate was then transferred to glass columns containing 10-15ml chitin beads (New England Biolabs, UK), which were previously washed with 100ml cold lysis buffer. In order to allow the Ub-intein-chitin fusion construct to bind to the chitin beads, the suspension (cell lysate/chitin beads) was incubated for 5h at 4°C with gentle shaking. Afterwards, to get rid of unbound proteins, the beads were washed with lysis buffer. Subsequently, 15ml of lysis buffer containing 50mM MesNa was passed though the beads and then refilled again till all beads were covered. The on-column cleavage, to gain the $HAUb_{75}$ – MESNa thioester product (**Figure 12**), was induced with an overnight incubation at 37°C. After incubation the flow-through containing the desired $HAUb_{75}$ – MESNa thioester product was collected followed by an additional rinsing step with 10ml lysis buffer to get the remaining product.

In contrast to the previously published methods the HA-Ub_{75} – MESNa thioester was purified to get rid of MESNa, which undergoes a competition reaction with thiol-reactive groups in the conjugation step. In order to perform the purification, the product was filtered with 2 µm NY filter (Millipore, France) and concentrated (~ 10ml) while exchanging the buffer to 50mM NaOAc, pH 4.5 using VIVASPIN-20 5000 MWCO (Sartorius Stedim Biotech GmbH, Germany) at 3000 x g and 15°C.

The purification was performed with cation exchange (CIEX) chromatography using the ÄKTApurifier 10 (GE HealthCare) system and a MonoS 10/10 column with a linear gradient from 0% buffer-CIEX A to 50% buffer-CIEX B. To avoid hydrolyzing

processes, the eluted fractions were immediately analyzed by MALDI-TOF MS. The fractions containing the appropriate $HAUb_{75}$ – MESNa thioester product were pooled and desalted via VivaSpin-1 3000 MWCO against 50 mM NaOAc (pH 4.5) to an end volume of 0.5 ~1 ml.

3.7.2 Generation of active-site directed probes

The generation of active site-directed probes is based on the ligation of reactive HAUb75 – MESNa thioester with an appropriate C-terminal electrophilic group (**Figure 12**), also termed “warhead”. These warheads were designed and synthesized using Horner-Wadsworth-Emmons reaction to predominantly produce the preferred E-form of the required glycine-based electrophilic group, more details are provided in the supplement 10.2 (in collaboration with Dept. of Chemical Biology, HZI). The warheads were then ligated with the recombinantly expressed HAUb lacking the C-terminal glycine (G_{76}) and carrying a reactive thioester group instead ($HAUb_{75}$ - MESNa), as described in the section above (3.7.1).

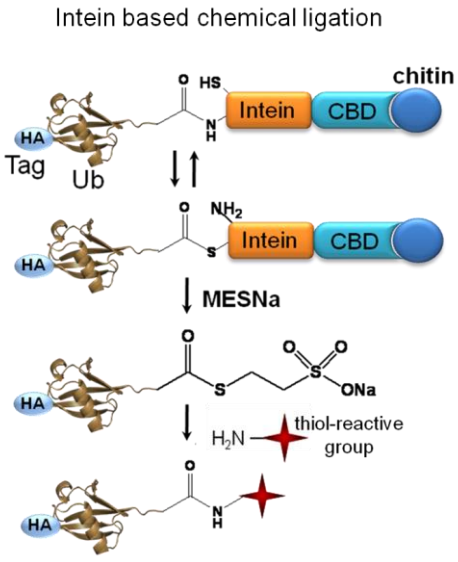

Figure 12. Schematical presentation of the Generation of HAUb derived active site- directed probes based on intein chemical ligation.

The produced amino functionalized thiol reactive groups (warheads) were dissolved in 100-200µl, 100mM HEPES by adjusting the pH value finally to pH 8 using 0.1M NH_4HCO_3. Alongside, the ligation step was improved by adding 2M S-NHS as biocatalyst to 500µl of $HAUb_{75}$ –MESNa and adjusted to pH 8 using $NaHCO_3$. Finally,

the active HAUb-derived thioester was ligated with the previously produced amino-functionalized warheads overnight at 37°C.

After the overnight incubation the probe product was filtered using 0.22µm NY membrane (Millipore, France) and the buffer was exchanged via VivaSpin 1ml -3000 MWCO concentrator. Afterwards, the probes were purified by utilizing the same setup as described in section 3.7.1, the appropriate fractions were pooled and concentrated by simultaneously exchanging the buffer to 50mM HEPES, pH 7.4 (storage buffer). Finally, the concentration was determined by Nanodrop Spectrophotometer (PEQLAB, Germany), and the probes were validated and characterized by ESI-Q-TOF MS / MALDI-TOF MS and stored at -80°C.

3.8 Cell harvesting and storage

In order to gain the high protein concentration of cell lysates and to get the possibility to work reproducibly in the following experiments by parallel handling parallel of different cell lines, cell pellets of each cell line were prepared and stored at -80°C.

Therefore, cells were cultivated until the confluence of 80-100% utilizing 150 mm uncoated culter dishes and harvested by placing the dish on ice.

For this purpose, the medium was discarded, the cells rinsed with ice cold PBS and scraped off from dishes. Following this, the cell suspension was directly transferred into ice-cold falcon tube. Afterwards the cells were pelleted by 950rpm centrifugation and at 4°C for 15 min. In the next step the supernatant was discarded, pellets washed two times with PBS and the pellets finally stored at -80°C.

3.9 Cell lysis

Frozen cells were thawed on ice and transferred into 2ml reaction tubes containing 300 ml glass beads (rinsed with PBS before use). To start the lysis, 1ml of lysis buffer and 250 units/ml benzonase (MERCK) were added. The high-speed vortexing for 40 min at 4°C supported the lysis with shear forces and was further enhanced by additional 10min sonication using an ice cold bath. To get a clear cell lysate, the suspension was transferred into a new reaction tube, centrifuged two times for 20min

at 18000 x g (4°C) and the clarified lysate finally transferred into a new reaction tube, which was stored on ice until usage.

3.10 Determination of protein concentration

The protein concentration (of cell lysates) was determined according to the Bradford assay[129]. The standard calibration curve was determined by using a dilution series of bovine serum albumin (BSA) from 0.1 – 1 mg/ml. All measurements were carried out in triplicates and were performed by an Infinite M200 Elisa reader (Tecan, Switzerland) at an absorption measurement at 595nm. The concentration measurement of ABP products was performed with Nanodrop using water or appropriate buffer as reference.

3.11 Activity based profiling by utilizing HAUB-VFEA probe

The profiling experiments using HAUb-VFEA were performed with the help of Anne Kummer as part of her master thesis.

The protein concentrations of all cell lysates were adjusted with 50mM HEPES (pH 8.0) to a final concentration of 9 mg/ml in an end volume of 1 ml. To enable the appropriate labeling after the adding of 0.8 µg of HAUb-VFEA, the samples were adjusted to a pH value of 7.5-8.0. The incubation of 2h at 37°C allowed HAUb-VFEA to react. The reaction was stopped by adding sodium dodecyl sulfate (SDS) to a final concentration of 0.3% (v/v) and further incubation of 15min at RT. Afterwards, the samples were subjected to an immunoprecipitation for the identification of probe-labeled enzymes,

3.11.1 HA-Immunoprecipitation of HAUb-VFEA-enzyme complex

After the enzyme labeling procedure with HAUb-VFEA (Activity based profiling by utilizing HAUb-VFEA probe, described above), the SDS concentration was further reduced to the final concentration of 0.1% using NET-buffer. Further on, 100µl of monoclonal anti-HA agarose beads (Sigma, clone HA-7) were washed with NET-buffer, placed into centrifuge columns with Polyethylene filter, ~30µm pore size (Thermo Fisher Scientific, USA) and filled with the samples. Afterwards, sealed

columns were incubated for 5h at 4°C by continuously rotating at 6 rpm. After the incubation the unbounded proteins were discarded by shortly spinning down the columns at 200 x g and washed twice with NET-buffer and 0.1M ammonium bicarbonate (NH_4HCO_3). Immunoprecipitated proteins were eluted with 4x sample buffer or digested directly on beads.

3.11.2 Tryptic on bead digest

To enhance the tryptic digest by providing trypsin the direct access to the proteins, the digest directly on beads was favored. In order to facilitate the protein identification, the proteins have to be reduced and carbamidomethylated. The protein reduction was carried out by covering the beads with 20mM DTT (in 0.1M NH_4HCO_3) followed by an incubation of 30min at 56°C. Afterwards the solution was discarded by shortly spinning down the column. The carbamidomethylation was achieved by addition of 55mM iodacetamide (in 0.1M NH_4HCO_3) and an incubation of 30min at RT in the dark. To get rid of left reagents, the beads were washed by spinning down two times with 0.1M NH_4HCO_3.

The digestion of precipitated proteins bound on the beads was executed by adding 4 µg of trypsin (Sequencing grade-Promega) dissolved in 10mM NH_4HCO_3, followed by an overnight incubation at 37°C and gently shaking at 70 rpm. The digested proteins were eluted from the beads by shortly spinning down, followed by additional two wash steps with 0.1% (v/v) trifluoroacetic acid (TFA, pH 3). To avoid some impurity, the samples containing the eluted proteins were centrifuged at 109000 x g for 20 min and the supernatant stored at 4°C for further usage.

Peptide Purification

Almost all commercially available agarose beads contain the plasticizer polyethylene glycol (PEG), which interferes with chromatography columns within mass spectrometric methods. To get rid of PEG from the peptide mixture, derived from the on-bead tryptic digest, a reverse phase (RP) chromatography approach was applied. Therefore, the samples were subjected to an Äkta Purifier system (GE Healthcare, Germany) just after the equilibration with 0.1% TFA (buffer A). After the binding of peptide on the self-packed C_{18} column (Merck, Germany) these were eluted with RP buffer B (without gradient). Although no gradient was applied, the peptides and PEG eluted differently. The fractions containing the corresponding peptides were pooled

and dried in a speedvac (vacuum concentrator, Thermo Fisher Scientific, USA). Afterwards, these were dissolved in 6% ACN in 0.1% formic acid (FA), sonicated for 5min and diluted to an end concentration of 3% ACN using 0.1% FA. To ensure the purity of the sample, the samples were centrifuged at 109000 x g for 20 min at 4°C and transferred into glass vials (Waters, USA) for further mass spectrometric analyses.

3.12 HA-Immunoprecipitation of UIPP-probe enzymes adducts

The crude cell lysate, prepared as described above, was diluted to a protein concentration of 6.25mg/ml (500µl total volume) using 50mM HEPES, (pH8.0). Then 0.8 µg of UIPP (Ub_{42-54} -K48(VA) or Ub_{54-72} –K63(VA)) was added and the pH-value adjusted to pH 8. As negative control, an aliquot of each cell lysate was treated exactly as the sample, however adding HEPES-buffer instead of UIPP. The samples were then incubated for 1h at 37°C to allow the probes to react. Afterwards, the reaction was stopped by adding SDS up to a final concentration of 0.3% (v/v) and incubated for 15 min at RT. Afterwards the cell lysate was further diluted to the final SDS-concentration of 0.1% using NET-buffer. To avoid contaminations, 100µl of monoclonal anti-HA agarose beads (Sigma, clone HA-7, 1:1 suspension) were transfer into spin columns (Thermo Fisher Scientific, USA) and washed with NET buffer. To achieve the precipitation of covalently bound probes, the diluted cell lysate-probe mix was added to the beads and incubated for 1h at 4°C with continuous rotation. After the incubation, the flow-through was discarded and the columns washed twice with NET-buffer. Finally, 50 µl of 2x reducing sample buffer was added, the columns sealed and incubated for 5 min at 97 °C. The probe-enzyme adducts were then eluted by spinning down at 200 x g. To assure the elution of all precipitated proteins, the beads were covered additionally by 50 µl of 0.1% formic acid (FA) and spun down again. The eluted proteins were then resolved with 4-12% SDS-PAGE and stained with Coomassie Brilliant Blue. The relevant gel-lanes were excised, tryptic digested (In-gel digestion protocol) and analyzed with LC-MS/MS.

3.12.1In-gel digestion

The excised gel pieces of interest were covered with 20mM DTT in 0.1M NH_4HCO_3 and incubated for 30min at 56°C. The solution was then discarded and the pieces dehydrated by adding acetonitrile (ACN) followed by 15 min incubation until these became white. ACN was exchanged by covering them with 55mM iodoacetamide in 0.1M NH_4HCO_3 followed by incubation for 30min at RT in the dark. Afterwards the solution was discarded, followed by dehydrating with ACN and drying the gel pieces using speedvac (Thermo Fisher Scientific). Subsequently, the gel pieces were washed twice with 0.1M NH_4HCO_3. For the tryptic digestion, the gel pieces were covered with 1µg trypsin (Promega Gold Standard), dissolved in 10mM NH_4HCO_3 and incubated overnight at 37°C. The resulting peptides were extracted by adding the same volume of ACN followed by an incubation of 15 min at 37°C. The supernatant containing the peptides was transferred into a new tube. To expand the extraction, the gel pieces were additionally covered with 5% formic acid, shaken for 15 min at 37°C, filled up with the same volume of ACN and incubated for further 15 min at 37°C. Finally, the supernatant was pooled with extracted peptides from the previous step. In order to prepare the peptides for mass spectrometry, the samples were desalted by C_{18} -ZipTip (Millipore, France) according to the manufacturer's protocol and filled in appropriate glass vials.

3.13 Mass spectrometry analysis

All LC-MS/MS data obtained by LTQ Orbitrap Velos (Thermo Scientific) were analysed using Mascot-Server 2.3.02 (Matrix Science, London, UK) / X! Tandem (the GPM, thegpm.org; version 2007.01.01.1) and Mascot Daemon 2.2.06.

The generated peptides originating from the HA-IP experiments were analyzed by LC-MS/MS, utilizing the state of the art spectrometer : Thermo Scientific LTQ Orbitrap Velos (Thermo Fisher Scientific, USA/Germany)

LC-MS/MS analyses of desalted samples were carried out on an Acquity ultraperformance LC system (Waters) connected to the LTQ Orbitrap XLVelos mass spectrometer. The injected peptides were separated on an analytical column (1.7-µm BEH130, 75 µm × 150 mm (Waters) with RP buffer A and RP B using linear gradients of 120 min or 60 min (depending on sample concentration) at a flow rate of 300 nl/min controlled with AcquityUPLC software V1.22. The ionization of eluting peptides

was performed by using PicoTip emitter needles (New Objective Inc.) at voltages of 1.7kV and a capillary temperature of 200°C.
To minimize repeated measurements of peptides, dynamic exclusion was set to 1 repeat count with 6sec repeat duration and 12sec exclusion duration.
XCalibur software (Thermo Finnigan).was used to control the Data-dependent acquisition of MS and MS/MS data.

Database searches were performed with the following parameters:

Fragment Tolerance: 0,40 Da (Monoisotopic)
Parent Tolerance: 20,0 PPM (Monoisotopic)
Instrument type: ESI-FTICR
Fixed Modifications: +36 on O (O+36), +57 on C (Carbamidomethyl)
Variable Modifications: +16 on M (Oxidation)

Databases: self compiled database containing 173 DUBs (homo sapiens and mus musculus), NCBI_2011 database (Homo sapiens)
Digestion Enzyme: Trypsin
Max Missed Cleavages: 1

X! Tandem was set up to search a self compiled DUBs database by assuming the digestion enzyme trypsin. And was searched with a fragment ion mass tolerance of 0.50 Da and a parent ion tolerance of 20 PPM. O+36 of pyrrolysine and iodoacetamide derivative of cysteine were specified in X! Tandem as fixed modifications, whereas oxidation of methionine was specified as a variable modification.

The tryptic-peptides generated by Activity based profiling utilizing HAUB-VFEA, were identified by subjecting to MASCOT and X!Tandem (self compiled database).

The tryptic-peptides generated by HA-Immunoprecipitation using UIPPs, were identified by subjecting to MASCOT NCBI (2011).

3.13.1 Criteria for protein identification and semi quantification

Scaffold (version Scaffold_3.2.0, Proteome Software Inc., Portland, OR) was used to validate MS/MS-based peptide and protein identifications. Peptide identifications were accepted if they could be established at greater than 95.0% probability as specified by the Peptide Prophet algorithm[2]. Protein identifications were accepted if they could be established at greater than 99.0% probability and contained at least 2 identified peptides. Protein probabilities were assigned by the Protein Prophet algorithm [3]. Additionally, due to the possibility of some false positive assignments originating from the relatively small self compiled database, all proteins were manually inspected and verified.

3.13.2 MALDI-TOF

Matrix-assisted laser desorption/ionization (MALDI) time of flight (TOF) was used for mass spectrometry analysis / monitoring of product generated during the intein-based chemical ligation.

The samples were prepared by depositing 1µl of sinapic acid protein matrix directly on the target plate and mixed afterwards with 1µl of desired sample.

After the mix solution is evaporated the spots were ionized (Laser)and measured in the linear mode. Data were analyzed with software of Bruker Daltonics (Coventry, UK), flexAnalysis™ .

Laser Frequency: 8.3 Hz

Laser Attenator	Offset:	70%
	Range:	20%

3.14 Activity-based shift assay

In order to prove the reactivity of active site-directed probes towards DUBs, these both components were mixed and the labeling potency of the probe was observed by a mass shift. This upwards mass-shifted band on the SDS-PAGE corresponds to the complex consisting of DUB and the covalently bound probe. Therefore, 0.5 – 1.0 µg of recombinant HIS_6-tagged DUBs were firstly pre-incubated in a DUB-reaction-buffer

for 15min at RT. Afterwards, 0.1-0.5 µg of particular active-site directed probe were added and the reaction mix incubated at 37°C for particular period of time. The reaction was stopped by adding 4X sample buffer, followed by 95°C incubation for 3min. Finally, the samples were resolved by SDS-PAGE and analyzed by immunoblotting. All experiments were conducted twice or more in the same conditions to ensure that the results were reproducible.

3.15 Immunoblotting (Western-Blotting)

The sample was reduced and alkylated with 4x reducing sample buffer, boiled for 3 min at 95°C and separated on SDS-PAGE acrylamide gels using the XCell SureLock^{TM} Invitrogen equipment. The proteins were transferred for 2h by "wet blotting" procedure using transfer buffer, Polyvinylidene Fluoride (PVDF) membrane and Invitrogen equipment (XCell blotting chamber). After the transfer the membranes were blocked for at least 3 hours in 5% milk in PBS (0.5% Tween 20) and washed afterwards 3x in PBS (0.5% Tween 20). The membranes were then immunoblotted with primary antibody diluted in 1% milk in PBS (0.5% Tween 20), washed 3x 15 min in PBS (0.5% Tween 20), and followed by 3 times 5 min washes and incubation in HRP-conjugated secondary antibody in 1% milk in PBS (0.5% Tween 20). The visualization of transferred proteins was performed with a LAS-3000 CCD-camera (Fujifilm Europe, Germany) and enhanced chemo luminescence Plus (ECL+) Western Blotting Reagent (GE Healthcare, UK).

3.16 Gel Electrophoresis

Shift assay analyses were carried out by using self-cast gels as summarized in **Table 6**. Therefore, 0.5-1.0µg of protein were applied to the gel wells and separated at 100V using Minigel-Twin chamber (Biometra, Germany) and 1X SDS running buffer. The PageRuler Prestained Plus Protein Ladder (Fermentas, Europe) was used to estimate the protein size. After the separation of proteins according their size, these were visualization by Coomassie brilliant blue.

Table 6. Composition of stacking and separating gel used for SDS-PAGE analyses.

Solution	stacking gel [ml]	Separating gel [ml] 10%	Separating gel [ml] 12%
SDS buffer A	---	2.5	2.5
SDS buffer B	2.5	---	---
MQ	6.1	4.2	3.5
Acrylamid/Bis (37.5:1)	1.4	3.3	4
TEMED	30µl	20µl	20µl
APS, 10%	60µl	50µl	50µl

In order to achieve sufficient separation of proteins in cell lysates, the profiling analysis after incubation with the particular probe or after ABPP approach, were carried out with precast gradient gels utilizing XCell SureLock®. The instruction for electrophoresis using the XCell SureLock® Mini-Cell (Invitrogen, UK) and the technical guide is available at www.invitrogen.com/manuels. Therefore, 25-50µg proteins were boiled at 95°C for 3min and loaded on the 1.0mm x 10/15 well, NuPAGE® -4-12% Bis-Tris gel. These were separated by applying 100V and using 1X NuPAGE® MOPS SDS Running Buffer.

3.17 Protein dyeing method -Coomassie staining

In order to visualize the proteins after the SDS-PAGE a dyeing method termed Coomassie-Brilliant-Blue-Silver was applied. Therefore, the gel was washed for 10min with deionized water and fixed overnight in fixing buffer. Afterwards, the gel was washed three times with deionized water for 30 min. In order to dye the in-gel proteins, the gel was covered with Coomassie-Brilliant-Blue-Silver solution and incubated overnight at RT. Finally, the gel was washed with deionized water until the protein bands appeared and the blue background disappeared.

4 Results

Deubiquitinating enzymes (DUBs) are involved in many crucial cellular regulatory events which directly influence disease and pathologies such as cancer or neurodegeneration and thus represent promising therapeutic targets. One important open question is the understanding of the molecular basis of DUBs specificity for different poly-Ubiquitin linkages and protein substrates.

To address this issue, promising ubiquitin derived tools termed activity-based probes (ABPs) were recently introduced. When these ABPs are applied in an in an activity based proteomic approach, these probes bind covalently to the catalytic residue of active DUBs and allow to be isolated, identified and characterize the DUBs under different physiological conditions. However, the evaluation of DUBs selectivity by those ABPs was not possible at the beginning of this thesis project.

The aim of this study was the improvement of ABPs by modulation of the well characterized probe (HAUb-VME) to examine the probe parameters that are most likely influencing the probe reactivity and selectivity. The ultimate aim was the generation of novel probes, which are able to bind DUBs selectively and thus give insights into their specificity towards ubiquitin linkages or substrates.

For the generation of the C-terminal Ub-ABPs a workflow was developed covering the following steps:

- Which stage(s) are improvable in order to optimize the previously introduced intein-based ligation[128] for generating HAUb derived probes?
  - The optimization steps should include the expression of HAUb, the ligation with C-terminal traps and its purification.
- Which parameters influence the behavior of ABPs?
  - New probes should be designed by systematical modulation of the reactivity and generated using an optimized synthesis workflow.
  - The newly generated probes should be evaluated by activity based profiling, immunoprecipitation and by binding assay towards recombinant DUB.
- Is it possible to generate highly reactive probes?

- Highly reactive probes should be designed and generated.
- The DUBeome of five different cell lines should be examined by new generated probes utilizing functional proteomics.

- To what extend is it possible to engineer selective probes by mimicking the iso-peptide bond?
  - Novel Di-ubiquitin-mimicking probes should be designed and generated based on structural composition of ubiquitin linkages.
  - Case study of representative probes should be conducted by activity based profiling.

4.1 Generation of novel activity based probes

4.1.1 Enhanced expression of starting product HAUb

The following description of the employed ligation method contains the significant optimization steps, whereas the relevant individual parameters are deposited in the method section.

In order to gain functionalized recombinant Ub, which is the starting product and the responsible part for specificity in Ub derived ABPs, the HA-Ub-intein-chitin fusion construct was expressed in BL-21star *E. coli*. To optimize the expression conditions bacterial cultures were induced with IPTG for 1h, 2h, 3h, and 4h at 20°C in the shaking flask and product formation was comparatively analyzed by SDS-PAGE (**Figure 13a**).

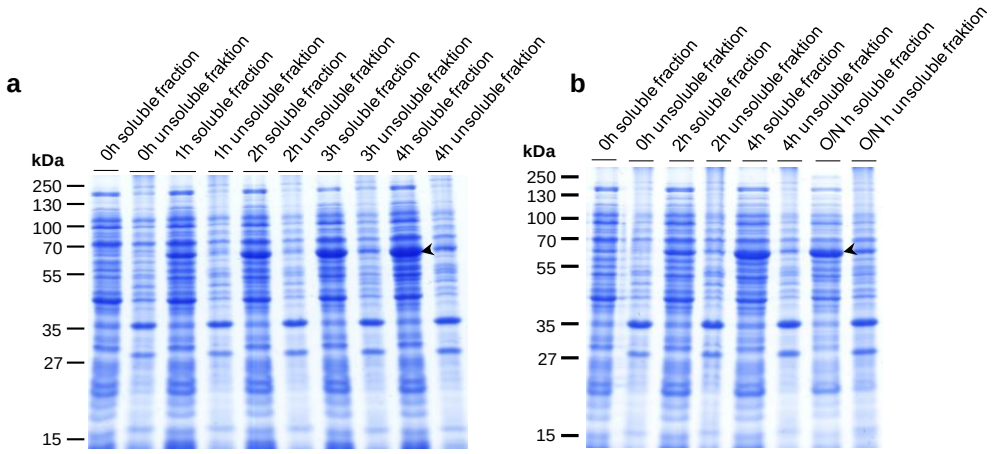

Figure 13. SDS-PAGE analysis of expression levels of HAUb in *E.coli* BL21 using 2L shaking flask (a) or 2L fermenter (b). Equivalent amounts of cell pellet were harvested and subjected to the BugBuster Protein Extraction reagent. Afterwards, the soluble and insoluble fractions were obtained by centrifugation (16000 x g). 50 µg from each cultivation time point was separated by 12% SDS-PAGE. The proteins were visualized by Coomassie Brilliant Blue staining. The arrows indicate the expression of HAUb-Intein fusion protein, the expression product of interest.

The observed product ration increased in the first three hours and kept constant afterwards. The observed difference between 3 and 4 hours cultivation time using a 2L shaking flask was apparently not significant.

With the goal to obtain sufficient yield from the intein-based ligation experiments, the cultivation time point was extended to overnight (O/N) and the expression induced in a 2L fermenter (**Figure 13b**).

On the one hand the HAUb expression was not enhanced by extending the cultivation time point to O/N, but on the other hand was not accompanied by obvious degradation byproducts. However, it has to be kept in mind that in contrast to shaking flasks, the fermenter could comprises a considerably higher end volume. In order to increase the expression yield and assure the reproducibility of further ligation experiments, it was decided to perform an O/N fermentation using a 5 L fermenter. The cell pellet yield after fermentation was measured as wet-pellet-mass and came to an yield of 200g which is 3 times higher than using shaking flasks. The correspondent *E.coli* growth curve using the fermenter is depicted in **Figure 14** which shows a representative growth curve.

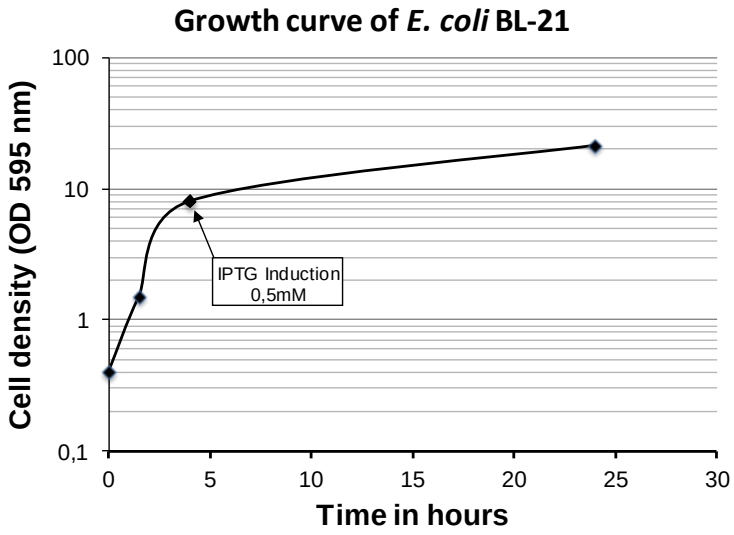

Figure 14. Growth curve of *E.coli* BL-21 in a 5 L fermenter.

Time course of relative cell density during the fermentation of *E.coli* BL21 at agitation speed of 800 rpm using a 5 L Labfors (Switzerland) fermenter.

4.1.2 Improved Workflow for sufficient generation of active site directed probes

Since HAUb-VME is a well characterized Ub-based active site-directed probe, its synthesis protocol was selected as a plattform and used as an approved reference[73]. Therefore, a recombinant expressed epitope-tagged Ub fusion protein was modified on its C-terminus by applying an intein-based chemical ligation (3.7) (**Figure 15**a). Briefly, a C-terminal fusion construct with an intein-chitin binding domain (CBD) was expressed, the cells were pelleted, resuspended and lysed. The suspension was clarified and incubated with chitin beads, which bind to the chitin-binding-domain present at the C-terminus of the fusion protein.

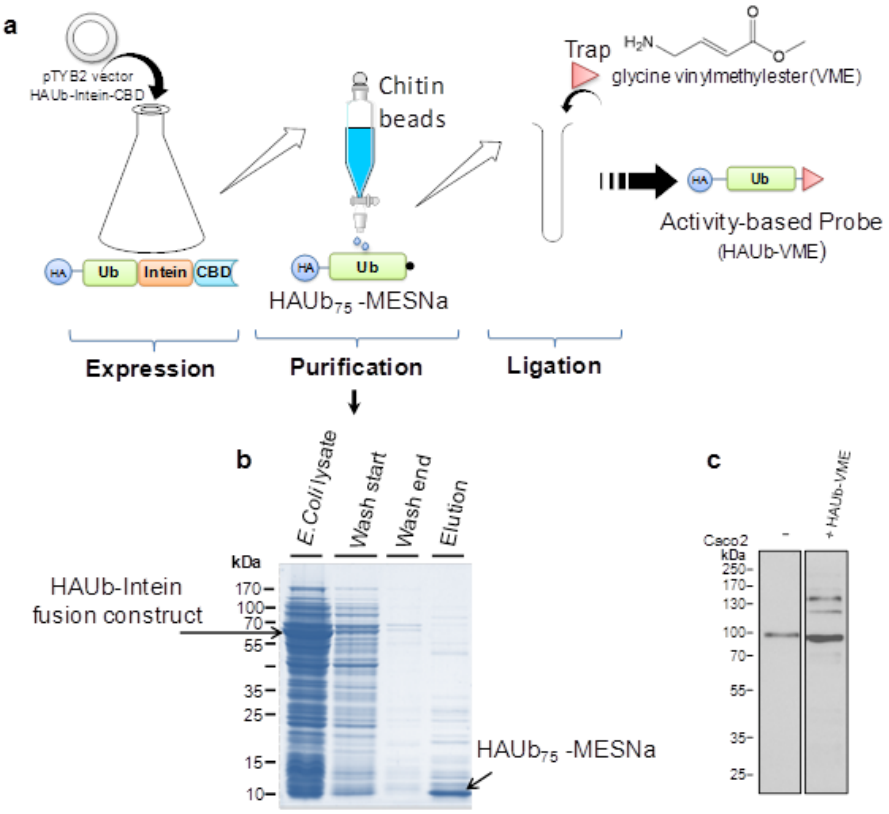

Figure 15. Synthesis workflow of activity based probe (ABP) and its validation. (a) Major synthesis steps for generation of activity based probes: Step 1, expression of a fusion protein with an intein and a chitin binding domain (CBD). Step 2, the fusion protein binds to a chitin affinity column. The HAUb was released from the column by a transthioesterification reaction by incubation with MESNa and resulted in reactive $HAUb_{75}$ –MESNa product. Step 3, The MESNa group was replaced by desired C-terminal reactive group (trap) in a chemical ligation step. (b) $HAUb_{75}$ –MESNa purification. The coomassie stained 12% SDS-PAGE shows the loaded lysate on chitin column; the flowthrough after the first and last washing step, and eluted $HAUb_{75}$ –MESNa collected after on-column cleavage

induced by MESNa. (c) Reactivity of the first generated HAUb-VME. The crude cell lysate (30µg) was incubated for 2h with 1µl of HAUb-VME, reduced with 4X sample buffer, resolved on 12% SDS-PAGE and immunobloted using α-HA antibody.

The addition of mercaptoethanesulfonic acid sodium salt (MESNa) resulted in elution of $HAUb_{75}$ –MESNa (**Figure 15b**) which lack the C-terminal glycine (G76), but carrying a reactive thioester group instead and is capable for chemical ligation. Due to the fact that $HAUb_{75}$ –MESNa is highly reactive and undergoes a fast hydrolysis, previous reports suggested to apply it directly to the chemical ligation step. Thus, this HAUb derived thioester ($HAUb_{75}$ –MESNa) was incubated overnight with the previously produced amino functionalized trap VME, to generate the desired HAUb-VME probe (**Figure 15a**). In contrast to all previous approaches, this ligation step was improved by adding Sulfo-NHS as bio-catalyst (as described in section 4.1.3).
In order to validate the probe reactivity, the generated HAUb-VME was incubated for 2h with crude cell lysate. Afterwards the sample was resolved by SDS-PAGE and its reactivity analyzed by α-HA immunoblotting (**Figure 15c**). However, in contrast to current literature, the labeling reactivity was relative weak and not satisfying. The reason was most likely the impurity of $HAUb_{75}$ –MESNa (**Figure 15b**, additional bands) and the missing information about the probe end concentration.
In spite of the paucity of ABP purity, most of the previous reports used the ABPs simply in excess[130]. To overcome these limitations, various efforts were made to purify the ABP.
Borodovsky et al. 2005 suggested to dialyze the probe and recommended the Pharmacia SMART cation exchange system. Unfortunately, the suggested column was not applicable for the ÄKTApurifier™ system used in this thesis work.
Alternatively, since the pH value was in the range of 6.5-8 pH before and after the ligation step, it was obviously to use an anion exchange chromatography without additional dialysis steps. Therefore, the usage of MonoQ anion exchange chromatography did not allow the purification of the end product, but enable the purification of $HAUb_{75}$ –MESNa (**Figure 16a**) which guaranteed an efficient conversion of the desired probe in the ligation step. Furthermore, in contrast to the previously published methods the HA-Ub_{75} –MESNa thioester was first of all purified to remove MESNa which could undergo a competition reaction with thiol-reactive groups in the further conjugation step. This purified product was then immediately

incubated with previously prepared trap carrying an electrophilic group (**Figure 15a**) to gain the respective ABP of interest by aminolysis of the C-terminal thioester.

After $HAUb_{75}$ –MesNa was purified and ligated to VME, the new generated HAUb-VME was tested by incubation with crude cell lysate (**Figure 16b**). In contrast to previously generated HAUb-VME (**Figure 15c**) the labeling reactivity increased apparently and was represented by additional appearing bands, distributed through all kDa ranges.

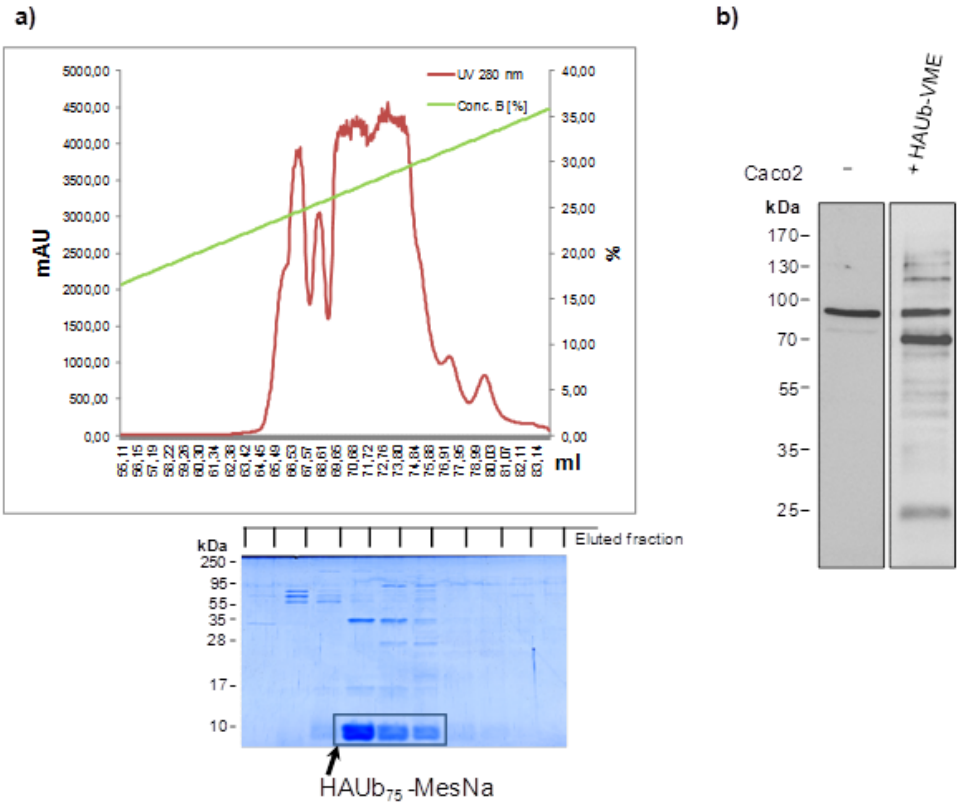

Figure 16. Purification of $HAUb_{75}$ –MesNa, and the reactivity of the consequent generated HAUb-VME. (a) The eluted solution obtained from chititin affinity column was adjusted to a pH 7.5 and loaded onto a anionic exchange column (MonoQ, GE, self packed). The protein was eluted using a gradient from 0 M to 1 M NaCl with a flow rate of 1 ml/min. The obtained fractions (2 mL) were analyzed by SDS-PAGE and coomassie staining. (b) Labeling potency of the generated HAUb-VME. The crude cell lysate (30µg) was incubated for 2h with 1 µlHAUb-VME, reduced with 4x sample buffer, separated on 12% SDS-PAGE and immunobloted using α-HA antibody.

The potency of new modulated active site directed probes (ABPs)

Regarding recent activity based protein profiling (ABPP) studies and their broad application for diverse enzyme classes, the question arises whether it is possible to modulate not only the reactivity of the active site-directed probes but also their selectivity.

In the next step, after the probe synthesis setup was established, the intent was to modulate the probe reactivity based on the well characterized HAUb-VME.

In contrast to previous efforts that tried to maximize the reactivity of the probes to capture as many DUBs as possible, a systematic approach to modulate the reactivity was set up, followed by an additional focus on improving the development of selective probes.

The previously introduced HAUb –VME, as gold standard in terms of high reactive probe, is an approved ABP in discovery of DUBs[128,131] and was therefore used as a reference in this study. To address the dependency of the reactivity on steric hindrance and electrophilicity, the HAUb-derived VME probe was first expanded by an ethyl ester group (VEE) and then by an additional methyl group on the electrophilic carbon (MVEE) of the α,β-unsaturated system (**Figure 17**).

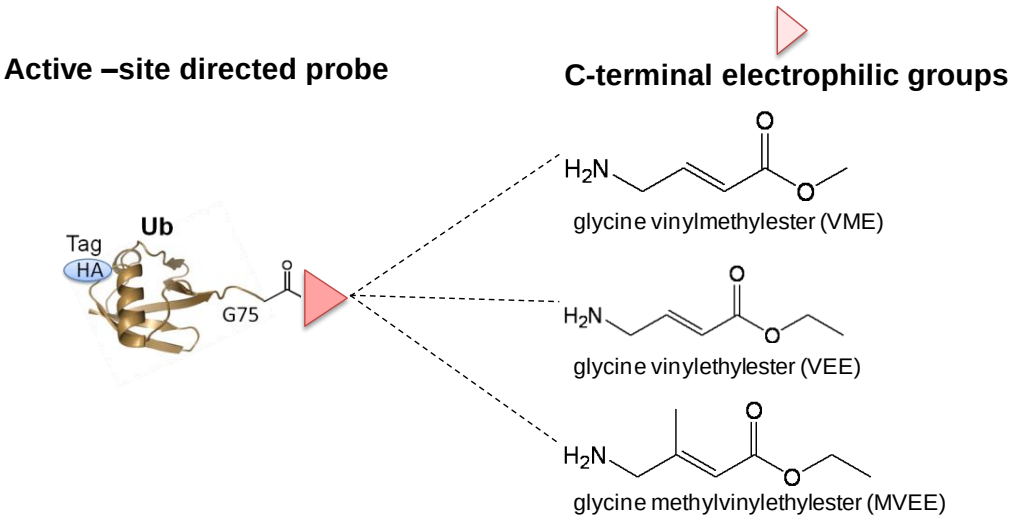

Figure 17. Newly generated HAUb derived probes with distinct C-terminal chemical groups.
Epitope-tagged Ub (HA-Ub) derived probes with different C-terminal reactive groups generated by intein based chemical ligation.

In order to compare the reactivity and selectivity of the newly developed probe panel, all three probes were incubated for 1.5 h with mammalian cell lysates derived from Caco2 cells. Covalently modified enzymes (DUBs) were then detected by immunobloting using anti-HA antibodies, following protein separation by SDS-PAGE.
The immunoblot showed comparable clustering of bands from 100 to 140 kDa upwards and is consistent with reports [128] about profiling with Michael acceptor containing probes. In contrast to clustering, the reactivity/intensity was negatively affected and diminished stepwise VME>VEE>MVEE (**Figure 18a**).
To proof whether this stepwise reactivity diminishing effect was cell line dependent, the ABPs were incubated with the well reported EL4 mouse lymphoma cell lysate[73].

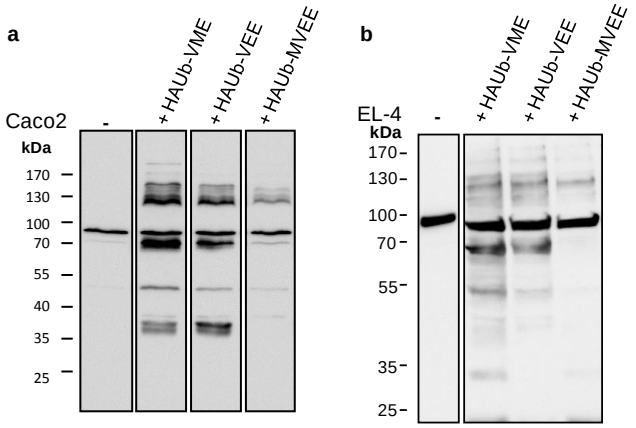

Figure 18. Distinct activity based protein profiling (ABPP) profiles obtained for total cellular extracts treated with HAUb-VME, HAUb-VEE or HAUb-VEE. Caco2 and EL4 cell lysates (30 µg) were incubated with 13µl or 10µl respectively of HAUb HAUb-VME, HAUb-VEE and HAUb-MVEE. The modified enzymes were separated by 4-12% reducing gradient SDS-PAGE and visualized by α-HA immunoblotting.

Remarkable was the reproducible stepwise diminished reactivity even after 2h incubation with a different cell line lysate (**Figure 18b**).
Comparing the ABPs among themselves, immunoblots indicated similar but not identical reactivities of HAUb-VEE and HAUb-MVEE. Therefore, the question came up, whether HAUb-VEE and HAUb-MVEE have the potency to label specific subgroups of DUBs.
In order to validate the stepwise diminished reactivity and to proof which subgroup of DUBs was exclusively labeled by HAUb-VEE or HAUb-MVEE, mass spectrometry

analyses were used. Therefore, the probes were incubated with total cell lysate (EL-4) as described above, followed by an anti-HA immunoprocipitation overnight. Subsequently, the DUB/probe complexes were eluted and subjected to SDS-PAGE. Appropriate gel lanes were excised, trypsin digested to generate tryptic-peptides, followed by identification of corresponding proteins (DUBs) via LC-MS/MS mass spectrometry.

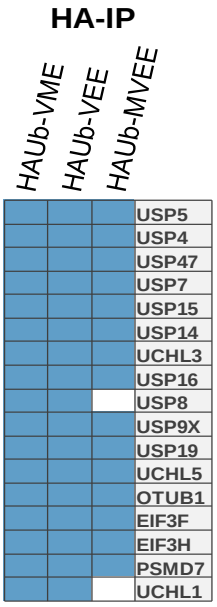

Figure 19. Qualiitative analysis of identified DUBs by applying activity based protein profiling (ABPP). The selective binding of DUBs was investigated by incubating HAUb-VME, HAUb-VEE or HAUb-MVEE with crude El-4 cell lysate. After overnight incubation of HA-tagged probes (40µl) with EL-4 cell lysate (3.4 mg/ml) followed by α- HA immunoprecipitation, the eluted proteins were separated by SDS-PAGE and Coomassie stained. Gel-lanes were excised, trypsin digested and analyzed by LC-MS/MS.

The immunoprecipitation and mass spectrometry analysis led to the isolation and identification of 17 known DUBs, whereas USP8 and UCHL1 were not labeled by HAUb-MVEE. Qualitatively, the mass spectrometric analyses revealed that all three probes bind basically the same DUBs and did not address specific subgroups as observed in immunoblotting analyses above. Moreover, the inspection of raw data indicated a slightl variation of applied probes amount (discussed in chapter 5.1). Therefore, in order to gain quantitative side by side analysis of probes, it was obviously that there was a need to declare the final probe concentration and purity.

To address this issue, the end product should be purified after the ligation step. The challenge was the small polarity and minor mass difference of the end product in comparison to the rest of components present in the ligation mixture.

Therefore, different columns and conditions were tested to purify the final product (e.g. HAUB-VME from HAUb / $HAUb_{75}$ –MesNa / HAUB-VME). The self packed CIEX column MonoS 5/50 showed the best performance. After the column conditions were optimized, the purification of the end product showed clearly two separated peaks representatively shown for HAUb-VME in **Figure 20a**. Thus, by using MonoS column the tighter elution peaks indicated the right composition of column material, column length, and the right conditions.

Usually, the chromatographic fractions are analyzed by applying SDS-PAGE, followed by Coomassie staining to validate the presence of the molecular weight of the expected product. This analysis procedure of the fractions is broadly applied by structural biologists, which is relatively fast and gives an approximate indication of the purity. The fractions containing the product of interest are thus identified and pooled afterwards. However, small differences of about 100 Da, which is the case for $HAUb_{75}$ -MESNa *vs.* ABP (e.g. HAUb-VME), can be not distinguished properly by observing a gel shift on SDS-PAGE. To circumvent this issue in this study, the eluted fraction analysis was carried out much faster and with more accuracy by applying the available mass spectrometry equipment (MALDI-TOF) instead. An example of the fraction analysis using mass spectrometry is provided in the supplementary data section (10.7).

As a consequence, all previously generated probes (HAUb-VME, HAUb-VEE, HAUb-MVEE) were purified according the established protocol, determined their appropriate concentration and were tested for their reactivity. Interestingly, the reactivity of all probes was slightly increased but the diminishing reactivity profile pattern (as observed before) did not change (**Figure 20b**).

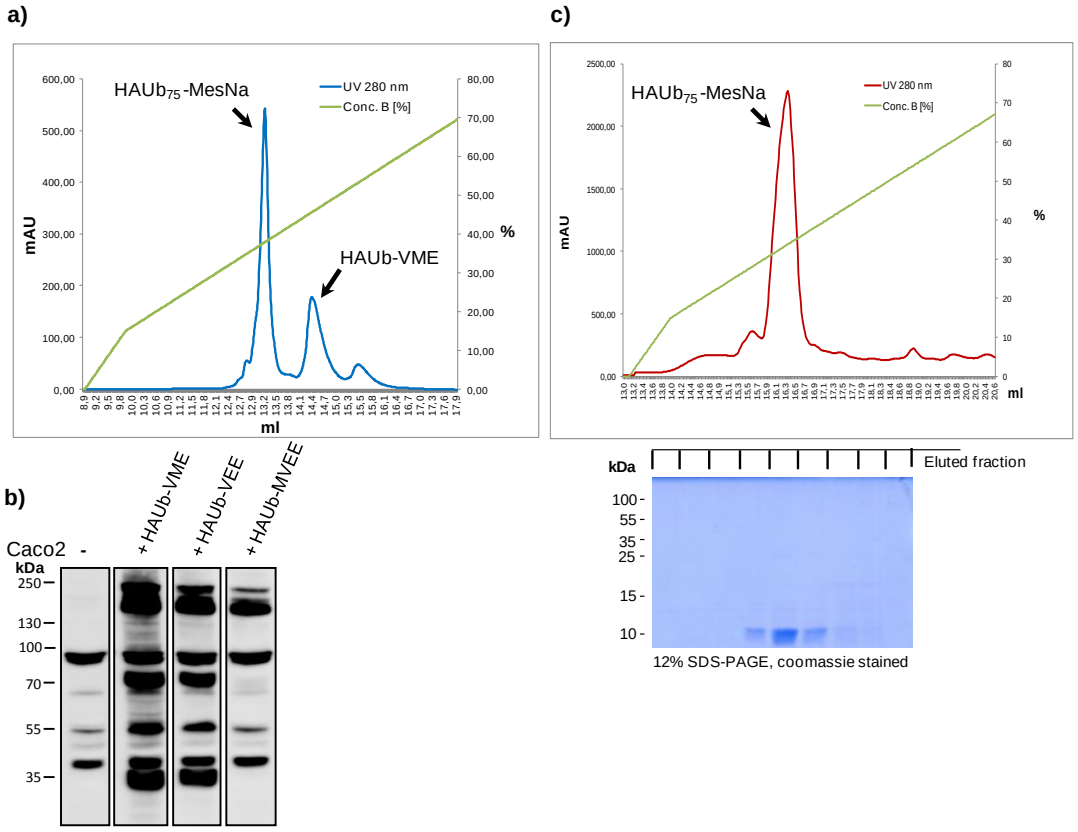

Figure 20. Purification of $HAUb_{75}$ –MesNa and HAUb-VME and the labeling potency of purified HAUb-VME, HAUb-VEE and HAUb-MVEE.

(a) Purification of HAUb-VME by applying CIEX chromatography (MonoS 5/50) after intein-based ligation, with a linear gradient from 0% to 80% buffer B, buffer A (50 mM NaOAc -pH 4.5), buffer B (50 mM NaOAc, 0.5 M NaCl –pH 4.5). (b) HAUb derived probes label distinct sets of proteins in Caco2 lysate and show distinct activity-based protein profiles. The purificated HAUb-VME derivatives (1 µM) were incubated for 2 h with 30 µg Caco2 crude cell lysate, resolved on 4-12 % gradient SDS-PAGE and visualized via α-HA immunobloting. (c) Purification of $HAUb_{75}$ -MESNa by CIEX chromatography (MonoS 10/10) after chitin on-column cleavage induced by MESNa. The separation was performed by a linear gradient from 0% to 90% buffer B, buffer A (50 mM NaOAc -pH 4.5), buffer B (50 mM NaOAc, 0.5 M NaCl –pH 4.5). The absorption at 280nm is shown in blue, the gradient of solvent B [%] is depicted in green.

Additionally, the purification of $HAUb_{75}$ –MESNa by MonoS –CIEX chromatography, showed in contrast to MonoQ purification a significant incease in purity. In comparison to Fig. 16, the UV280 nm absorption peak was tighter and the Coomassie stained SDS-PAGE presented less background (**Figure 20c**). It was then supposed, that the usage of pure $HAUb_{75}$ –MesNa would additionally increase the ligation efficiency.

Therefore, the purification of $HAUb_{75}$ –MesNa using MonoS was inserted into the final probe-generation-workflow.

To summarize, the probe generation starting from the “simple” workflow (**Figure 15**), was improved by adding two further purification steps, including direct MALD-TOF MS monitoring of eluted fractions (**Figure 21**). Applying MALD-TOF MS analyses instead of Coomassie stained SDS-PAGE, allowed even to distinguish between $HAUb_{75}$ –MesNa vs. HAUb-VME and thus the pooling of appropriate fractions.

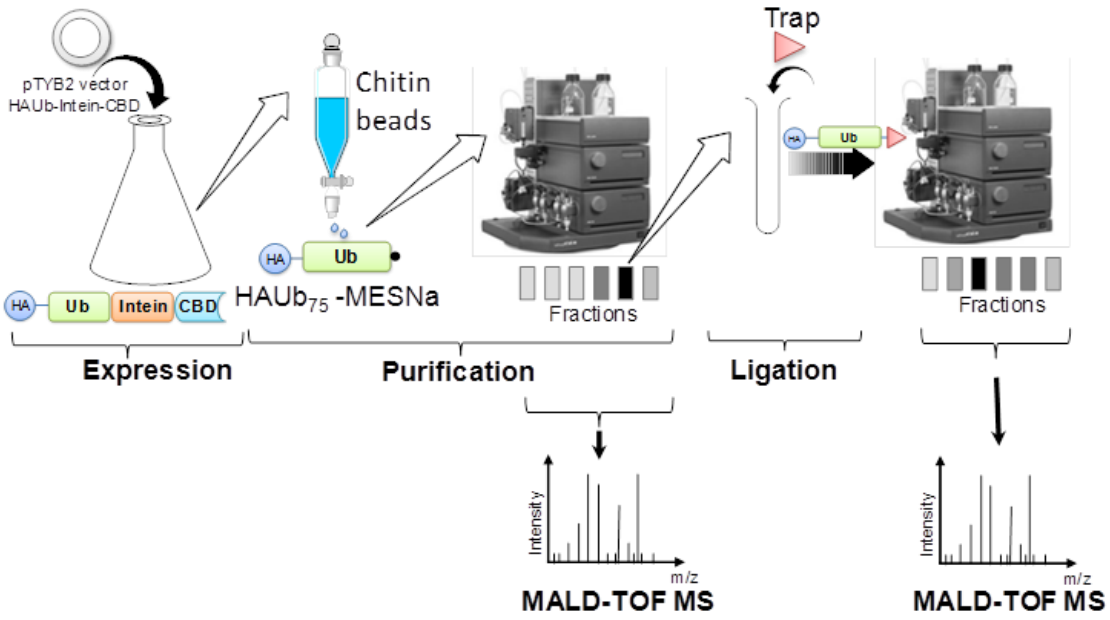

Figure 21. Optimized ABP synthesis workflow.

Major synthesis steps for generation of activity based probes: Step 1, expression of a fusion protein with an intein and a chitin binding domain (CBD). Step 2, the fusion protein binds to a chitin affinity column. The HAUb was released from the column by on column cleavage induced by MESNa. and resulted in $HAUb_{75}$ –MESNa chemical ligation capable product. Step 3, The $HAUb_{75}$ –MESNa was purified using MonoS 10/10 CIEX chromatography. Eluted fractions were analyzed by MALDI MS and pooled appropriately. Step4, subjecting of purified $HAUb_{75}$ –MESNa to chemical ligation, whereby the MESNa group is replaced by desired C-terminal reactive group (trap). Step 5, the end product (probe) was purified. Eluted fractions were analyzed by MALDI MS and pooled appropriately. After determining the concentration, the desired probes were stored at -80°C.

4.1.3 Improving chemical ligation by varying the catalyst

The classical intein chemical ligation was carried out whereas a synthetic peptide or protein carrying the C-terminal alpha thioestergroup was mixed with peptide or protein containing an N-terminal cysteine residue. This intermixture ensures the highly efficient and chemo selective intermolecular reaction to build the thioester connected product. The thioester rearranges to the native peptide bond by an S->N acyl transfer. In the present study, this traditional intein chemical ligation was modified by using a N-nucleophile instead of the S-nucleophile (cystein residue) as described above. This kind of ligation can only be enabled by introducing a N-hydroxysuccinimide (NHS) (**Figure 22a**) catalysis, which converts a thioester to an amine-reactive NHS ester. This intermediate then has the ability to react with an N-nucleophile to form a stable amide bond (**Figure 22b**).

Importantly, contrary to all previously reported intein-based ligations, the ligation method used in this study was improved by subjecting N-hydroxysulfosuccinimide (Sulfo-NHS) (**Figure 22a**) instead of NHS. Sulfo-NHS was much more soluble in an aqueous solution and thus more efficient in generating the necessary amine-reactive Sulfo-NHS esters.

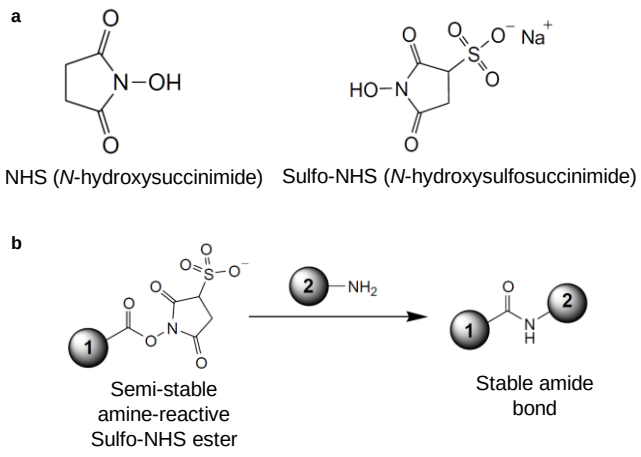

Figure 22.. Structures of NHS and Sulfo-NHS, including the reaction of amine-reactive Sulfo-NHS ester and amine on molecule. **a**) Structures of NHS and Sulfo-NHS chemical modification reagents. **b**) Semi stable amine reactive Sulfo-NHS ester intermediate #1 react with an amine on molecule #2, yielding a conjugate of the two molecules joined by a stable amide bond (modified from Thermo Scientific Pierce, www.piercenet.com).

4.1.4 Extension of probe repertoire by high reactive probes

Beside the modulation of steric hindrance, the second attempt intended to increase the reactivity due to altered electrophilicity by replacing the methyl ester (VME).
The free carboxy group of the new VA warhead (**Figure 23**) enabled the introduction of fluoro-ethyl substituents. Thereby the preparation of the vinyl monofluoroethyl amide (VFEA) and vinyl trifluoroethyl amide (VF_3EA) probes was accomplished.

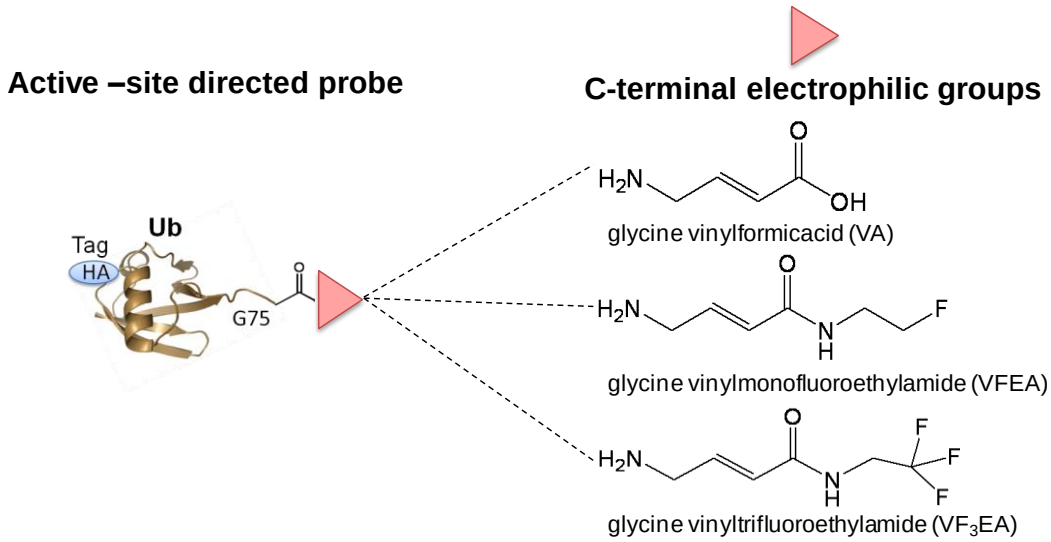

Figure 23. Newly generated highly reactive HAUb derived activity based probes containing distinct C-terminal chemical groups. Epitope-tagged Ub (HA-Ub) ligated with different C-terminal reactive groups generated via intein based chemical ligation.

To examine the reactivity of all five newly developed HAUb-derived probes towards DUBs, the whole set was subjected to the recombinant deubiquitinating enzyme UCHL-3 (**Figure 24**). The successful labeling of UCH L-3 is demonstrated by a ~ 10.5 kDa shift, and represents the covalent binding of the respective probe to the DUB *in vitro*. The activity-based DUB shift assay showed distinct labeling profiles. The higher reactivity of the HAUb-Monofluoroethyl amide probe compared to HAUb-VME as indicated before, is also demonstrated in this assay.

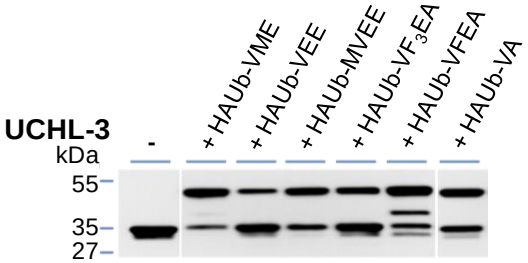

Figure 24. The potency of newly generated ABPs to bind covalently DUBs.
Activity profiling assay shows the reactivity of the synthesized HAUb derived active site-directed probes with recombinant HIS_6-taged DUB UCH-L3. Recombinant DUB (1µM) was incubated with the indicated probe (1µM) at 37°C for 2 h and immunoblotted with anti-HIS_6 antibody. Probe reactivity was investigated by UCH-L3 shift formed by probe / enzyme adducts.

In order to compare the selectivity of the newly generated probe panel, all probes were subjected to a crude cell lysate. For this purposes the well characterized EL4 mouse lymphoma cell lysate was incubated with the ABPs and modified enzymes were visualized by anti-HA immunoblotting (**Figure 25**).

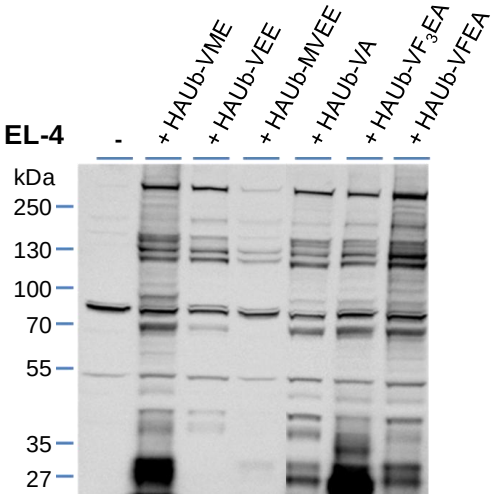

Figure 25. Distinct activity-based DUB labeling profiles by using newly generated ABPs. The probes containing various C-terminal electrophilic groups present distinct activity labeling profiles. Lymphoma EL-4 cell lysate (30µg) was incubated with appropriate probes (1µM), separated by 4-12 % gradient SDS-PAGE, and immunoblotted with the anti-HA monoclonal antibody. HAUb-VME with known broad selectivity spectrum for diverse DUBs, was used as a comparison.

In terms of additional bands and higher reactivity, the HAUb- derived Monofluoro probe (HAUb-VFEA) shows indeed a higher labeling efficiency compared to HAUb-VME (**Figure 25**). In contrast, the trifluoro substituted probe shows less reactivity towards DUBs. The main difference could be a stronger electron withdrawing effect

from three versus one fluorine atom which could influence the coordination into the active-site or the stabilization of the probe itself.

In conclusion, a variation of the substituents of the Michael acceptor demonstrates that it is possible to fine tune the reactivity of ABPs. Concerning the reactivity, only a stepwise diminishing reactivity, without formation of new bands (**Figure 20**, **Figure 25**) were observed, which most likely indicates a lack of selectivity.

However, whether the high reactivity observed for HAUB-VFEA also corresponds to increased DUB labeling, was initially unclear and is a subject to investigations in the next chapter.

Using the improved synthesis and purification protocol from this study, it was now possible to design and synthesize a set of five new ABPs (HAUb-VEE, HAUb-MVEE, HAUb-VA, HAUb-VFEA and HAUb-VF_3EA) and one reference probe (HAUb-VME). These six Michael acceptor containing probes should all react at the position corresponding to the C-terminal carbonyl group G76 of ubiquitin, respective of the specific position where ubiquitination or deubiquitination occur. Each HAUb-derived active site-directed probe was characterized using nanospray time-of-flight mass spectrometry (Q-TOF 2 TM, Micromass) by direct injection.

A representative ESI-MS measurement of ABP products is shown for HAUb-VFEA (**Figure 26**), which represents the observed mass in agreement with the theoretical mass. The variation of the theoretical and the observed (measured) mass of only 55 ppm is an indication for an accurate measurement and successful ligation. The high peak intensity and the low background noise indicate the relatively high purity of the probe.

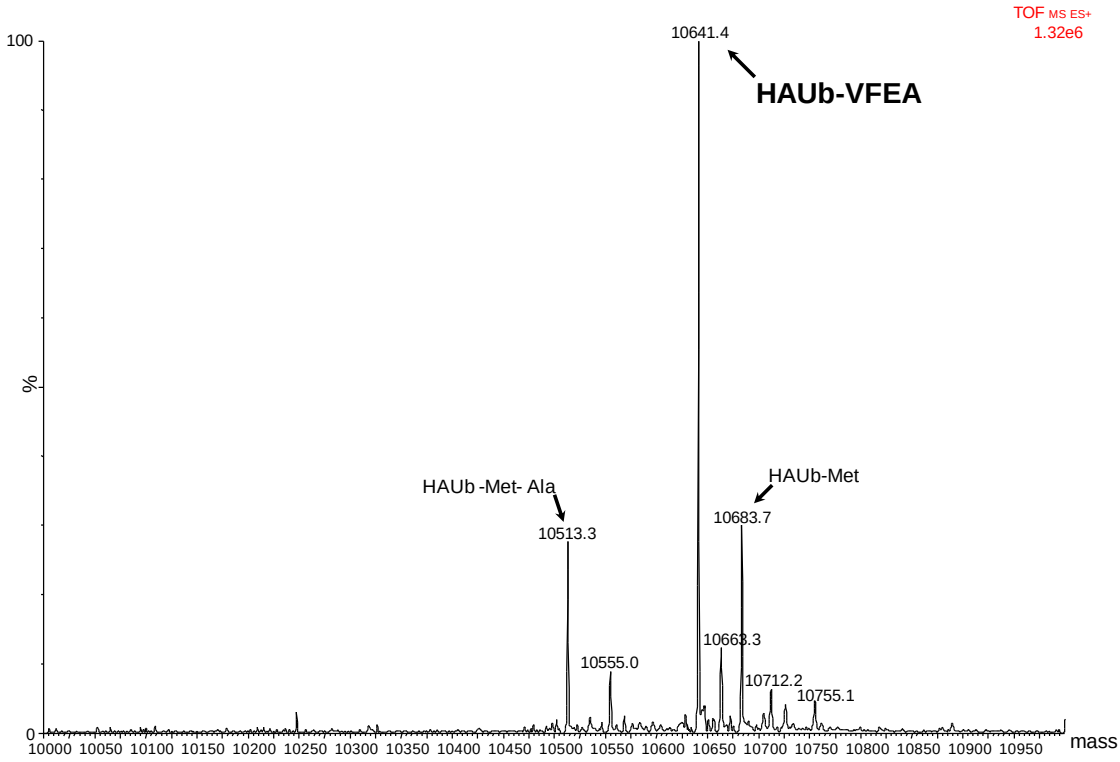

Figure 26. ESI-MS (Q-TOF) spectra of the ligation product HAUb-VFEA.
The deconvoluted mass spectrum of the intein-based ligation product showed a mass that corresponds to the expected HAUb-VFEA product (theoretical $[M+H]^+$= 10641.98, observed $[M+H]^+$ = 10641.40).

The theoretical and observed masses for all generated probes are listed below. The calculated masses were derived from the composition of theoretical mass of HAUb (10716.18 Da), the desired C-terminal electrophilic group (**Figure 17, Figure 23**), minus the eliminated water molecule which occur during the liagation step.

Synthesized active site directed probes:

HAUb-VME - **ESI-MS** (*m/z*): $[M+H]^+$ calc.: 10610.95; found, 10610.42

HAUb-VEE - **ESI-MS** (*m/z*): $[M+H]^+$ calc.: 10624.97; found, 10624.20

HAUb-MVEE - **ESI-MS** (*m/z*): $[M+H]^+$ calc.: 10638.98; found, 10638.10

HAUb-VA - **ESI-MS** (*m/z*): $[M+H]^+$ calc.: 10596.94 ; found, 10596.42

HAUb-VFEA - **ESI-MS** (*m/z*): $[M+H]^+$ calc.: 10641.98; found, 10641.40

HAUb-VF3EA - **ESI-MS** (*m/z*): $[M+H]^+$ calc.: 10677.96; found, 10677.10

4.2 Distribution of active DUBs in selected cell lines

4.2.1 DUB profiling using new active site directed probe HAUb-VFEA

Chemical probes are able to report the distinct activity of enzymes, rather than merely their expression levels, which defines their functional roles in cell physiology. This ability to label enzyme active sites can in some cases even be carried out in vivo[132,133] and provides high-content proteomic information. One of these approaches using chemical probes applies this methodology to covalently label enzyme active sites and is termed activity-based protein profiling (ABPP)[134].

In order to evaluate whether the newly developed HAUb-VFEA probe has the ability to label a broad spectrum of DUBs, it was therefore applied in an ABPP approach to analyze the entirety of available DUBs in four different cell lines.

The experiment described below (using HAUb-VFEA) to address above question were performed together with master student Anne Kummer under my supervision.

Due to the good characterization and wide applicability in the research field the following four cell lines (in addition to EL-4) were used to examine HAUb-VFEA in the ABPP approach: HeLa S3, MCF-7, A549 and Jurkat E6-1.

The cells were grown to 90-100% confluence, harvested and immediately lysed. Each cell lysate (9 mg/ml) was incubated with the newly developed ABP – HAUb-VFEA (0.8 µg) and the covalently bound DUBs were pulled down by anti HA-Immunoprecipitation. The eluted proteins were trypsinized on beads, purified via reversed phase HPLC and analyzed by LTQ-Orbitrap LC-MS/MS. The protein identification was carried out by MASCOT database search and the assigned spectra evaluated via Scaffold 3.0 (Proteome Software, US). The same workflow without HAUb-VFEA was used as a negative control. The experiment was performed in two biological replicates and the merged data were used for further Scaffold evaluation. Protein detections were accepted if they could be established at peptide probability or more than 95,0% and the protein identifications were accepted if they could be established at a probability

of 50,0% or more and contained at least 1 identified peptide

The activity-based protein profiling with HAUb-VFEA achieved a total number of 67 identified DUBs (**Figure 27**) including members from all five subclasses, which corresponds to a total coverage of 69% of all annotated DUBs.

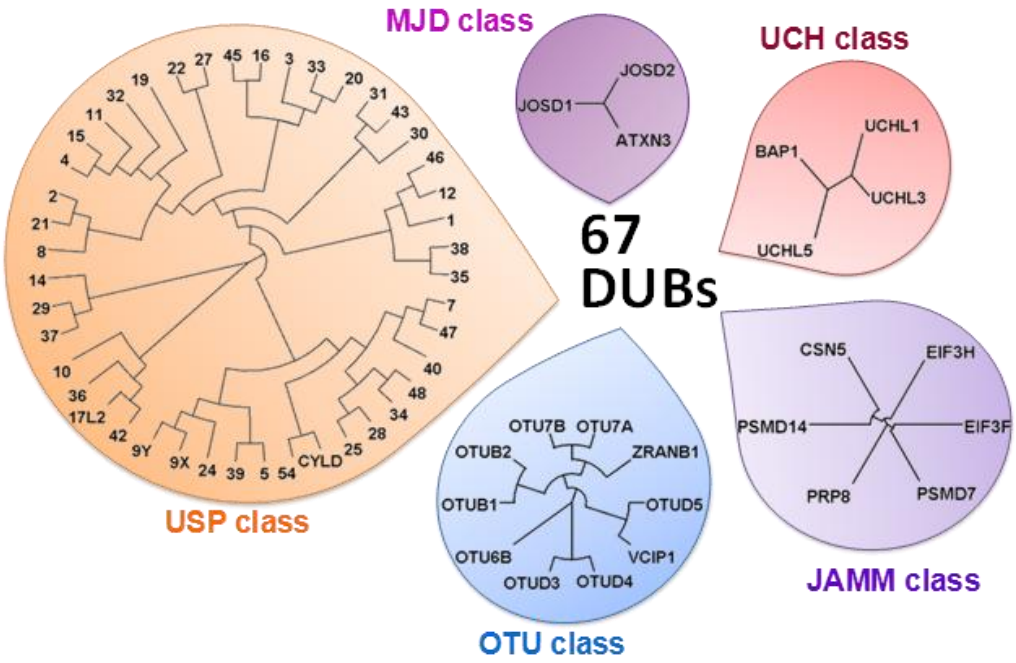

Figure 27. Identified DUBs from anti-HA immuno-precipitation using the HAUb-VFEA probe and their distribution to the corresponding sub-classes. The DUB sequences were aligned with the ClustalW2[135] algorithm and visualized by generation of guided trees using Dendroscope 3.0[136].

Interestingly, also metalloproteases from the JAMM class which contain a Zn^{2+} dependent active site composition could also be detected. However, whether their identification is based directly on covalent binding to HAUb-VFEA or through involved complexes remains to be clarified in detail. Comparing the modified DUBs among the five cell lines, the amount and distribution of detected DUBs seems to be rather similar (**Figure 28**) with the exceptions of the HeLa S3 cell line that in comparison expressed relatively more DUBs of the OTU subclass. Taking the activity based probing into account, 47 active DUBs were identified in A549, 42 in EL-4, 53 in HeLa S3, 56 in Jurkat and 51 in MCF-7. However, in consideration of the activity based

profiling, the detected DUB distribution among the cell lines may either be due to enzyme activity or abundance.

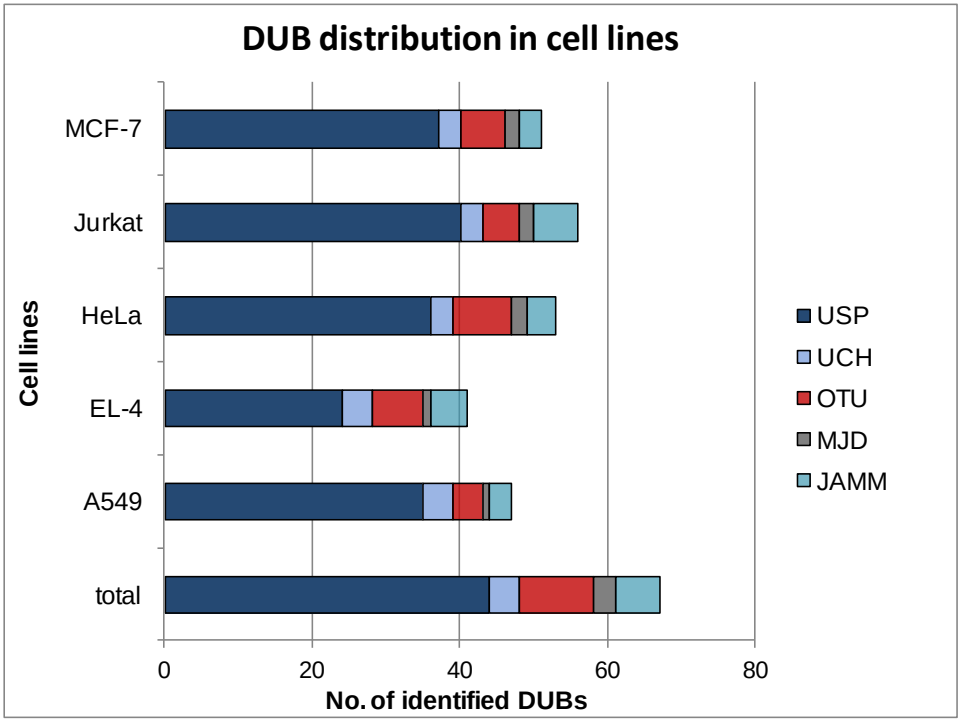

Figure 28. Count of identified DUBs and their distribution among four cell lines. DUBs were detected by applying HAUb-VFEA in the ABPP approach and their corresponding distribution in different cell lines is depicted.

To examine the distribution of DUBs in these cell lines semi-quantitatively, the LTQ LC-MS/MS unique spectra were evaluated with Proteome Software Scaffold 3.0, normalized by their molecular masses, clustered with Cluster 3.0[137], and visualized by Java TreeView[138]. Thus, the DUBs with their respective MS spectral counts are shown as resulted heat maps (**Figure 29**).

The cell lines display an overall similar DUB distribution, but also distinct DUB subsets were detected. This is illustrated for instance by UCHL3, UCHL5, USP4,USP5, USP7, USP8, USP14, USP15,USP19, USP46, USP47, OTU6B and OTU7B that differ in their quantitative occurrence but were identified in all cell lines. Other candidates like, USP21, USP29, USP39, USP45, USP54, OTUD3 OTUD5, were found only in one cell line. On the other hand, DUBs including OTUB1, OTUB2,

UCHL1, USP1, USP3, USP22, USP35,USP38, USP17L2, CYLD and VCIP135 show high intensity in certain cell lines only. Beyond the distinct DUB intensities the representation by the heat map also revealed subgroups patterns within the cell lines. The upper part of the heat map of the USP class seems to represent DUBs with high abundance or activity whereas the lower part of the USP class, containing the majority of members, displays more specific allocation (**Figure 29**).

Furthermore, DUBs like CYLD, USP38, USP20, USP30 show remarkable similar patterns intensity of among all cell lines.

DUBs like OTU7B and OTU6B from the second largest OTU subclass exhibit high intensity which corresponds either to high abundance or to high activity in the positive cell lines. Interestingly in this class, HeLa S3 cells contain the most detected OTU and two exclusive members but at the same time lacks OTUB2.

Concerning the remaining DUB subclasses UCH and MJD, distinct distribution patterns were also detected. Also worth mentioning is the detection of all known UCH class members, of which UCHL3, UCHL5 and BAP1 seems to be highly active, whereas UCHL1 occurs exclusive only in EL-4 and A549 cell line. Furthermore, the MJD subclass is covered by the highly intense Ataxin3 among all cell lines and contain by narrowly distributed JOSD1 and JOSD2.

Although matalloproteases execute a non Cys triggered catalytical mechanism, six DUBs could be identified. However, comparing the DUB intensities from the JAMM class with other DUB classes it is noticeable that these are considerably weaker.

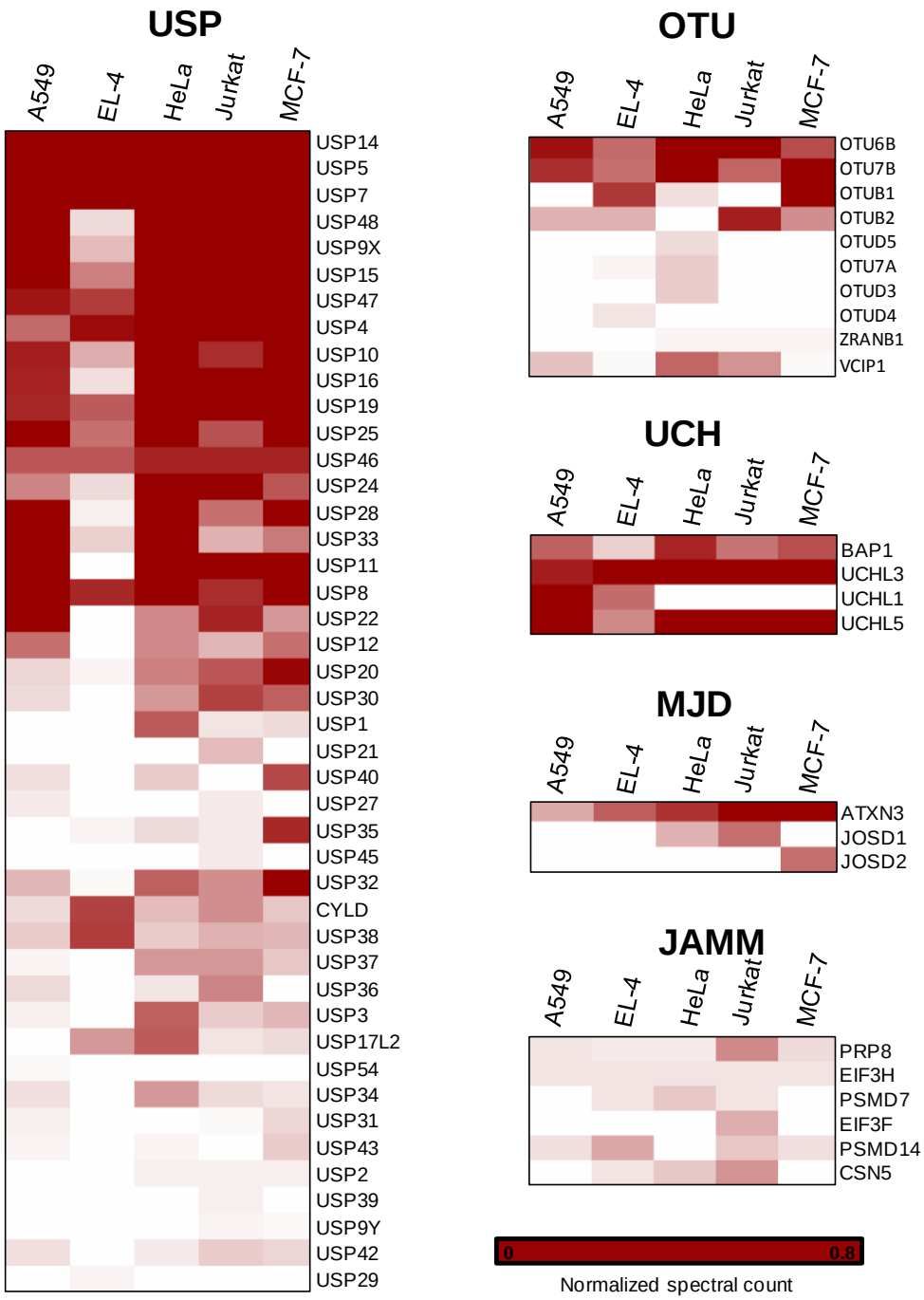

Figure 29. DUBs identification and semi-quantitative analysis in different cell lines by ABPP.

After 5h incubation of HA-tagged HAUB-VFEA with appropriate cell lysate (9 mg/ml) followed by α- HA immunoprecipitation, the proteins were digested directly on beads LC-MS/MS. MS spectral counts corresponding to unique peptides (10.4) identified by LC-MS/MS were normalized according the molecular weight clustered by Cluster 3.0 and visualized as heatmaps by Java TreeView. (V.1.1.6). Ubiquitin-Specific Proteases (USP), Ubiquitin C-terminal Hydrolases (UCH), Machado-Josephin Disease domain containing proteases (MJD), Ovarian Tumor domain containing DUBs (OTU), metalloenzyme domain containing DUBs (JAMM).

To conclude, the ABPP approach using HAUb-VFEA clearly demonstrated the high reactivity of HAUb-VFEA towards DUBs and detected both widely as well as specific distributions of active DUBs in distinct cell lines, whereas the Jurkat cell line contained the highest number of detected DUBs.

4.3 Generation of isopeptide bond mimicking ABPs to cast insights of the specificity and selectivity of DUBs

The molecular mechanism of DUB specificity for different poly-Ubiquitin linkages and substrate proteins are still poorly understood. The previously introduced ABPs attempt to address this issue, but due to their broad and high reactivity do not provide information on the substrate selectivity or linkage specificity of DUBs. While the labeling specificity of probes can be partially tuned, proteases that do display restricted substrate selectivities might escape the generic probe labeling approach.

4.3.1 The concept, design and sought out parameters for novel ABP

Under the consideration that the previously described ABPs were only a poor structural mimetics of substrates which DUBs likely encounter in the cell, it was reasoned that features of the ubiquitinated target protein should be implemented in the probe design to improve the specificity. Therefore, the intent was to develop a new class of ABPs for characterizing the selectivity of DUBs. A novel branched Ubiquitin Isopeptide Activity Based Probe (UIPP) was engineered in order to address the specificity of different DUBs, their detection, enrichment and to gain further insights into deubiquitination machinery (**Figure 30**). Instead of modifying one ubiquitin unit only C-terminally, an approach to generate mimetics of a di-ubiquitin or of any ubiquitinated target protein was established. To achieve such probe specificity, the UIPPs incorporate the isopeptide linkage and the target sequence of the ubiquitinated protein of interest allowing it to achieve the desired probe specificity. The distal ubiquitin unit is expressed as recombinant protein linked via its C-terminus to the ε-amino group of a lysine within a synthesized peptide which mimics the proximal Ub unit. The peptide sequence can in principle also be derived from any ubiquitinated target protein. Previous studies that used Ub-peptide based substrates, demonstrated that a minimal chain length of 8 amino acids is already sufficient to

evoke DUB reactivity[10]. On the other hand the peptide length should not exceed 20 amino acids to avoid proteasomal degradation[139-140]. The peptide design was also based on structural considerations with the aim to mimic the native fold. Thus, those constructs could be promising to capture ubiquitin linkage-specific DUBs.

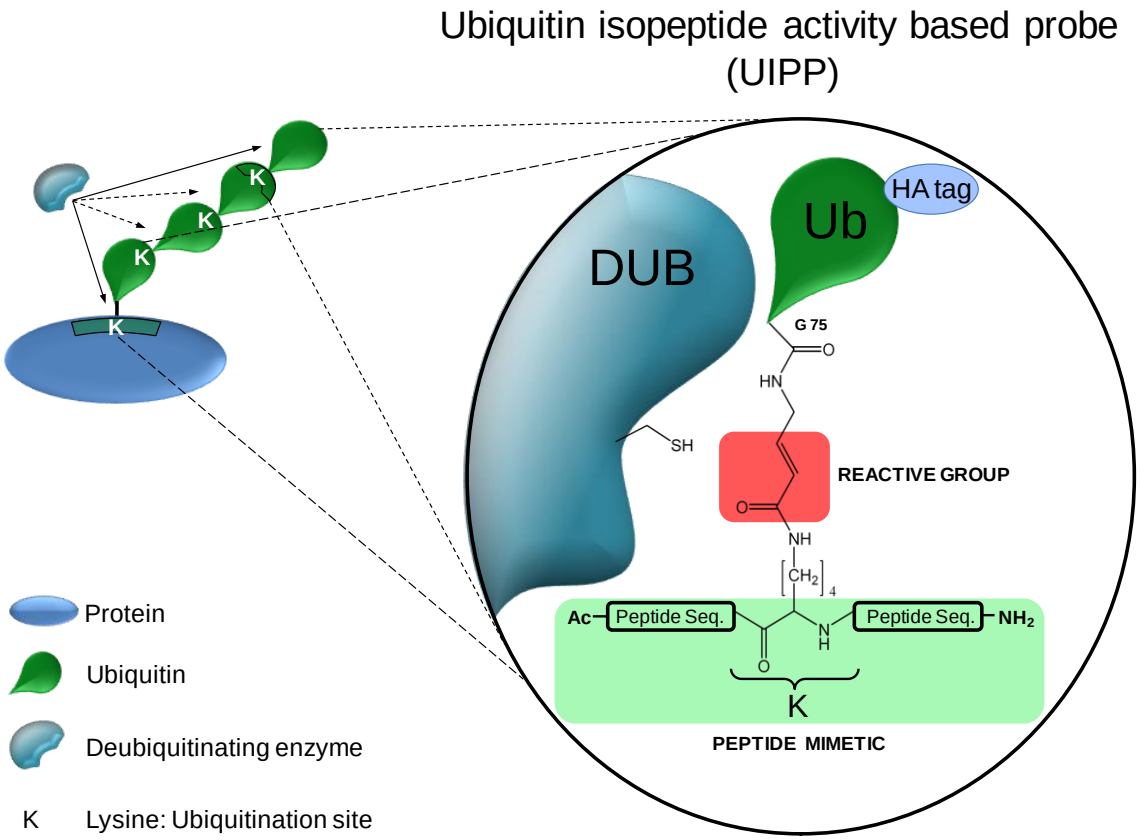

Figure 30. Novel systematically designed ubiquitin isopeptide activity based probes (UIPPs). The innovative UIPP concept mimics the isopeptide bond between two Ub-molecules or Ub-molecule and protein, which is the DUB substrate, and thereby enables the formation of a covalent bond between the particular DUB and its substrate. The property of covalent capture is given by the intrinsic reactivity of the Michael acceptor group, highlighted in red. The specificity was achieved by full length ubiquitin and the chosen peptide sequence, originating from next Ub-unit or the target protein of interest, shaded in green.

The close inspection of ubiquitin sequence in context to ubiquitin-linkages revealed that each of the seven lysine residues in Ub create an unique sequence and

structure, which might be used for specific recognition by DUBs[30] (**Table 7**). Therefore, this insight was used for the rational behind the design of chain specific Ub-isopeptide probes.

Recent biochemical characterizations have revealed the specificity relevance of this C-terminal sequence, showing that the fourth and third amino acid (Arg74 and Gly75) are crucial for ubiquitin recognition by DUBs[141]. This relevance was also validated in the first structure of a DUB with a diubiquitin, which illustrates the Ub-linkage specificity of AMSH-LP due to the specific recognition of the Lys63 sequence context[106]. For the new probe design it was thus reasoned that it is sufficient enough to use a peptide fragment that contains the side-chain-modified lysine residue derived from the proximal Ub unit. To enable the covalent capture of DUBs with particular linkage specificity, the novel UIPPs are equipped with a Michael acceptor group in direct proximity to the isopeptide bond. For the preparation of the UIPPs the previously introduced modified intein-based chemical ligation (3.7) was used.

Table 7. Ubiquitin linkage context for all types of polyubiquitin chains.

Linkage residues	**Ubiquitin (lys) linkage context**	***Accessible nearby residues***
Ub-Lys$_6$	Phe, Val, Lys$_6$, Thr, Leu	His$_{68}$, Thr$_{66}$, Thr$_{12}$
Ub-Lys$_{11}$	Thr, Gly, Lys$_{11}$, Thr, Ile	Thr$_9$
Ub-Lys$_{27}$	Val, Lys$_{27}$, Ala	Glu$_{24}$, Asp$_{52}$
Ub-Lys$_{29}$	Ala, Lys$_{29}$, Ile	Asp$_{32}$, Glu$_{18}$
Ub-Lys$_{33}$	Gln, Asp, Lys$_{33}$, Glu, Gly	Not explicit
Ub-Lys$_{48}$	Phe, Ala, Gly$_{48}$, Lys, Gln, Leu	Ala$_{46}$
Ub-Lys$_{63}$	Asn, Ile, Gln$_{63}$, Lys, Glu	Not explicit

Modified and extended from Urbé *et al.* (2009).

4.3.2 Synthesis of Ubiquitin Isopeptide Activity Based Probe (UIPP)

As one of the new C-terminal ABPs in the “probe-tuning” experiments (4.1.4), glycine vinyl formic acid (VA) was synthesized, which is the key intermediate for the preparation of the UIPPs. VA was used to selectively modify the ε-amino-group of lysine within a peptide which had been synthesized by Fmoc solid phase peptide synthesis. The VA-modified peptide (**Table 8**) was then used in a modified intein-

based chemical ligation to generate the isopeptide bond between the free amino group of the VA modified peptide and the C-terminus of a recombinant HA-Ub_{75}-thioester. The UIPP construct that resulted after chemical ligation carries the Michael acceptor group instead of Gly76, which is bound to the ε-amino group of the lysine within the Ub mimetic peptide (**Figure 31a**). Thus this construct mimics a di-Ub unit while carrying an electrophilic reactive group next to the isopeptide bond for covalent capture of DUBs. To validate the UIPP concept, the well studied K_{48}- and K_{63}-polyubiquitin linkages were selected. Thereby two ubiquitin derived peptide sequences containing a thiol reactive group and a single free amino group (**Table 8**) were subjected to a chemical ligation with $HAUb_{75}$ –MESNa to generate two di-Ub mimicking probes (K48-UIPP: HAUb-Ub_{42-54} –K_{48}(VA) and K63-UIPP: HAUb-Ub_{42-54} –K_{63}(VA)) respectively (**Figure 32**).

Table 8. Properties of the thiol reactive peptide traps used for the synthesis of novel UIPPs.

Isopeptideprobe	**Peptide sequence**	**Mass**
$Ub_{(42-54)}$ –K_{48}(VA) (K48-UIPP)	Ac-RLIFAG-**K_{48}(VA)**-QLEDGR-NH2	1626.936
$Ub_{(54-72)}$ –K_{63} (VA) (K63-UIPP)	Ac-RTLSDYNIQ-**K_{63}(VA)**-ESTLHLVLR-NH2	2410.327

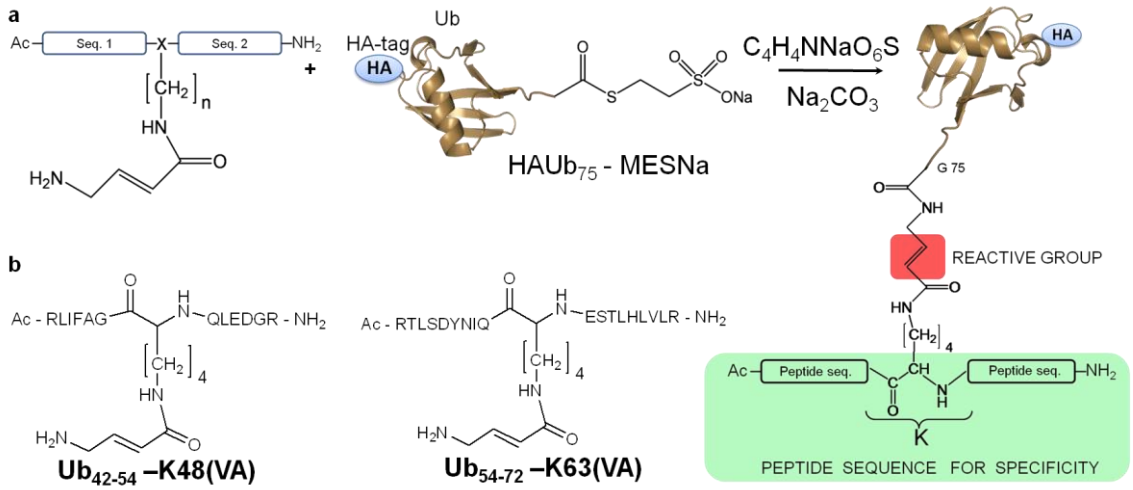

Figure 31. Synthesis of ubiquitin isopeptide activity based probe (UIPP). **a)** The generation of desired UIPPs is achieved by the chemical ligation mechanism from the intein-based ligation approach.. The capability for covalent capture is given by the intrinsic Michael acceptor properties of the substructure highlighted in red. The specificity was achieved by full length ubiquitin and the chosen peptide sequence, originating from next Ub-unit or the target protein of interest, shaded in green. **b)** Ubiquitin originating peptide sequences containing a C- terminal thiol-reactive group, were subjected to a chemical ligation (a) to generate the desired UIPPs which mimic the K_{48} or K_{63} ubiquitin linkage.

All HAUb-derived UIPPs were characterized using nanospray time-of-flight mass spectrometry (Q-TOF 2 ^{TM}, Micromass) via direct injection.

The successful generation of novel K48/K63-UIPP products is illustrated below (**Figure 32**), which represents the observed mass in agreement with the theoretical mass.

The difference between theoretical and observed (measured) mass of 43 ppm for K48–UIPP and 40ppm for K63–UIPP, is an indicative for an accurate measurement and successful ligation, since these values are in the range of the accuracy of the instrument resolution. The high peak intensity and the low background noise indicate the relatively high purity of the probe.

a)

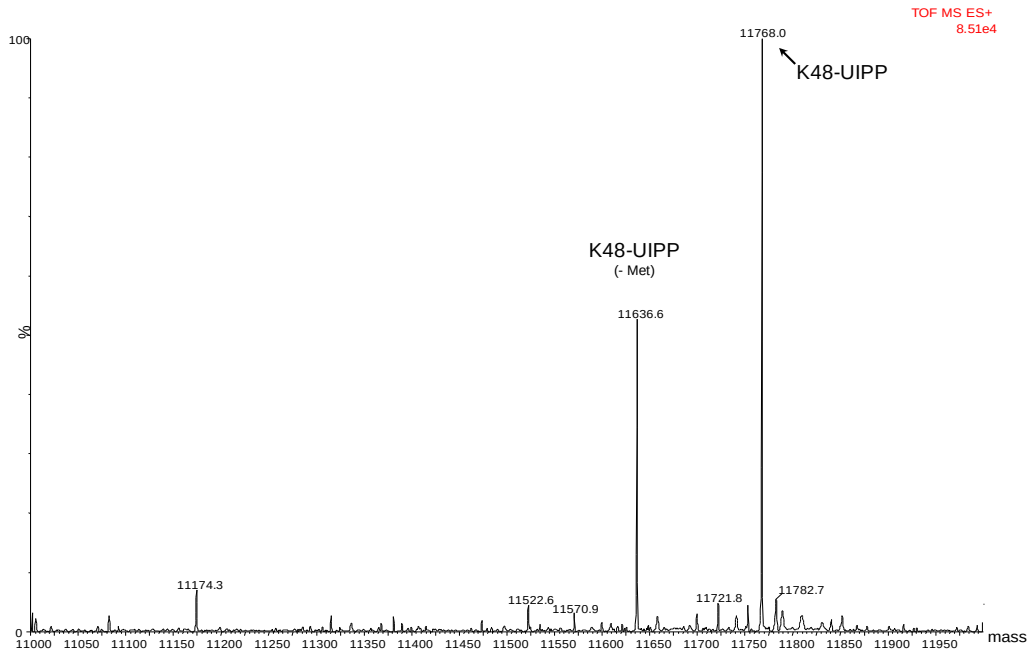

b)

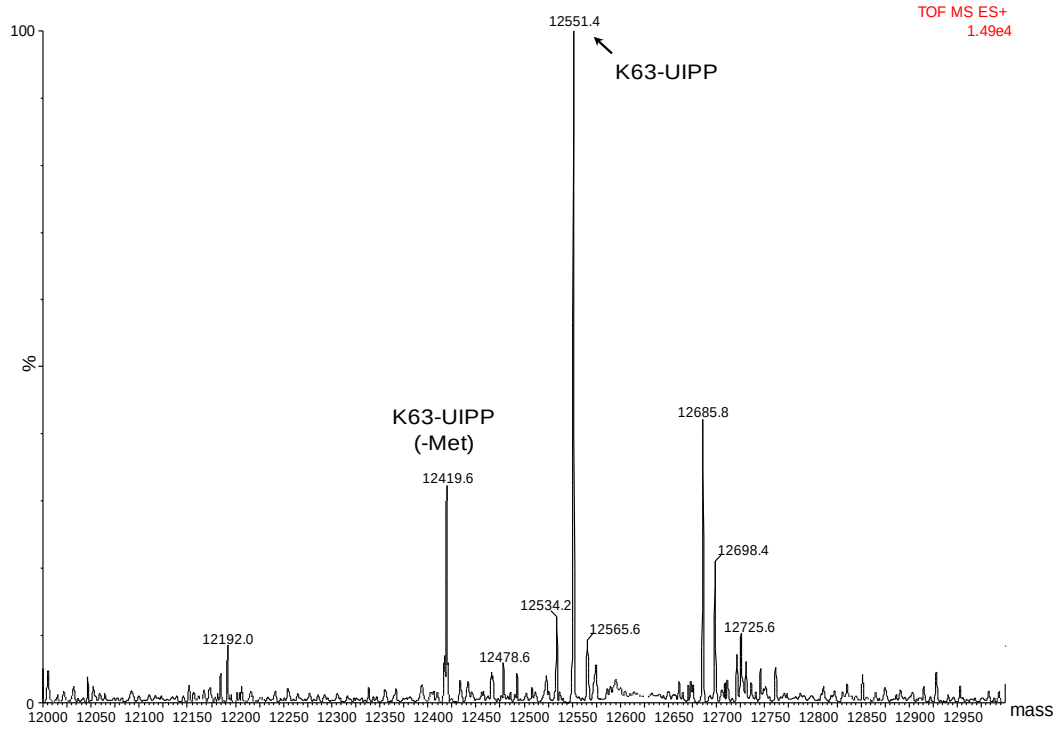

Figure 32. ESI-MS (Q-TOF) spectra of the ligation products K48-UIPP (a) and K63-UIPP(b).

The deconvoluted mass spectrum of the intein-based ligation products showed a mass that corresponds to the expected UIPP products (theoretical K48-UIPP $[M+H]^+$= 11768.5, observed 11768.0, theoretical K63-UIPP $[M+H]^+$= 12551.9, observed 12551.4). The masses 11636.6 and 12419.6 are explained by loss of N-terminal methionine due to the bacterial methionine amino peptidase (MetAP) activity in E.coli.

The theoretical and observed masses are listed below. The calculated masses were derived from the composition of theoretical mass of HAUb (10159.6 Da), the desired C-terminal electrophilic peptide sequence (**Table 8**), minus the eliminated water molecule which occur during the liagation step.

Generated Ubiquitin Isopeptide Activity Based Probes:

HAUb-$Ub_{(42-54)}$ –K_{48}(VA):
ESI-MS (*m/z*): [M+H]+ calc.: 11768.5 ; found, 11768.0
HAUb-$Ub_{(54-72)}$ –K_{63}(VA):
ESI-MS (*m/z*): [M+H]+ calc.: 12551.9 ; found, 12551.4

4.3.3 UIPP reactivity and selectivity

As proof of concept two UIPP probes (**Figure 33a**) were generated and used for a case study to test their selective binding to DUBs with known poly-Ub linkage-specificity. The two UIPPs that were generated and used in the assay were designed to either mimic K_{48}-linked di-Ub (K48-UIPP) or K_{63}-linked di-Ub (K63-UIPP) respectively. Applying these probes in a shift assay, recombinant USP15, which is known to bind both K_{48}- and K_{63}-linked poly Ub chains[104] reacted with both UIPPs, confirming the expected reactivity of both probes. In contrast to USP15, for UCH-L3 it has been suggested that it hydrolyses K_{48}-linked byproducts from proteasomal degradation processes[142] and indeed, recombinant UCH-L3 showed a clear preference for labeling by K48-UIPP. Furthermore, applying the UIPPs and recombinant Ataxin-3 in the shift assay, no reactivity could be observed (**Figure 33b**). These observations show the ability of UIPPs to selectively and covalently label DUBs *in vitro*.

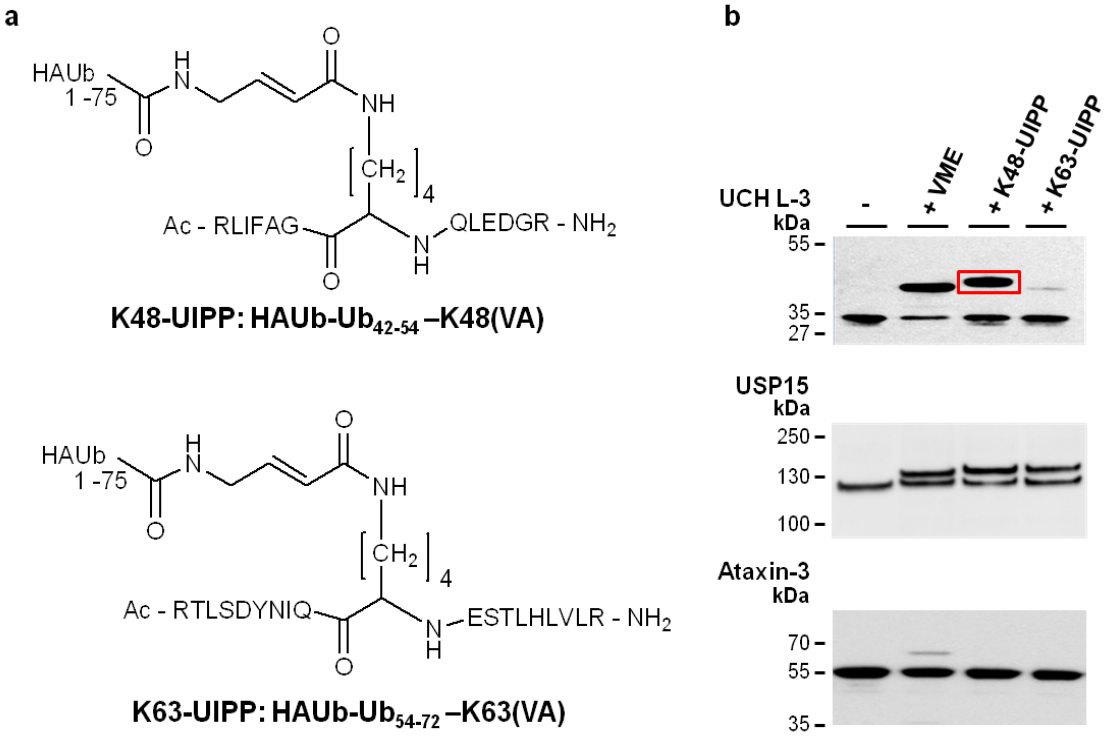

Figure 33. Selectivity of novel isopeptide probes towards recombinant DUBs (UCH-L3, USP15 and Ataxin-3) *in vitro*. (**a**) Chemical structures of the generated K_{48}- and K_{63}-linkage UIPPs.
(**b**) Selectivity of the K_{48}- and K_{63}-UIPPs towards recombinant DUBs. Recombinant HIS_6-tagged UCH-L3, Ataxin3 and USP15 were incubated for 10 min with the UIPPs, separated by 12% SDS-PAGE and immunoblotted with an anti-HIS_6 monoclonal antibody. Probe selectivity was investigated by checking the formation of UCH-L3 /Ataxin3/ USP15 probe-enzyme adducts. The band representing the UCH-

L3-K48-UIPP adduct (outlined in red, was isolated, digested with trypsin and analyzed by MALDI-TOF MS/MS (**Figure 34**).

In order to confirm the ability of the UIPPs to covalently capture DUBs by targeting their active site, a shift assay as shown in **Figure 33** was carried out, followed by Coomassie staining. The up shifted band (outlined in red) was trypsinized and analyzed by MALDI-MS. Besides the fragments corresponding to either UCH L-3 or Ub, the tryptic peptide containing the active site cysteine residue of UCH-L3 covalently bound to the isopeptide probe could also be detected (**Figure 34**).

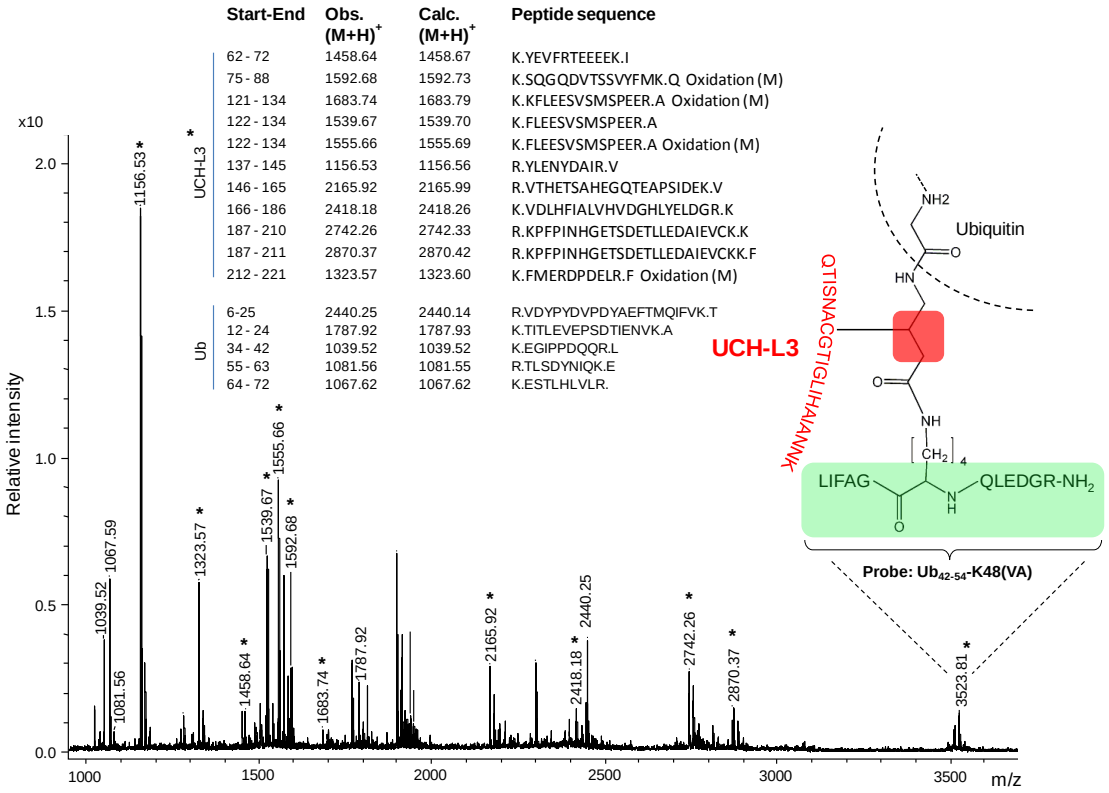

Figure 34. MALDI-TOF MS peptide mapping of the UCH-L3 - Ub_{42-54}-K48(VA) isopeptide probe covalent adduct. Peptides originating from tryptic digestion of the complex of UCH-L3 (*) and ubiquitin (■) isopeptide probe (Fig. 2b) were detected by MALDI-TOF MS using the Mascot (Matrix Science) search engine (Sprot database, 1 missed cleavage, precursor tolerance: 100 ppm). Next to UCH-L3 and Ub derived tryptic peptides, an additional mass peak (m/z 3523.81) was detected corresponding to the fragment of DUB/probe –complex (theoretical mass 3522.87, $[M+H]^+$ = 3523.81,), mapping the covalent adduct to the UCH-L3 derived peptide 89-108 (see inserted scheme).The delta mass can be attributed to that trypsin converts the C-terminal amide on the synthetic peptide (ends on

Arg) to free carboxylate. Additionally, the isopeptide probe was found to be covalently bound to the active site cysteine (Cys^{95}) present in the UCH-L3 derived peptide as confirmed by MS/MS fragmentation analysis (data not shown).

4.3.4 Novel UIPPs in biological applications

In cases where the DUB specificity information is missing, the iso-peptide probe can be used to “fish” a subset of DUBs with distinct specificity. For this purpose, a probe can be incubated with a crude cell lysate, followed by immunoprecipitation, protein digestion and mass spectrometric analysis. As a proof of the profiling capacity, the K48-UIPP and K63-UIPPs were incubated with crude Jurkat cell lysate, separated by SDS-PAGE, and immunoblotted with anti-HA antibody (**Figure 35**). The ABP–HAUb-VME used as a ontrol shows a broad reactivity, whereas both UIPPs display both common and distinct activity profiles, underlining their different linkage specificities.

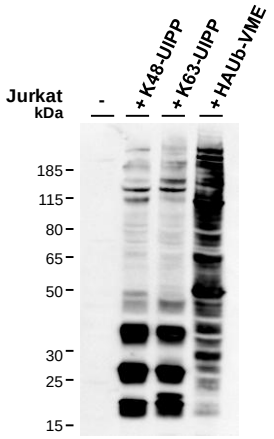

Figure 35. Activity-based profiling using novel UIPPs reveal distinct labeling patterns. Jurkat cell lysates (25 µg) were incubated with the indicated UIPPs, resolved on 4-12% gradient SDS-PAGE, and immunoblotted with anti-HA monoclonal antibody.

DUB identification was achieved using a functional proteomics approach by incubating the UIPP probes with the cell lysate, followed by immunoprecipitation of the covalently bound protein with anti-HA antibody-agarose beads. Precipitated proteins were eluted, seperated by SDS-PAGE and visualized by Coomassie staining (**Figure 36**). Proteins of the K48-UIPP, K63-UIPP and HAUb-VME gel-lanes were trypsinized and the derived peptides analyzed by LTQ-Orbitrap LC-MS/MS. To highlight the specificity differences of UIPPs, corresponding unique spectra were

clustered and visualized using a heatmap (**Figure 36**). The ABPP approach with HAUb-VME revealed 34 identified DUBs in total whereas a subgroup of 22 was captured by the UIPPs in a partially complementary way. Regarding the subgroup, a cluster of preference could be obtained for K48-UIPP as well as for K63-UIPP whereas only 3 (USP28,USP12,USP22) out of 22 DUBs were specifically captured by K48-UIPP. It is important to note that, the distribution of UIPP-DUB labeling specificity is more graded and not exclusively UIPP allocated. However, a good Ub-linkage evidence was observed for USP5, 7, 10, 12, 22, 28 and USP9X which show a strong preference for UIPP-K48, whereas K63-UIPP preferentially labeled USP16, 19, 38 and BAP1.

The data presented here demonstrate that the novel UIPPs are selective labeling reagents for DUBs and can efficiently capture their targets in an activity-dependent manner in crude cell lysates and *in vitro*. Therefore, this novel ABP approach seems to be an ideal tool to study DUBs selectivity towards ubiquitin-linkage specificity not only *in vitro* but also in a more biological environment. Due to its novelty, the UIPP constellation was patent.

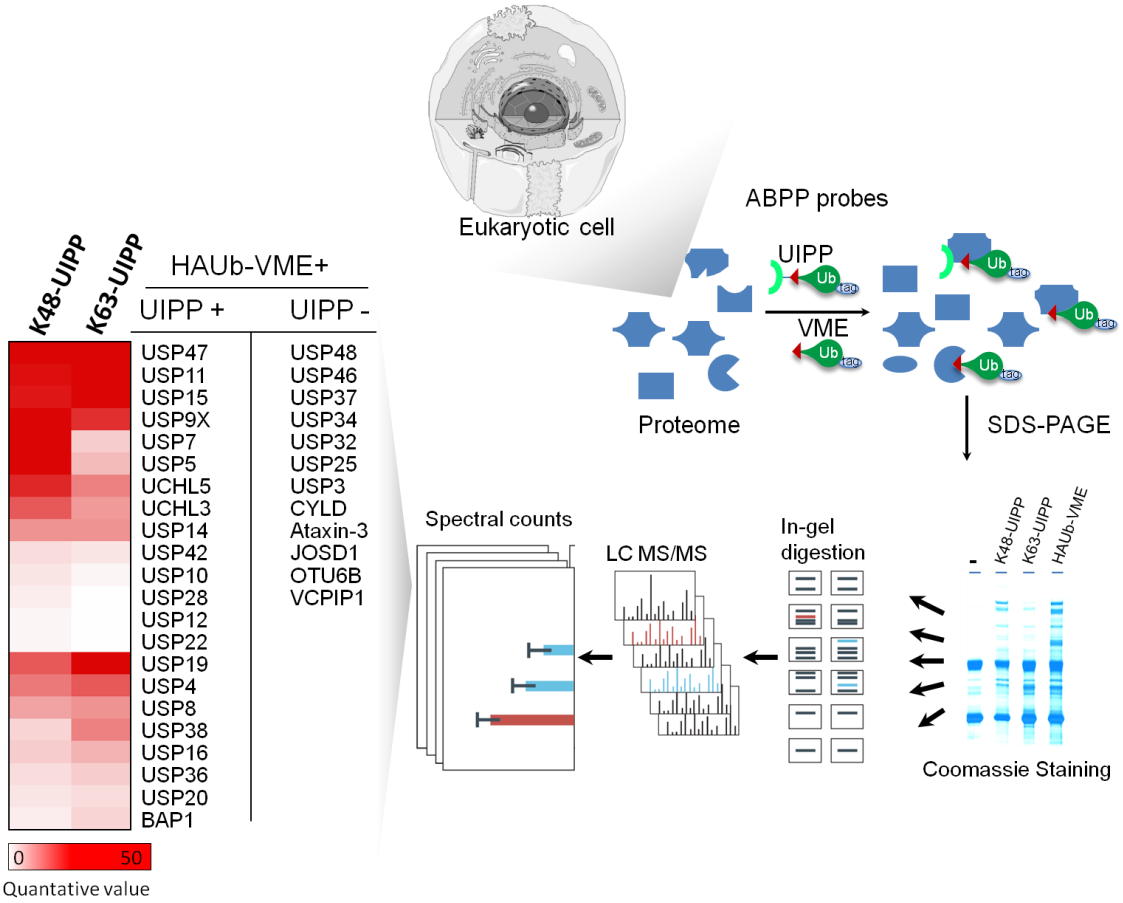

Figure 36. HAUb derived active site-directed UIPPs containing various thiol-reactive groups show distinct activity labeling profiles. The selective binding of DUBs was investigated by incubating K48- and K63-UIPPs with crude Jurkat cell lysates. After 1h incubation of HA-tagged UIPPs with Jurkat cell lysate (6.25 mg/ml) followed by α- HA immunoprecipitation, the eluted proteins were separated by SDS-PAGEand Coomassie stained. The excised gel-lanes were trypsinized and analyzed by LC-MS/MS. Heatmap of DUBs identified by incubating K48- and K63-UIPPs with crude Jurkat cell lysates. MS spectral counts corresponding to unique peptides (supplementary table 2) identified by LC-MS/MS were normalized with Scaffold 3.0 (Proteome-Software, Portland), and visualized with TreeView (V.1.1.6). 34 DUBs were detected by HAUb-VME (VME), whereas a subgroup of 22 DUBs was also labeled by UIPPs in a partially complementary fashion.

5 Discussion

5.1 Modulation potency of active-site directed probes

The utility of ABPs for mechanistic studies has been repeatedly confirmed by new studies. Recent mechanistic studies , e.g. addressing the E3 ligase ARF-BP1, revealed the importance of multiple cysteine residues for its ubiquitination activity by using HAUb-VME[143]. Similar studies also demonstrated the usefulness of C-terminal variation to address further enzyme groups like E3 ligases but did not improve the capture selectivity within one enzyme class. Furthermore, the specificity-conferring part of the probe assemblage (e.g. Ub), is a very important component that dramatically influences probe selectivity[144] and can stabilize proteins for crystallization purposes as well[108].

Concerning the ABP modulation attempts in this study, beginning with C-terminal variations of HAUb-VME, fine-tuning of reactivity was more successful than that of selectivity. Examination of the label profiling showed comparable intensity clustering upwards of 100 kDa and diminished enzyme labeling downwards (**Figure 20b**, **Figure 25**), which is consistent with recent reports for profiling with Michael acceptor probes[131,130]. Probe reactivity clearly is negatively affected by the structure of the reactive groups, which was deduced from the systematical extension from VME to VEE and further to MVEE. Thus, the VME-derived probes showed graded reactivity (VME>VEE>MVEE), corresponding to increasing steric hindrance, whereas the overall labeling efficiency was diminished and did not show additional specificity representing bands.

It must be noted that the effect is not the same for each band as for some of the bands the effect is stronger, which suggests that some DUBs seem to be more sensitive regarding higher steric demands. Unfortunately, these observations were only in conformity with HAUb-MVEE, which was not able to bind UCHL1 and USP8 in the immunoprecipitation assay (**Figure 19**). Nevertheless, closer inspection of raw data in terms of intensity and spectral counts did not conform with the expected stepwise diminishing effect, as described above. In addition, UCHL1 and USP8 belong to different DUB subclasses, show a sequence homology of only 5.4% (ClustalW) and there are absolutely no indications in the literature from which one could infer that the absence of probe-binding to these DUBs was due to their specificity.

However, the immunoprecipitation assay illustrated the capability of probes to bind DUBs covalently and revealed 17 identified DUBs.

To conclude, the attempt of modulating only the C-terminal electrophile of current ABPs offers the chance to modulate the reactivity but not the selectivity of HAUb derived probes.
However, a broad reactivity towards DUBs might be useful for large scale profiling approaches intending to explore the diversity of DUB expression in different tissues, cell lines or stimulating experiments.
The higher reactivity of the HAUb-VFEA probe compared to HAUb-VME as mentioned before is also observed in the reactivity band shift assay (**Figure 24**). This fact was confirmed by an additional band detected at around 40 kDa, which is also slightly visible after labeling with HAUb-VME. Running a 12% SDS-PAGE, staining with Coomassie, excising the band followed by tryptic digestion identified UCHL3 as the contents of this additional band (data not shown). The occurrence of UCHL3 in this lower running band (ca. 40 kDa) was also confirmed by the manufacturing company Enzo Life Sciences^{R} and specified as truncated UCHL3.
It has been shown previously that fluorine could interact favorably with peptidic N-H, and might orient the ligand towards electronegative regions of receptor sites[145]. Thus in addition to the electron-withdrawing effect, which causes higher electrophilicity at the β-carbon of the Michael acceptor group, introduction of a fluoro-substituent might also cause a favorable pre-orientation of the ABP and should be considered in further probe designs. However, as the comparison of diminished reactivity from monofluoro- to trifluoro-substituted probe demonstrated, the implementation of multiple fluro-substituents should be carefully considered. The reduced reactivity in case of trifluoro-substituent may duo to highly electron withdrawing effect which also leads to probe instability.
To conclude, there are still potentials to modulate the probe reactivity by amplified incorporating of steric hindrance and electronwithdrawing components.

5.2 High abundance versus high activity, correlation between ABPP and transcriptomic data

Numerous studies have applied activity-based protein profiling (ABPP) using chemical probes that are active-site directed and thus detect the activity status of proteins in complex mixtures. This begs the question: Which factors directly affect measured parameters and which of these contribute to DUB identification? From the biological point of view the identification could depend on the amount of expressed protein and its current activity status. As a complement to that, the probe affinity, reactivity and its amount influence the DUB identification during the ABPP approach as well.

To address the question concerning the correlation between activity and abundance of detected DUBs in different cell lines, mRNA data from BioGPS[146] were extracted and correlated with the ABPP data from this study. BioGPS is a gene annotation portal that includes gene annotations and relationships from the NCI-60 panel of human cancer cell lines[147]. In the following correlation analysis the EL-4 cell line was excluded due to missing information in BioGPS.

The correlating interpretation of mRNA and ABPP data described below underlie the assumption, that mRNA data represent protein expression level whereby ABPP data the abundance of active proteins.

In order to evaluate these two datasets from the objective perspective, a classification into different subgroups was carried out.

The classification criteria into subgroups include mRNA intensities, MS spectral counts, their correlation and the level differences in all four cell lines.

The overall comparison between mRNA and ABPP data indicated three major groups (i) correlated, (ii) partially correlated and (iii) not correlated (**Figure 37**).

The main criterion for the division into the correlated group was the relationship between ABP and mRNA, which was retained through all cell lines. Therefore, the progression of levels (trend) together with the correlation of ABP and mRNA (positive/negative sign) was taken into consideration (e.g. – ABP/+mRNA (MCF-7), -ABP/+mRNA (A549), …).

The relevance for the assignment to the “partially correlated” category was the partial consistence of the trend and the sign of the levels from ABP and mRNA data, which were not maintained through all five cell lines.

The “not correlated” category covers all other candidates, including those without any observable trend of cell lines, without any correlation between ABP/mRNA data and some cell line types with missing ABP data. Moreover the classification took candidates into account, whereas the numbers of unique spectra and mRNA intensity (x axis) varied dramatically.

The first group shows parallel good correlation between the mRNA and ABPP datasets and is representatively shown for USP22 and USP15 (**Figure 37a**). The DUBs assigned to this subgroup maybe regulated more at the DNA/RNA level. High protein abundance is also supported by high counts of MS spectra in the ABPP approach. In addition, recent reports[148,149,150] on USP22 corroborate this assumption also. However, the mRNA expression level does not necessarily correspond to the amount of active protein in a cell. In case of USP4, which is also sorted to the first group, a recent study detected an auto-inhibited form after translation[151]. In this case the DUB is functional but not active, and probably activated after the structural rearrangement induced by binding the active site-directed HAUb-VFEA.

About 39 % of the detected DUBs that differ in their ratio and the level trend regarding one or two cell lines were classified to the second “partial correlated” subgroup.

Representative examples for this group are UCHL3 and USP47 (**Figure 37b**). UCHL3 displays an obvious inconsistence for mRNA as shown for A549 and HeLa, while the spectral counts are more equally distributed. Taking into account the high intensity scaling for mRNA, the functional importance and high activity of UCHL3, the data are consistent with the available literature[84]. The differences between the cell lines might indicate that UCHL3 could be used as a marker for cells (cell lines) from diseased tissues.

With respect to USP47, the cell lines MCF-7 and A549 illustrate a controversial correlation.

Nevertheless, the mRNA data are consistent in comparison with large-scale tissue mRNA profiling data[152]. The high spectral count and mRNA levels of USP47 suggest both high activity and functional importance of this DUB, which indeed is supported

by a recent publication demonstrating its importance for DNA repair and maintaining genome integrity[153].

The third classification subgroup comprises of 46% of DUBs without any correlation of mRNA and ABPP dataset. Two representatives of this subgroup shown shown for examples are USP1 and USP2 (**Figure 37c**). The high variations between mRNA and ABPP data could indicate a regulation on both ways, either at the transcriptional level or through different protein activity. Furthermore, these observations suggest a directed DUB regulation in certain cell lines / tissues depending on DUB functionality, as shown in a recent report for USP1, where the authors describe that USP1 expression in mesenchymal stem cells stabilized ID proteins, inhibited osteoblastic differentiation, and enhanced proliferation[154]. Remarkable for USP2 is the low intensity (see scaling of both y-axes) that might hint at a more sensitive regulation of this DUB, an observation that is certainly worthwhile following up in additional experiments.

Further comparison diagrams (ABP data *versus* mRNA data) can be provided on the request by Cellular Proteom Research group (HZI).

To conclude, the more general overview of classification of DUBs in the three presented subgroups demonstrates a valuable comparison between transcriptomics and protein activity data. Concerning these data, it seems that DUBs are mostly regulated post-translationally, since most of the DUBs were classified to the third “no correlation” subgroup. All DUBs in this group are lacking a correlation between mRNA and ABPP data, therfore it is highly likely that their activity is regulated separately. Furthermore, post-translational modifications play a role in regulating the activity of DUBs, such as reported for Ataxin3 whereas the catalytic activity status is influenced by its ubiquitination[155], or by phosphorylation for OTUB1[156]. In addition, DUB activity is also affected by certain conformational changes[157,109], as already mentioned in the introduction. The mRNA studies presented here together with the ABPP data using HAUb-VFEA suggest that the absence of correlation in mRNA and ABPP data is due to distinct DUB regulation mechanisms rather than just enzyme appearance. Regarding the activity of proteins, active site-directed probes can provide high content proteomic information about the active state of enzymes and their active site conformation *in vivo.*

In addition, attention should be also paid to the fact that the applied concentration of HAUb-VFEA in this study was considerably low when compared to all previously

published ABPP investigations. The increase of concentration can enhance the reactivity / sensitivity but on the other hand also reduce the specificity.

The data presented in this study supply the research community with the information, which probe could be used in which cell line in order to get access to a particular DUB. This information could be useful for the choice of an appropriate cell line for the design of DUB-oriented projects.

For instance , in order to perform functional studies with USP35, it is recommended to use MCF-7 as an appropriate cell line.

Therefore, it would be desirable for this case to have already representatively DUB-profiled cell lines, permitting an easy selection of the right cell line for the intended study of a particular DUB or vice versa.

a) Correlated

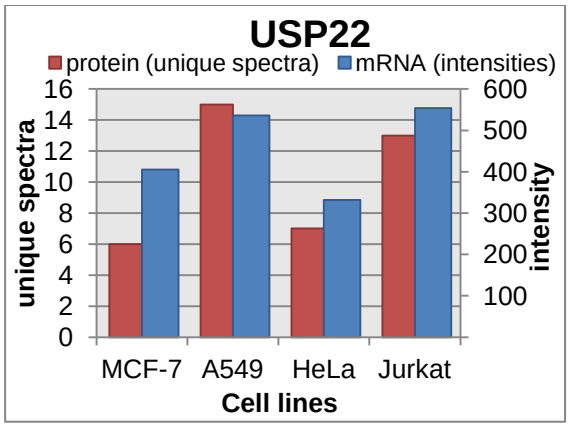

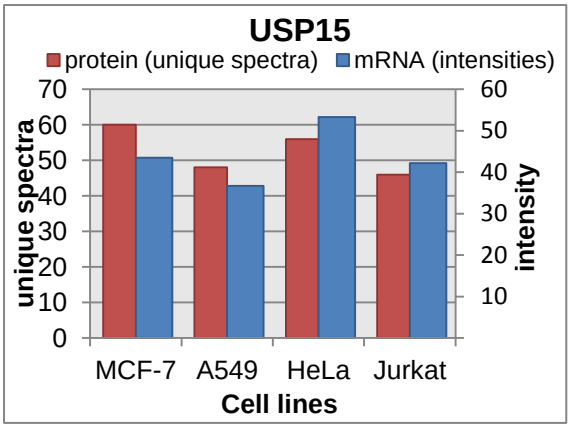

b) Partial correlated

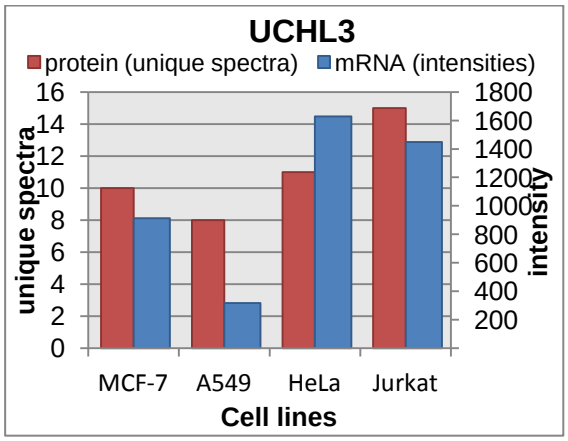

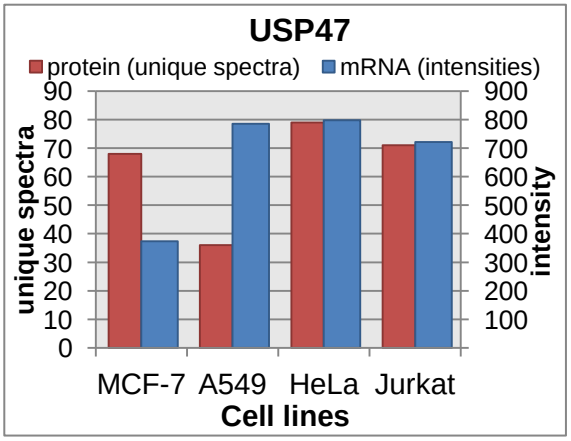

c) No correlation

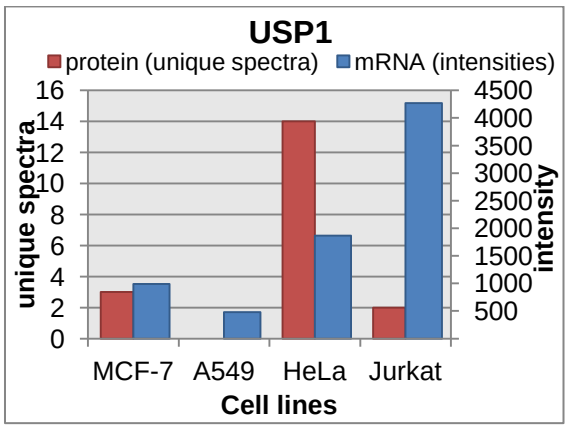

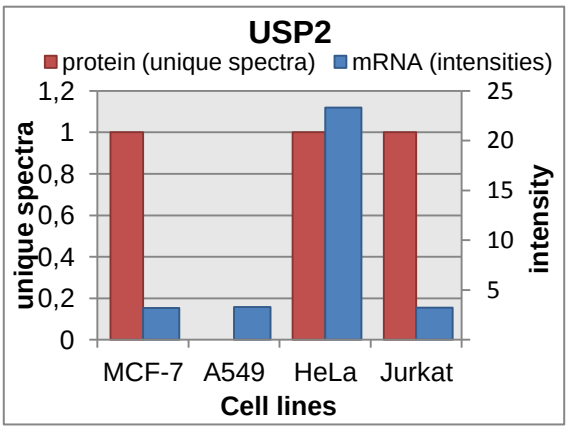

Figure 37. Comparison of mRNA and the obtained ABPP data using HAUb-VFEA. Depicted are mRNA and ABPP spectral count data for correlation purposes. Chosen are DUBs which are representative for the following groups a)correlated, b)partial correlated, and c)no correlation. The extracted mRNA data from the NCI-60 cell panel[147] (BioGPS) covered 39 DUBs also detected in the ABPP approach using HAUb-VFEA. The counts of unique spectra are shown on the primary y-axis, the mRNA-intensities on the secondary y-axis. In case of multiple spots on a microarray the intensities

were averaged. The diagrams of the remaining DUBs can be found in the supplement. Picture partially adapted from Anne Kummer (Master Thesis).

5.2.1 HAUb-VFEA profiling potency towards metalloproteases

Previously introduced ABPs[158,108] and the probes from this study were engineered to target conserved nucleophiles in the active site of proteases. Taking the differences of the MP catalytic mechanism[159] into account, their direct targeting by HAUb-VFEA can likely be excluded. Furthermore, several JAMMs are allocated in protein complexes and thus were more likely pulled down as a byproduct of protein complexes such as the proteasome, which may explain the low detected intensitys in contrast to other DUB subclasses. Accordingly to this observation, further investigations have to be carried out to clear the remained question whether all other less detected DUBs were pulled down as byproducts as well.

However it is clear that HAUb-VFEA is a functional and highly reactive active site-directed probe and it could be managed to retrieve these DUBs successfully even though the probe was not originally designed to achieve this.

Nevertheless, considering certain existing examples of electrophile-based covalent inhibitors[160]and covalent probes proven effective for presenilin[161] and creatine kinase[162], Alan Saghatelian and colleges engineered recently also an ABP for MPs[163].

5.2.2 Comparison of HAUb-VFEA versus gold standard HAUb-VME

Posttranslational interactions and modifications modulate the functional state of enzymes and different large-scale profiling methods have been applied to monitor these. One such technique is termed ABPP and uses the popular active-site directed probe HAUb-VME, which was first designed in 2002[128]. In five different studies utilizing HAUb-VME the identification of 46 DUBs was described[7-9,167,168].

Regarding the DUB profiling in the mostly used EL-4 cell line, 29 DUBs were detected using HAUb-VME[128,166], compared to 42 DUBs labeled by HAUb-VFEA in this study.

The direct comparison of the “gold standard” HAUb-VME and HAUb-VFEA shows an overlap of 44 commonly labeled DUBs (**Figure 38**). Concerning the DUB identification and the distribution in their DUB subclasses, HAUb-VFEA labeling covered

exclusively 23 additional DUBs distributed among all subclasses. In contrast, HAUb-VME additionally modified 2 DUBs, USP13 and A20. The list of identified DUBs used for the comparison is provided in the supplement section 10.5.

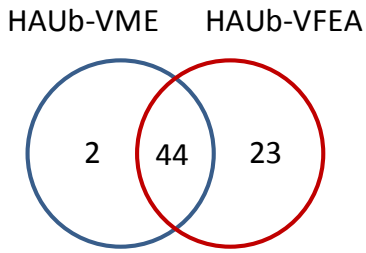

Figure 38. Comparison of DUBs identified by the new HAUb-VFEA versus "gold standard" HAUb-VME (Venn diagram). All detected DUBs identified by HAUb-VFEA in this study versus DUBS labeled by HAUb-VME, are summarized from all known ABPP-HAUb-VME approaches performed to date[73,128,131,130,169-58].

Several previous studies have utilized HAUb-VME but were predominantly carried out in the EL-4 cell line. HAUb-VME will certainly may have the potential to detect more DUBs in further cell lines, Since the labeling power of probes is restricted also by (i) probe property, (ii) the performance of measuring apparatus and (iii) at the biological system itself[128].

These points clearly show the advantage of HAUb-VFEA, which was already utilized in profiling experiments of different cell lines by using state of the art instruments.

Huib Ovaa *et al.* 2004 for example, showed the activity profiles of DUBs in different cell types using HAUb-VME, but detected in summary only 11 DUBs.

Thus, the utilization of up to date instruments could allow to increase the sensitivity and the more detailed description of DUB profiles between different cell types. However, the direct evaluation and the high number of 16 DUBs exclusively captured by HAUb-VFEA (in contrast to all HAUb-VME reports up to date) suggest a broader reactivity and thus, is more than comparable with HAUb-VME.

In summary, HAUb-VFEA demonstrates increased reactivity compared to HAUb-VME and is a suitable active site-directed probe for DUB profiling approaches.

5.3 The potency of novel UIPPs

In contrast to recently introduced synthetic di-Ubiquitines[170], the newly developed UIPPs possess a Michael acceptor system instead of Gly76 of the distal Ub, thus enabling the covalent capture of DUBs. This allows for the capture and sampling of DUBs with distinct target specificities, and formation of stable DUB-UIPPs complexes facilitates crystallization attempts. Knowledge of target specificities and structure of the enzyme bound in its active conformation is also important for the design of specific inhibitors of DUBs

5.3.1 Evaluating the reactivity and selectivity of recombinant DUBs using UIPPs

The gel shift assays of UIPPs demonstrated not only the reactivity but a certain potency for DUB selectivity as well (**Figure 33b**). In addition, the presence of only one (rather than multiple) up-shifted band hints at reactivity towards one active cystein residue[143].

The reactivity of USP15 towards both UIPPs provides a kind of guideline, a hint to its Ub-linkage preference, and is consistent with current knowledge of its deubiquitination specificity[104]. USP15 and USP4 are closely related proteins containing both an integrated Ubl fold within the catalytic domain and share a sequence identity of 70%. A recent publication established that the catalytic activity of USP4 is regulated by its Ubl fold, and closely related proteins, such as USPs 6, 11, 15, 19, 31, 32 and 43, probably also regulate DUB activity through their Ubl domain[151]. Thus, the observed UIPP reactivity supports again the importance of “activity- based probes”.

In contrast to USP15, UCHL3 has been reported to be able to cleave K_{48} linked poly-Ub but not K_{63}-linked poly-Ub[104,171,172]. The gel shift assay with recombinant UCHL3 certified a clear preference for binding to the K_{48}-UIPP and supports the assumption that UCHL3 may recognize proteasomally pre-processed K_{48}-linked proteins[142].

Regarding Ataxin-3, recent studies observed that di-Ub chains, whether K_{63}- or K_{48}-linked, are unsuitable Ataxin-3 substrates[173,174]. Additionally, the Ub preference was evaluated by crystallography using HAUb-chloroethylamine, which allowed the

determination of the first crystal structure for a Josephin-Ub complex and attests once again the potential of ABPs in structural analysis[175].

The DUB Ub-linkage specificity concerning the sequence context[141,106] could be remarkably demonstrated by proof of concept UIPPs with the chosen peptides, $Ub_{(42-54)}$ –K_{48}(VA) and $Ub_{(54-72)}$ –K_{63}(VA).

There can be no doubt that the interaction of distinct amino acids from both, substrate and residues in the active site of DUBs, contribute to DUB specificity.

Importantly, the prerequisite for their correct orientations is determined by structural constraints. The sequence length of the investigated peptides (**K_{48}-Pep**: $Ub_{(42-54)}$ –K_{48}(VA), **K_{63}-Pep**: $Ub_{(54-72)}$ –K_{63}(VA)) was deliberately chosen to cover these structural features from ubiquitin and contains indeed different structural components (**Figure 39**). On the one hand, the K_{48}-Pep poses a compact structure and is shorter than K_{63}-Pep, which might explain the high preference of UCH L-3 towards K_{48}-UIPP (**Figure 33b**). On the other hand, K_{63}-Pep provides more sequence context and is much more flexible in comparison to the ordered structure of K_{48}-Pep. (**Figure 39a**). Thus it should fit better into the catalytic groove of a DUB. Beside the structural aspects, each peptide contains a different potential distribution which attributes to distinct charge preference in the catalytic groove as well. For example K_{48}-Pep. presents a positive charged area around K_{48} which suggest that this to interact with DUBs which display more negative charged surface around the active-site.

Additionally, K_{63}-Pep exhibits more hydrophobic surface patches (**Figure 39b**) and therefore should have more potential to interact with the DUBs. However, the applied gel shift assay (**Figure 33b**) demonstrated different DUBs preferences towards UIPPs, which cannot be explained by peptide length or structure alone, but obviously depends on the DUB binding sites as well. The cases where UIPPs did not bind the DUB can be attributed firstly to the sequence context of the five missing Ub-linkages (K6, K11, K27, K29, K33) and secondly to the lack of further hydrophobic ubiquitin patches, which naturally interact with certain DUB domains.

Furthermore, due to a similar structural element (β-sheet) around the Ub-linkage, it can be postulated that K6 and K11 polyubiquitin chains have the same function as K48 polyubiquitin chains. The participation of K11 polyubiquitin chains in proteasomal degradation was also recently reported[77]. In contrast, the lysines K27, K29 and K33 jut out from an α-helix (**Figure 1**) and thus may serve for other cellular functions.

These structural deductions are presently only hypotheses but should nevertheless being considered when evaluating these unconventional and poorly understood ubiquitin chains.

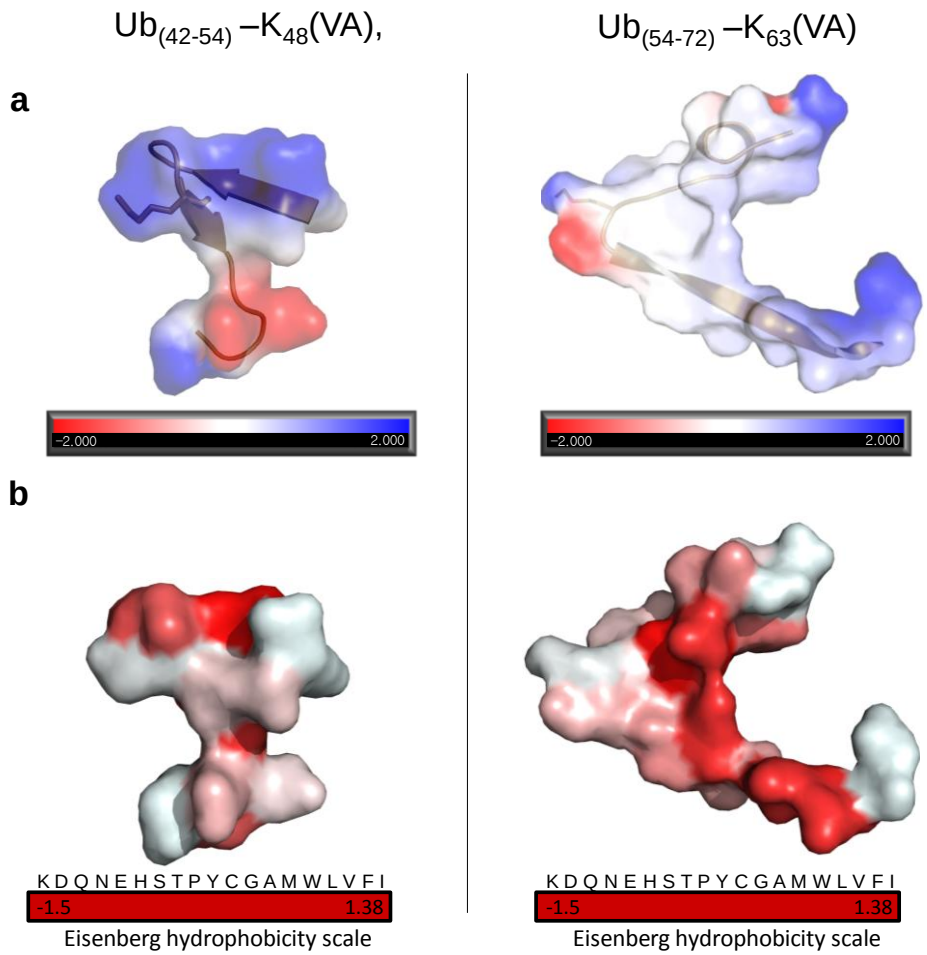

Figure 39. Potential distribution and hydrophobicity mapping of Ub(42-54)–K_{48}(VA) and $Ub_{(54-72)}$ – K_{63}(VA) peptides used for the UIPP design. (a) The calculations by DelPhi webserver show distinct potential distribution and hydrophobic areas on the surface of the ubiquitin-derived peptides. The lysines (K_{48} and K_{63}) shown as sticks are exposed on the surface and ready to engage in interactions. (b) Molecular surface is colored by the hydrophobicity of the residues according to the Eisenberg scale (Eisenberg *et al.*, 1984). The pictures were generated using *The PyMOL Molecular Graphics System,* 2008 (PDB-ID: 1UBI).

5.3.2 Application of UIPPs in biological environment

The ABPP approach with UIPPs clearly highlights the potential of the new UIPPs to capture and characterize linkage-specific DUBs from cell lysates (**Figure 36**). Although the reactive groups of HAUb-VME and the UIPPs are similar, the comparison of detected DUBs certifies again the high reactivity of HAUb-VME and the ability of UIPPs to label a particular subgroup of DUBs. However, it has to be kept in mind that this is a proof-of-concept study and only two (K48/K63) out of seven possible Ub-linkages were mimicked. Taking this into account, mimicking the other five Ub-linkages using the UIPP design, a coverage of 39 DUBs and more can be expected. A further important point is the difference of covered DUB classes. Interestingly, only two (USP and UCH) out of five DUB classes were targeted by the present ABPP/UIPP approach, although ABPP/HAUb-VME addressed at least one DUB out of four DUB classes (USP, UCH, OUT, MJD). CYLD (USP class) and Ataxin-3 (MJD class) for instance, seem to prefer K63 polyubiquitin linkages[176,173], whereas A20, as an OTU class member, prefers K48 polyubiquitin in vitro[104]. On the other hand *in vivo* studies, as for A20, describe its cleavage preference for K63 polyubiquitin chains. This example again represents the discrepancy between *in vitro* and *in vivo* studies and highlights the lasting need for clarification of DUB linkage preference, and using probes such as UIPPs *in vivo* would be an important step forward. The DUBs of the fifth class (JAMM) were generally missing, which is most likely due to the different catalytic mechanism of metalloproteases, as discussed already in the introduction section.

Why UIPPs didnot label DUBs from other DUB classes stil has not been completely understood, although for some of these the deubiquitinating preference for K48/K63 Ub-linkages are well described. An explanation could be that the remaining DUBs (covered only by HAUb-VME) cleave polyubiquitin chains exclusively, since UIPPs mimic more a di-Ub or distinct branched Ub variant, rather than polyubiquitin. Furthermore, the DUB-Ub substrate recognition is not fully understood to date and often depends on the additional DUB-internal multiple Ubiquitin Binding Domain (UBD), which first binds a number of ubiquitin variants in order to activate the DUB catalysis[104].

The labeling of certain DUBs by UIPPs may not be realized which could be explained by the fact that UBD is missing in the UIPP design, but is needed for the DUB activation.

Additionally, the polyubiquitin recognition and processing by DUBs can be performed as whole chain amputation, distal/endo trimming or long-chain binding[15,177] (**Figure 40**) and have to be taken into account for the evaluation of Ub-linkage preferences. Especially for K63-linked polyubiquitin chains it remains to be clarified whether these chains are cleaved from their proximal or distal ends.

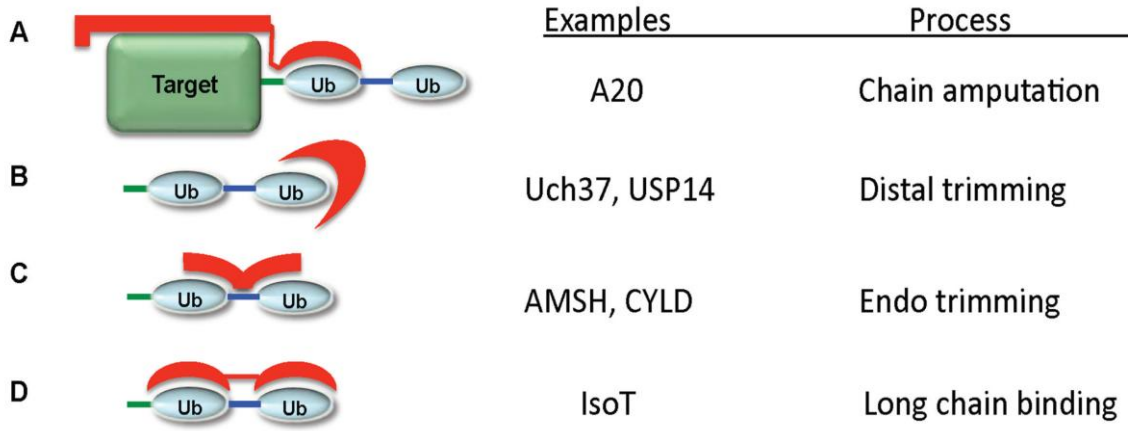

Figure 40. Possible mechanisms of polyubiquitin recognition by DUBs.
A) DUBs can recognize both, the target protein and the polyubiquitin chain. **B)** DUBs can trim the polyubiquitin chain beginning with distal ubiquitin. **C)** DUBs may bind simultaneously two ubiquitins by interacting with both ubiquitins that surround the isopeptide bond. **D)** DUBs could recognize polyubiquitin through the use of multiple UBDs. Ubiquitin is depicted in blue, the target protein in green, and the polyubiquitin receptor in red (Reyes-Turcu & F.E. Wilkinson, K.D, 2009).

According to the “Ub-linkage preference” illustrated by heat maps (**Figure 36**), K48-UIPP is highly reactive towards USP5. Interestingly, this finding is in accordence with shift assay (in this study) and a recent publication, which established that USP5 recognizes the C-terminal Gly-Gly motif and also is a known dedicated ubiquitin recycling DUB, which is highly active against unattached Ub-chains as well[178]. Regarding USP7, the preference for K48-linked di-Ub was recently reported[179]. Nevertheless, labeling of DUBs by both UIPPs also gives a clue about their Ub-

linkage specificity. DUBs which are likely to be multifaceted in their Ub-linkage specificity, like USP15, which is consistent with recent literature was also labeled by both UIPPs[104]. In addition, it has been suggested that certain USP members show cross-reactivity to ubiquitin-like proteins, such as NEDD8, as well[180].

To answer this question, the generation of UIPPs including any conceivable Ubl-derived peptide sequence could be used for the assembly of Ubiquitin-like Isopeptide Activity Based Probe (UBL-IPP). With this strategy it is now possible to modify each lysine of the target protein with ubiquitin via an isopeptide linkage thatcontains the reactive Michael acceptor group. This opens up not only the possibility to synthesize UIPPs with all seven possible di-Ub linkages, but also to derive peptide sequences from putative ubiquitination sites[181] of distinct target proteins. This represents a significant advantage as compared to examining their specificity using recombinant enzymes, as the enzymatic properties of DUBs may change within their biological environment.

Nevertheless, the ABPP approach with novel K48/K63-UIPPs already provides substrate selectivity for only 34 DUBs, but it should be stressed that this represents a sizable subfraction of ~100 human genome-encoded DUBs, which bind either K48 or K63 Ub-linked chains. According to this, the result of profiled DUBs represents a specific DUB-sub-proteome.

To conclude, the application of UIPPs in different induction assays, such bacterial infections, could provide a certain DUB sub-proteome and at the same time information about their substrate selectivity.

Furthermore, the evaluation of DUB's Ub-linkage preference using UIPPs followed by DUB implementation in signaling pathways can provide useful information about its biological significance. Taking this into account, one example will be presented for USP7, serving as proof-of-concept, followed by discussing the infection-associated DUB USP19[182].

The reported interaction between p53 and USP7 (HAUSP) serves as an ideal representative example. Recent studies described the deubiquitinating activity of USP7 towards p53 and its protection from proteasomal degradation by acting as a direct antagonist of Mdm2 (E3 Ub-ligase)[183]. Since all proteins labeled with K48-polyubiquitin chains are destined for proteasomal degradation it is believed that p53 is likely to be labeled with K48-polyubqiuitin chains. This widespread assumption is

supported by the UIPP-ABPP results in this study, where USP7 shows a clear preference for K48-UIPP.

Furthermore, functional studies indicating that the binding of Epstein-Barr nuclear antigen 1 (EBNA1) to USP7 inhibits its deubiquitination of p53[184], suggests that some viruses alter the activity of USP7 to manipulate the proteasomal cellular events.

In cases like USP19, the cellular function and interaction network is not as well described as for USP7, thus UIPP-ABPP results could give important and exiting insights into their biological relevance. Due to the fact that USP19 is a relatively large enzyme of 145 kDa, the recombinant expression and biochemical characterization is not a simple task. All USP19 publications up to date have indeed reported deubiquitinating activity, but not the types of Ub-linkages that were processed. The last reported function of USP19 was the transcriptional modulation of major myofibrillar proteins[185] and that its resides on the ER to most likely rescue the ERAD substrates from degradation[182]. Since USP19 showed a clear preference for the K63-UIPP probe (**Figure 36**), further examination with those interacting proteins should be carried out in the context of K63-linked ubiquitination. Also, further USP19 knock-down or silencing experiments should not only be evaluated in terms of degradation but also in the context of induction in transcription, protein sorting into the multivesicular bodys[186], autophagic clearance[187], protein trafficking and DNA repair[31].

Besides the possibility to elucidate the ubiquitin linkage specificity of DUBs by using UIPPs, the UIPP approach could also be used to identify DUBs which deubiquitinate particular targets. In case of substrates where the ubiquitination site is known, the development of specifically constructed UIPPs could enable the detection of DUBs which most probably regulate their ubiquitin status, for instance DUBs in the E-cadherin pathway.

E-Cadherin is an epithelial cell-cell adhesion receptor, forms a key component of epithelial cell adhesion, and plays an important role during developmental morphogenesis and wound healing[188]. Recent reports demonstrated that the surface protein (InlA) of *Listeria monocytogenes* interacts with E-cadherin, triggers its ubiquitination and promotes the internalization of the bacterium[189].

Although it was reported that E-cadherin is ubiquitinated by the ubiquitin-ligase Hakai, its antagonist (DUB) is still unknown. Due to the implication of E-cadherin in different signal transduction pathways, the interaction network is relatively broad and covers various possible DUBs (**Figure 41**).

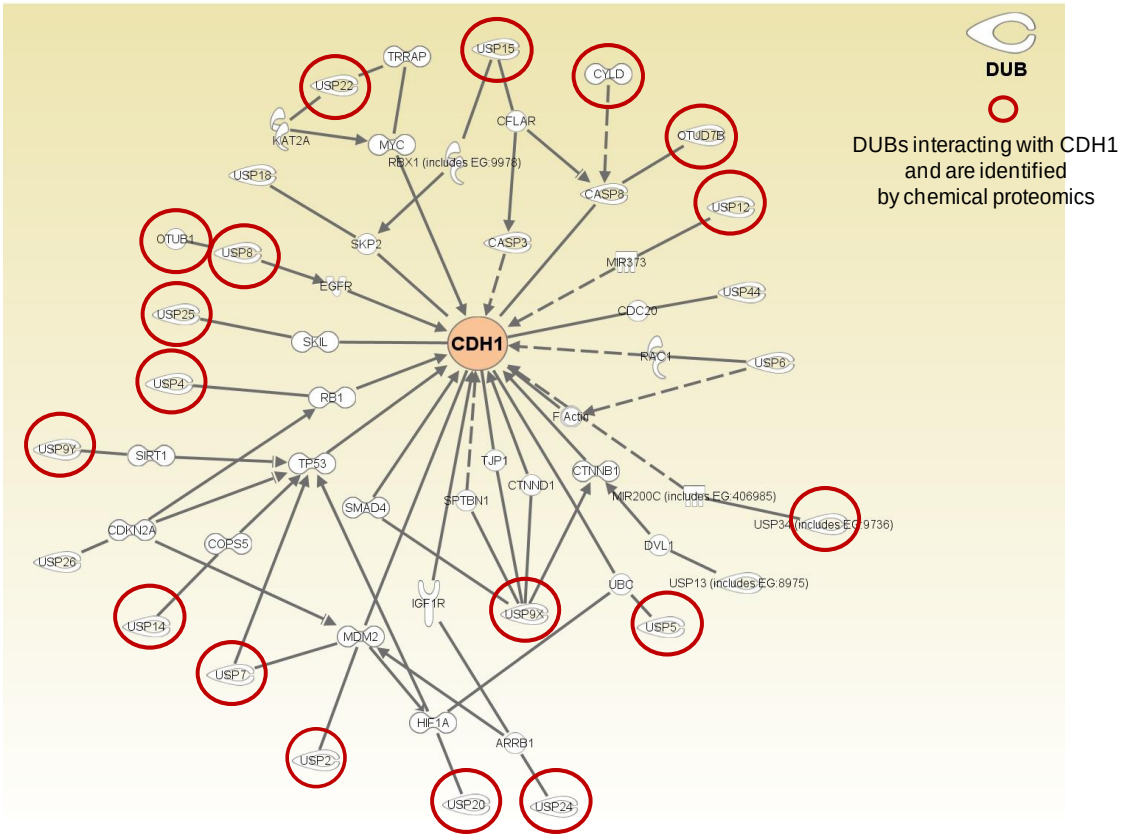

Figure 41. Schematic plot of USP19 and its interaction partners constructed with 2011 Ingenuity Systems.

Thus, it remains a challenge to identify the DUB responsible for the deubiquitination of E-cadherin. The generation of specific UIPPs containing the sequence that covers the ubiquitination site of E-cadherin (**Figure 42**) could solve this issue and represent an unprecedented tool. Furthermore, the application of an E-cadherin-UIPP in a functional proteomic approach has the advantage to address many DUBs in a single experiment.

In addition, the access to DUBs and their monitoring during *Listeria* infection using probes developed in this study could reveal how intracellular *Listeria* influence host DUBs.

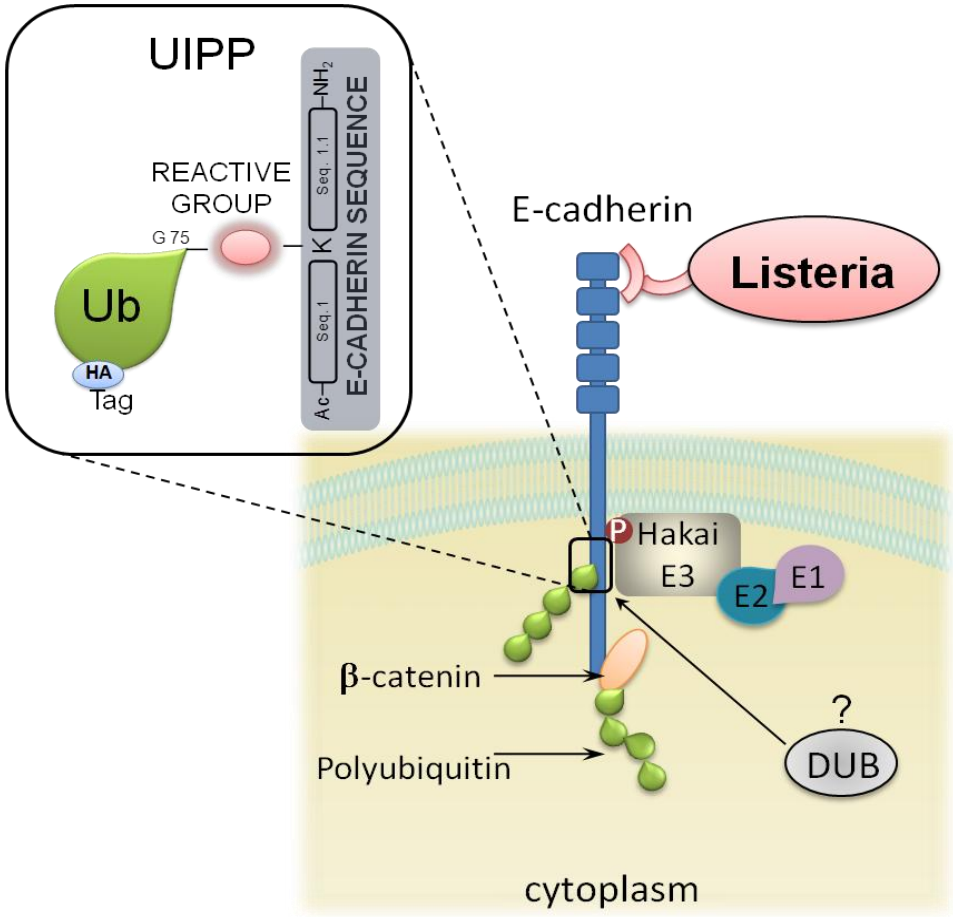

Figure 42. Schematic model of an UIPP constellation to discover possible DUBs which regulate the ubiquitin status of E-cadherin during *Listeria monocytogenes* infection.

6 Outlook

The most obvious next step of development is to continue to improve of the reactivity and selectivity of ABPs as well as their applicability in ABPP approaches. The pilot approach of systematically modulating HAUb-VME reactivity demonstrated that in future for instance the probe reactivity might be enhanced by introducing a more electron-withdrawing group including Fluorine. HAUb-VFEA, designed in this study, showed a slightly higher reactivity as the gold standard HAUb-VME and could be utilized for a broad range of activity-based DUB profiling experiments. However, to ensure the wide range reactivity for exploring the DUB profiles in further profiling experiments it would be an advantage using a mixture of different ABPs, similar to already commercial available inhibitor cocktails. Such a strategy would be sensible, e.g. to profile the DUB activity before and post infection to identify DUBs that are putatively involved in the infection process of interest, as described for UCHL1[190].

After choosing a DUB of interest from a DUB profiling experiment the same or a more selective ABP could be used to enrich this DUB and examine it for PTMs, which may explain its up or downregulating activity. This kind of analysis could be performed by mass spectrometry and would give insights into the PTM status in a more biological context, an advantage compared to *in vitro* modifications.

Furthermore in order to expand the utilization of probes for *in vivo* application, the development of cell permeable probes would allow profiling enzymes directly in living cells. First experiments to realize such probes have already been published[191]. These probes are mostly based on small molecules to ascertain their ability to cross the membrane. Unfortunately Ub-derived probes, which are more selective towards targets related to the native substrate Ub, cannot passively permeate the cytoplasmic membrane. Additionally, probes containing the HA tag are not cell permeable *per se*[192]. To meet this challenge the HAUb-derived construct could be reduced to two peptides containing instead HA another tag, such as a FLAG tag. Another completely different approach would be the utilization of cell penetrating peptides (CPPs) which have the ability to shuttle proteins or even nanoparticles into living cells[193]. Moreover, fluorescent probes developed in the last decades allow a “real time” imaging of the dynamic assembly, localization and turnover of target proteins in living cells[194].

The design of mechanism-based probes directed against receptors or proteins in the cell membrane would even allow imaging distinct cell types and under optimal conditions replace antibodies. Nevertheless, the combination of antibody-linked

active site-directed probes may provide more target specificity and would be a novel attempt, which was not attempted until now.

The creation of ABPs based on Ubiquitin-like proteins such as Nedd8, ISG15 and SUMO has already been demonstrated[130] and is a promising innovation which should further be developed to shed light on the function of these poorly investigated protein modifications. In addition, their characterization could be facilitated by structure analyses as there are as yet no structures of ISG15 or NEDD8 bound to DUBs available.

The fact that ubiquitin-like modifications were mainly observed monomeric and not forming poly-Ubl chains suggests that these kinds of modifications could be more easily mimicked by the UIPP approach as well.

Although the UIPP strategy is at an early stage of development, it illustrates the potential of peptide integration for studying the chemistry of DUB selectivity. The advantage of peptides as specificity-contributing units was recently demonstrated with photo-activated cross-linking of peptides in studies of the human hypoxia inducible factor system[195]. Further advantages of using peptides were already covered in the discussion section, e.g. mimicking a whole ubiquitinated protein by combining ubiquitin and a peptide originating from the protein of interest. This construct could be incubated with a crude cell extract followed by immunoprecipitation, and can thus disclose the DUB that is very likely responsible for regulating the ubiquitination status of the “mimicked” targeted protein.

The current understanding of DUB specificity is still incomplete, due to among other things, the unavailability of well-defined ubiquitin chain substrates or assays. This issue could be addressed by generating the further five UIPPs to cover all possible ubiquitin chain linkages.

Despite the elegant design at using peptides, the idea could be extended to implement full length ubiquitin using the recently patented and published UB synthesis protocol from Huib Ovaa’s lab[170].

In general terms, the latest increase of covering sub-proteomes by ABPP focuses mainly on hydrolase activities and should be extended to other enzyme classes. Recently notable examples, such as the whole ABP panel from Cravatts laboratory directed against multiple cytochrome P450s[196] have been published. Additionally, the Lin group recently described ABPs targeting cell surface receptor CD38[197], and first ABP attempts from Licht et al. were directed towards ion channels[198]. The advantage

of the ABPP approach is the utilization of the natural affinity of native ubiquitin, permitting the use of enzymes combined with small active site-directed probes. This advantage could be used not only to profile enzyme activities or test the affinity of inhibitors in competitive assays, but also for probe design based on already validated inhibitors for certain enzymes. This kind of approach would clearly accelerate the development of additional ABPs. Furthermore, generating ABPs by using drug compounds as a source of proven inhibitors may be a practical approach to evaluate their affinity. Thus, development of inhibitors with widespread affinity could be avoided and the side effects resulting from this would be prevented in the first place. In order to improve pharmaceutical relevance of ABPs, the last and ultimate goal would be the integration of ABPP into several high-throughput technologies to facilitate the understanding of enzyme function in complex biology networks and pathologies resulting from their malfunction. A good step forward with a multidimensional profiling strategy that combines activity-based proteomics and metabolomics[199] was recently demonstrated.

The present study established the potential of broadly reactive ABPs, their fine-tuning and paved the way to generate more selective activity-based probes. The availability of such ABPs would facilitate the proteomic analysis of pathogens to identify new targets and alleviate the search for new drugs against multi-resistant strains. To investigate this possibility Staphan Sieber's group recently used a small generated library of β-Lactones and applied ABPP to prokaryotes to identify specific target enzymes, which are crucial for bacterial viability and virulence[200,201].

7 SUMMARY

Ubiquitin is a 76-amino-acid protein and contains seven Lysine residues at the positions 6, 11, 27, 29, 33, 48, and 63. The covalent attachment of ubiquitin *via* the C-terminus of ubiquitin to lysine residues of target proteins (or ubiquitin itself) is termed ubiquitination and is a widespread regulatory post-translational modification. Beside monoubiquitin also topologically different polyubiquitin chains (Ub-linkages) exist which regulate a wide range of cellular processes. As with most other post-translational modifications, ubiquitination is a reversible process, which is enabled by deubiquitinating enzymes (DUBs) that remove the ubiquitin or truncate (trim) polyubiquitin chains. Therefore, DUBs have an analogous role to phosphatases and are functionally as important as ligases or kinases, thus representing an attractive therapeutic target. Unfortunately, the mechanism and function of DUBs are poorly understood and recent research efforts focused on the development of suitable biochemical tools to obtain new insights into the specific mechanisms of members of this recently discovered enzyme class. Useful tools termed activity-based probes (ABPs) are implemented by conversion of ubiquitin into a suicide substrate, which possesses a C-terminal reactive group. By utilizing the ABPs in a functional proteomics approach, these probes interact and bind covalently to the catalytic Cys residue of active DUBs. However, because of their relatively unspecific binding of different DUB proteases and thereby broad reactivity, the examination of all aspects of DUB selectivity and specificity cannot be addressed. The aim of this study was the improvement of the ubiquitin ABP by generating specific probes to clarify DUB linkage and substrate specificity issues. In addition, the novel designed probes should be validated and evaluated in respect to their biological applications in functional proteomics experiments.

The ABP synthesis procedure described in previous publications was improved by additional purification steps and by utilizing Sulfo-NHS as a nucleophilic catalyst.

To investigate the reactivity profile of ABPs two directions were pursued: the dependence of DUB labeling on steric hindrance and the influence of increased electrophilicity by fluorination. Concerning steric hindrance, the reactivity diminished stepwise by expanding the gold standard ABP (HAUb-VME) with an ethyl ester group (VEE) and further by additional attachment of a methyl group to the electrophilic carbon atom (MVEE). However, the effect of increased electrophilicity by replacing

alternatively the methylester from HAUb-VME with a monofluoroethylamide-group (HAUb-VFEA) showed indeed higher labeling efficiency compared to HAUb-VME.

To conclude, using the improved synthesis protocol, it was possible to design and synthesize a set of five new ABPs (HAUb-VEE, HAUb-MVEE, HAUb-VA, HAUb-VFEA and HAUb-VF_3EA), showing distinct activity-based DUB labeling profiles.

The activity-based protein profiling using the most reactive probe (HAUb-VFEA) designed in this study revealed an overall of 67 active DUBs in five different cell lines (A549, EL-4, MCF-7, Jurkat E6-1 and HeLa S3). These results demonstrate not only the high reactivity of HAUb-VFEA but also show the distinct active DUB populations of each cell line, respectively. The focus of the next investigation was the development of novel ubiquitin-based ABPs to also allow targeting of DUBs with distinct Ub-linkage specificities. The intention was to develop a new class of ABPs for characterization of the Ub-linkage preference of DUBs within the activity profiling assay. The result was novel peptide branched Ubiquitin Isopeptide Activity Based Probes (UIPPs). In contrast to standard ABPs, the novel UIPPs contain not only the ubiquitin with a C-terminal reactive group, but also an additional freely selectable peptide sequence. The peptide sequence can originate from ubiquitin or from any ubiquitinated target protein. Thus, an UIPP mimics an isopeptide bond present within di-ubiquitin or an ubiquitination site from a protein of interest. This constellation represents a new type of ubiquitin-based reactive probe concept and was patented in 2011.

Due to the fact that DUBs distinguish the Ub-linkages most likely by Ub-linkage sequence context, the well studied K48 - and K63 polyubiquitin linkages were mimicked to validate the UIPP concept. Indeed, the respective probes showed a selective labeling behavior towards USP15, UCHL3 and Ataxin-3 in an activity shift assay, thus validating the peptide based approach. The ability of the UIPPs to covalently capture DUBs by targeting their active-site residue was further confirmed by mass spectrometry analysis.

Using cell lysates, the activity-based profiling comparison *versus* HAUb-VME indicated also their potential of capturing different Ub-linkage specificities from complex proteomes.

In order to evaluate the DUB Ub-linkage specificity in more detail in a biological environment, a functional proteomics approach was applied to crude cell lysates. Good evidence for Ub-linkage preference was observed for DUBs such as USP5, 7,

10, 12, 22, 28 and USP9X which show a strong binding preference for K48-UIPP, whereas K63-UIPP preferentially labeled USP16, 19, 38 and BAP1.

In conclusion, the ABPs and UIPPs created in this study were found to be enabling tools to capture active DUBs and study their selectivity towards ubiquitin-linkage specificity in a complex proteome. The crystallization of DUBs in their active conformation in complex with UIPPs would provide an important advance towards the design of specific inhibitors of DUBs. It can be expect that the use and application of UIPPs may facilitate drug design and expand the repertoire of targeted molecular therapies.

7.1 Zusammenfassung

Ubiquitin ist ein kleines aus 76 Aminosäuren bestehendes Protein und beinhaltet sieben Lysinreste an den folgenden Positionen: 6, 11, 27, 29, 33, 48, 63. Die Kovalente Bindung von C-terminalen Ende des Ubiquitins mit dem Lysinrest des Zielproteins wird Ubiquitinierung bezeichnet und ist eine weitverbreitete posttranslationale Modifikation. Neben der Monoubiquitinierung existieren auch topologisch verschieden Polyubiquitinketten (Ubiquitinverknüpfungen) die ein breites Spektrum an Zellulären Prozessen regulieren. Wie auch bei anderen posttranslationalen Modifikationen, ist die Ubiquitinierung ein reversibler Prozess, wobei das Ubiquitin durch Deubiquitinierungs Enzyme entfernt oder die Polyubiquitin Ketten verkürzt werden. Demnach, sind DUBs ein Analogon zu Phosphotasen und funktionell ebenso wichtig wie Ligasen oder Kinasen und repräsentieren somit ein attraktives therapeutisches Ziel. Bedauerlicherweise ist der Mechanismus und die Funktion von DUBs nur wenig verstanden und deswegen sind derzeitige wissenschafliche Bemühungen fokussiert geeignete biochemische Tools zu entwickeln, um eine Einsicht in den spezifischen Mechanismen von diesen erst kürzlich endeckten enzymklasse zu bekommen.

Vielversprechend sind die Aktivität basierten Sonden (activity based probes -ABPs) dessen Aufbau ein modifiziertes Ubiquitin beinhaltet, welches am C-terminus eine reaktive Gruppe trägt. Bei der Anwendung dieser ABPs im funktionsbasierten Proteomiks Ansatz interagieren diese mit aktiven DUBs und binden kovalent an dessen katalytischen Aminosäurenrest. Allerdings zeigen diese eine unspezifische Bindung und eine breit gefächerte Reaktivität auf, so dass die Untersuchung der DUBs hinsichtlich Ihrer Selektivität und Spezifität nicht möglich ist.

Ziel dieser Arbeit war es die Reaktivität der Sonden weiterhin zu verbessern und die fundamentale Frage der DUB Spezifität anhand neue entwickelter, spezifischer Sonden zu klären. Dabei sollten die neu designten Sonden synthetisiert, validiert und im biologischen Kontext mit der funktionalen Proteomik evaluiert werden. Das zuvor in der Literatur beschrieben Syntheseprotokoll wurde durch zusätzliche Aufreinigungsschritte und den Zusatz von S-NHS, einem neuen Bio-Katalysator, deutlich verbessert. Das Reaktivitäts-Verhalten der ABPs wurde anhand der Abhängigkeit der molekularen sterischen Hinderung und des Einflusses von elektrophilen Grupen untersucht. Ausgehend von dem Gold Standard-ABP (HAUb-VME) und der systematischen Erweiterung mit einer Ethyl Gruppe (zu HAUB-VEE)

und einer weiteren Methyl Gruppe (zu HAUB-MVEE), nahm die Reaktivität stufenweise ab. Dennoch, das alternative Ersetzen der Methylester Gruppe von HAUB-VME mit der Monofluorgruppe (HAUb-VFEA) zeigte eine höhere Reaktivität im Vergleich zum Goldstandard HAUB-VME.

Zusammengefasst, unter Verwendung des verbesserten Syntheseprotokolls ist es gelungen fünf neuartige ABPs (HAUb-VEE, HAUb-MVEE, HAUb-VA, HAUb-VFEA und HAUb-VF_3EA) mit unterschiedlichen aktivitätsabhängigen DUB Bindungsprofilen zu synthetisieren. Das aktivitätsbasierte Profiling unter Verwendung des neuen hoch reaktiven HAUb-VFEA ermöglichte das detektieren von 63 aktiven DUBs in fünf verschiedenen Zelllinien (A549, EL-4, MCF-7, Jurkat E6-1 and HeLa S3). Diese Ergebnisse repräsentieren nicht nur die hohe Reaktivität von HAUB-VFEA, sondern zugleich auch das „DUBeom“ der einzelnen Zelllinien.

Der nächste Fokus dieser Arbeit war die Entwicklung neuer ABPs durch Einführung zusätzlicher Elemente die die Spezifität der DUBs hinsichtlich der Ubiquitin-Verknüpfung ansprechen. Die Intention war es eine neue Klasse von ABPs zu implementieren die es ermöglicht die DUBs Präferenz hinsichtilich der Ubiquitin-Verknüpfung in einem aktivitäts-basierten Assay zu profilen.

Das Resultat war eine neue Art von reaktiven Ubiquitin-Peptid basierten Sonden (Ubiquitin Isopeptide Activity Based Probe (UIPP)).

Im Gegensatzt zu standard ABPs beinhalten die UIPPs nicht nur Ubiquitin mit einer C-terminalen reaktiven Gruppe, sondern noch eine zusätzliche frei wählbare Peptidsequenz. Im Prinzip kann diese Peptid Sequence entweder von Ubiquitin oder von einem erdenklich ubiquitinierten Protein stammen. Demnach ist ein UIPP eine Nachahmung von einem Di-Ubiquitin oder einer Ubiquitinierung von gewünschten Proteinen. Da diese Konstellation eine völlig neue Art vom reaktiven Tool darstellt, wurde diese 2011 patentiert.

Aus dem Fakt, dass die DUBs die Ubiquitinverknüpfungen höchstwahrscheinlich anhand der Konsensus Sequenz unterscheiden, wurden die gut charakterisierten K_{48} - und K_{63} Polyubiquitin Verküpfungen ausgewählt um das UIPP Konzept zu validieren. Ein Aktivität-Shift-Assay zeigte in der Tat ein selektives Verhalten gegenüber USP15, UCHL3 und Ataxin-3, welches auch für den Peptid basierte Ansatz spricht.

Die Fähigkeit der kovalenten Bindung an das aktive Zentrum von DUBs wurde anhand Massen Spektrometrischer Analysen bestätigt.

Das aktivitätsbasierte Profiling im Zelllysat versus HAUB-VME deutete ebenfalls auf dessen Potential verschiedenen Ubiquitinverknüpfungen zu imitieren.
Der Funktionelle Proteomiks Ansatz in einem Zelllysat evaluierte die Spezifität bezüglich der Ubiquitinverknüpfung in einem mehr biologischen Milieu. Gute Anzeichen wurden für DUBs wie USP5, 7, 10, 12, 22, 28 und USP9X beobachtet, die eine deutliche Bindungspräferenz zu K48-UIPP aufzeigten, wobei K63-UIPP vorzugsweise USP16, 19, 38 und BAP1 gebunden hat.
Zusammengefasst, die in dieser Arbeit neu entwickelten ABPs und UIPPs repräsentieren ein ideales Tool zur Anreicherung von aktiven DUBs und für die Charaktereisierung dessen Spezifität bezüglich Ubiquitinverknüpfungen in einem biologischen Milieu. Die Kristallisation von DUBs in ihrer aktiven Konformation komplexiert mit UIPP würde ein wichtiges Requisit bieten, welches zur Generierung neuer DUB Inhibitoren nützen könnte.
Es kann angenommen werden, dass die Verwendung von UIPP das Drug Design beschleunigen und das Repertoire an molekularen Therapien erweitern könnte.

8 References

1. Pickart, C.M. & Eddins, M.J. Ubiquitin: structures, functions, mechanisms. *Biochimica et biophysica acta* **1695**, 55-72 (2004).

2. Welchman, R.L., Gordon, C. & Mayer, R.J. Ubiquitin and ubiquitin-like proteins as multifunctional signals. *Nature reviews. Molecular cell biology* **6**, 599-609 (2005).

3. Voges, D., Zwickl, P. & Baumeister, W. The 26S proteasome: a molecular machine designed for controlled proteolysis. *Annual review of biochemistry* **68**, 1015-68 (1999).

4. Song, L. & Rape, M. Reverse the curse–the role of deubiquitination in cell cycle control. *Current opinion in cell biology* **20**, 156–163 (2008).

5. Daniel, J. Multi-tasking on chromatin with the SAGA coactivator complexes. *Mutation Research/Fundamental and Molecular* **618**, 135-148 (2007).

6. Adhikari, A., Xu, M. & Chen, Z.J. Ubiquitin-mediated activation of TAK1 and IKK. *Oncogene* **26**, 3214-3226

7. Lee, E.G. Failure to Regulate TNF-Induced NF-kappa B and Cell Death Responses in A20-Deficient Mice. *Science* **289**, 2350-2354 (2000).

8. Janice A., F. Deubiquitinating Enzymes: Their Roles in Development, Differentiation, and Disease. **Volume 229**, 43-72 (2003).

9. Jiang, Y.-hui & Beaudet, A.L. Human disorders of ubiquitination and proteasomal degradation. *Current opinion in pediatrics* **16**, 419-26 (2004).

10. Kattenhorn, L.M., Korbel, G. a, Kessler, B.M., Spooner, E. & Ploegh, H.L. A deubiquitinating enzyme encoded by HSV-1 belongs to a family of cysteine proteases that is conserved across the family Herpesviridae. *Molecular cell* **19**, 547-57 (2005).

11. Rytkönen, A. & Holden, D.W. Bacterial interference of ubiquitination and deubiquitination. *Cell host & microbe* **1**, 13-22 (2007).

12. Misaghi, S. et al. Chlamydia trachomatis-derived deubiquitinating enzymes in mammalian cells during infection. *Molecular microbiology* **61**, 142-50 (2006).

13. Lindner, H. a Deubiquitination in virus infection. *Virology* **362**, 245-56 (2007).

14. Sompallae, R. et al. Epstein-barr virus encodes three bona fide ubiquitin-specific proteases. *Journal of virology* **82**, 10477-86 (2008).

15. Reyes-Turcu, F.E. & Wilkinson, K.D. Polyubiquitin binding and disassembly by deubiquitinating enzymes. *Chemical reviews* **109**, 1495–1508 (2009).

16. Raasi, S., Varadan, R., Fushman, D. & Pickart, C.M. Diverse polyubiquitin interaction properties of ubiquitin-associated domains. *Nature structural & molecular biology* **12**, 708-14 (2005).

17. Lenkinski, R.E., Chen, D.M., Glickson, J.D. & Goldstein, G. Nuclear magnetic resonance studies of the denaturation of ubiquitin. *Biochimica et Biophysica Acta (BBA) - Protein Structure* **494**, 126-130 (1977).

18. Baker, R.T. & Board, P.G. The human ubiquitin-52 amino acid fusion protein gene shares several structural features with mammalian ribosomal protein genes. *Nucleic acids research* **19**, 1035-40 (1991).

19. Ozkaynak, E., Finley, D., Solomon, M. & Varshavsky, A. The yeast ubiquitin genes: a family of natural gene fusions. *The EMBO journal* **6**, 1429 (1987).

20. Bloom, J., Amador, V., Bartolini, F., DeMartino, G. & Pagano, M. Proteasome-mediated degradation of p21 via N-terminal ubiquitinylation. *Cell* **115**, 71-82 (2003).

21. Pickart, C.M. Ubiquitin in chains. *Trends in biochemical sciences* **25**, 544–548 (2000).

22. Ikeda, F. & Dikic, I. Atypical ubiquitin chains: new molecular signals. "Protein Modifications: Beyond the Usual Suspects" review series. *EMBO reports* **9**, 536-42 (2008).

23. Kim, H.T. et al. Certain pairs of ubiquitin-conjugating enzymes (E2s) and ubiquitin-protein ligases (E3s) synthesize nondegradable forked ubiquitin chains containing all possible isopeptide linkages. *The Journal of biological chemistry* **282**, 17375-86 (2007).

24. Kirkpatrick, D.S., Denison, C. & Gygi, S.P. Weighing in on Ubiquitin: The Expanding Role of Mass Spectrometry-based Proteomics. *Nature cell biology* **7**, 750 (2005).

25. Bailey, D. & O'Hare, P. Comparison of the SUMO1 and ubiquitin conjugation pathways during the inhibition of proteasome activity with evidence of SUMO1 recycling. *The Biochemical journal* **392**, 271-81 (2005).

26. Geoffroy, M.-C. & Hay, R.T. An additional role for SUMO in ubiquitin-mediated proteolysis. *Nature reviews. Molecular cell biology* **10**, 564-8 (2009).

27. Schoenfeld, A.R., Apgar, S., Dolios, G., Wang, R. & Aaronson, S.A. BRCA2 is ubiquitinated in vivo and interacts with USP11, a deubiquitinating enzyme that exhibits prosurvival function in the cellular response to DNA damage. *Molecular and cellular biology* **24**, 7444 (2004).

28. Behrends, C. & Harper, J.W. Constructing and decoding unconventional ubiquitin chains. *Nature structural & molecular biology* **18**, 520-8 (2011).

29. Grabbe, C., Husnjak, K. & Dikic, I. The spatial and temporal organization of ubiquitin networks. *Nature reviews. Molecular cell biology* **12**, 295-307 (2011).

30. Komander, D., Clague, M.J. & Urbé, S. Breaking the chains: structure and function of the deubiquitinases. *Nature reviews. Molecular cell biology* **10**, 550-63 (2009).

31. Adhikari, A. & Chen, Z.J. Diversity of polyubiquitin chains. *Developmental cell* **16**, 485-6 (2009).

32. Xu, Y., Cao, H. & Chong, K. APC-targeted RAA1 degradation mediates the cell cycle and root development in plants. *Plant signaling & behavior* **5**, 218-23 (2010).

33. Ubiquitin Drug Discovery & Diagnostics Conference 2011.

34. Ranjani Varadan, Assfalg, M. & Fushman, D. Using NMR spectroscopy to monitor ubiquitin chain conformation and interactions with ubiquitin-binding domains. *Methods in enzymology* **399**, 177-92 (2005).

35. Jentsch, S. The ubiquitin-conjugation system. *Annual review of genetics* **26**, 179–207 (1992).

36. Scheffner, M., Nuber, U. & Huibregtse, J.M. Protein ubiquitination involving an E1-E2-E3 enzyme ubiquitin thioester cascade. *Nature* **373**, 81-3 (1995).

37. Disteche C.M., Zacksenhaus E., Adler D.A., Bressler S.L., Keitz B.T., C.V.M. Mapping and expression of the ubiquitin-activating enzyme E1 (Ube1) gene in the mouse. *Mamm Genome* **3**, 156-61 (1992).

38. Scheffner, M. & Huibregtse, J. Identification of a human ubiquitin-conjugating enzyme that mediates the E6-AP-dependent ubiquitination of p53. *Proceedings of the* **91**, 8797-801 (1994).

39. Chau, V. et al. A multiubiquitin chain is confined to specific lysine in a targeted short-lived protein. *Science* **243**, 1576 (1989).

40. Carvalho, A.F. et al. Ubiquitination of mammalian Pex5p, the peroxisomal import receptor. *The Journal of biological chemistry* **282**, 31267-72 (2007).

41. Cadwell, K. & Coscoy, L. Ubiquitination on nonlysine residues by a viral E3 ubiquitin ligase. *Science (New York, N.Y.)* **309**, 127-30 (2005).

42. Wang, X. et al. Ubiquitination of serine, threonine, or lysine residues on the cytoplasmic tail can induce ERAD of MHC-I by viral E3 ligase mK3. *The Journal of cell biology* **177**, 613-24 (2007).

43. Hough, R., Pratt, G. & Rechsteiner, M. Purification of two high molecular weight proteases from rabbit reticulocyte lysate. *Journal of Biological Chemistry* **262**, 8303 (1987).

44. Pickart, C. Targeting of substrates to the 26S proteasome. *The FASEB journal* 1055-1066 (1997).

45. Xu, P. et al. Quantitative proteomics reveals the function of unconventional ubiquitin chains in proteasomal degradation. *Cell* **137**, 133-45 (2009).

46. Matsumoto, M.L. et al. K11-linked polyubiquitination in cell cycle control revealed by a K11 linkage-specific antibody. *Molecular cell* **39**, 477-84 (2010).

47. Ostendorff, H.P. et al. Ubiquitination-dependent cofactor exchange on LIM homeodomain transcription factors. *Nature* **416**, 99–103 (2002).

48. Sijts, E.J. a M. & Kloetzel, P.M. The role of the proteasome in the generation of MHC class I ligands and immune responses. *Cellular and molecular life sciences : CMLS* **68**, 1491-502 (2011).

49. Piotrowski, J., Beal, R. & Hoffman, L. Inhibition of the 26 S proteasome by polyubiquitin chains synthesized to have defined lengths. *Journal of Biological* **272**, 23712-21 (1997).

50. Hammond-Martel, I., Yu, H. & Affar, E.B. Roles of ubiquitin signaling in transcription regulation. *Cellular signalling* (2011).

51. Strous, G.J., van Kerkhof, P., Govers, R., Ciechanover, a & Schwartz, a L. The ubiquitin conjugation system is required for ligand-induced endocytosis and degradation of the growth hormone receptor. *The EMBO journal* **15**, 3806-12 (1996).

52. Rotin, D., Staub, O. & Haguenauer-Tsapis, R. Ubiquitination and endocytosis of plasma membrane proteins: role of Nedd4/Rsp5p family of ubiquitin-protein ligases. *Journal of Membrane Biology* **176**, 1–17 (2000).

53. Katzmann, D.J., Babst, M. & Emr, S.D. Ubiquitin-dependent sorting into the multivesicular body pathway requires the function of a conserved endosomal protein sorting complex, ESCRT-I. *Cell* **106**, 145–155 (2001).

54. Stang, E., Johannessen, L.E., Knardal, S.L. & Madshus, I.H. Polyubiquitination of the epidermal growth factor receptor occurs at the plasma membrane upon ligand-induced activation. *Journal of Biological Chemistry* **275**, 13940 (2000).

55. Patnaik, a, Chau, V. & Wills, J.W. Ubiquitin is part of the retrovirus budding machinery. *Proceedings of the National Academy of Sciences of the United States of America* **97**, 13069-74 (2000).

56. Kumar, S., Tomooka, Y. & Noda, M. Identification of a set of genes with developmentally down-regulated expression in the mouse brain. *Biochemical and biophysical research communications* **185**, 1155–1161 (1992).

57. Jones, J. et al. A targeted proteomic analysis of the ubiquitin-like modifier nedd8 and associated proteins. *Journal of proteome research* **7**, 1274–1287 (2008).

58. Whitby, F.G., Xia, G., Pickart, C.M. & Hill, C.P. Crystal structure of the human ubiquitin-like protein NEDD8 and interactions with ubiquitin pathway enzymes. *The Journal of biological chemistry* **273**, 34983-91 (1998).

59. Loeb, K.R. & Haas, a L. The interferon-inducible 15-kDa ubiquitin homolog conjugates to intracellular proteins. *The Journal of biological chemistry* **267**, 7806-13 (1992).

60. Ebstein, F. et al. Maturation of human dendritic cells is accompanied by functional remodelling of the ubiquitin-proteasome system. *The International Journal of Biochemistry & Cell Biology* **41**, 1205-1215 (2009).

61. Liu, C., Chang, R., Yao, X., Qiao, W.T. & Geng, Y.Q. ISG15 expression in response to double-stranded RNA or LPS in cultured Fetal bovine lung (FBL) cells. *Veterinary research communications* **33**, 723-33 (2009).

62. Vertegaal, A.C.O. et al. Distinct and overlapping sets of SUMO-1 and SUMO-2 target proteins revealed by quantitative proteomics. *Molecular & cellular proteomics : MCP* **5**, 2298-310 (2006).

63. Mark Hochstrasser Identification of SUMO-Interacting Proteins by Yeast Two-Hybrid Analysis. *Methods Mol Biol.* **497**, 1-13 (2009).

64. Wang, Y. et al. Identification and developmental expression of Xenopus laevis SUMO proteases. *PloS one* **4**, e8462 (2009).

65. Schmidtke, G. et al. The UBA domains of NUB1L are required for binding but not for accelerated degradation of the ubiquitin-like modifier FAT10. *The Journal of biological chemistry* **281**, 20045-54 (2006).

66. Canaan, A. et al. FAT10/diubiquitin-like protein-deficient mice exhibit minimal phenotypic differences. *Molecular and cellular biology* **26**, 5180-9 (2006).

67. Nijman, S.M.B. et al. A genomic and functional inventory of deubiquitinating enzymes. *Cell* **123**, 773-86 (2005).

68. Davies, J.E., Sarkar, S. & Rubinsztein, D.C. The ubiquitin proteasome system in Huntington's disease and the spinocerebellar ataxias. *BMC biochemistry* **8 Suppl 1**, S2 (2007).

69. Wertz, I.E. et al. De-ubiquitination and ubiquitin ligase domains of A20 downregulate NF B signalling. *Nature* **430**, 694–699 (2004).

70. Hussain, S., Zhang, Y. & Galardy, P.J. DUBs and cancer: the role of deubiquitinating enzymes as oncogenes, non-oncogenes and tumor suppressors. *Cell cycle (Georgetown, Tex.)* **8**, 1688-97 (2009).

71. Reyes-Turcu, F.E. & Wilkinson, K.D. Polyubiquitin binding and disassembly by deubiquitinating enzymes. *Chemical Reviews* **109**, 1495-1508 (2009).

72. Lam, Y. a, Xu, W., DeMartino, G.N. & Cohen, R.E. Editing of ubiquitin conjugates by an isopeptidase in the 26S proteasome. *Nature* **385**, 737-40 (1997).

73. Borodovsky, a et al. A novel active site-directed probe specific for deubiquitylating enzymes reveals proteasome association of USP14. *The EMBO journal* **20**, 5187-96 (2001).

74. Verma, R., Aravind, L., Oania, R. & McDonald, W. Role of Rpn11 metalloprotease in deubiquitination and degradation by the 26S proteasome. *Science* **298**, 611-5 (2002).

75. Henry, K., Wyce, A., Lo, W. & Duggan, L. Transcriptional activation via sequential histone H2B ubiquitylation and deubiquitylation, mediated by SAGA-associated Ubp8. *Genes &* **17**, 2648-2663 (2003).

76. Haglund, K., Sigismund, S. & Polo, S. Multiple monoubiquitination of RTKs is sufficient for their endocytosis and degradation. *Nature cell* **5**, 461-466 (2003).

77. Ye, Y. & Rape, M. Building ubiquitin chains: E2 enzymes at work. *Nature reviews. Molecular cell biology* **10**, 755-64 (2009).

78. Sieburth, D. et al. Systematic analysis of genes required for synapse structure and function. *Nature* **436**, 510-7 (2005).

79. Barrios-Rodiles, M., Brown, K., Ozdamar, B. & Bose, R. High-throughput mapping of a dynamic signaling network in mammalian cells. *Science* **307**, 1621-5 (2005).

80. Clague, M.J. & Urbé, S. Endocytosis: the DUB version. *Trends in cell biology* **16**, 551-9 (2006).

81. Row, P.E. et al. The MIT domain of UBPY constitutes a CHMP binding and endosomal localization signal required for efficient epidermal growth factor receptor degradation. *The Journal of biological chemistry* **282**, 30929-37 (2007).

82. Ernst, R., Mueller, B., Ploegh, H.L. & Schlieker, C. The otubain YOD1 is a deubiquitinating enzyme that associates with p97 to facilitate protein dislocation from the ER. *Molecular cell* **36**, 28-38 (2009).

83. Larsen, C.N., Krantz, B.A. & Wilkinson, K.D. Substrate specificity of deubiquitinating enzymes: ubiquitin C-terminal hydrolases. *Biochemistry* **37**, 3358–3368 (1998).

84. Butterworth, M.B. et al. The deubiquitinating enzyme UCH-L3 regulates the apical membrane recycling of the epithelial sodium channel. *The Journal of biological chemistry* **282**, 37885-93 (2007).

85. Dayal, S. et al. Suppression of the deubiquitinating enzyme USP5 causes the accumulation of unanchored polyubiquitin and the activation of p53. *Journal of Biological Chemistry* **284**, 5030 (2009).

86. Li, M., Brooks, C.L., Kon, N. & Gu, W. A dynamic role of HAUSP in the p53-Mdm2 pathway. *Molecular cell* **13**, 879-86 (2004).

87. Shen, C. et al. Calcium/calmodulin regulates ubiquitination of the ubiquitin-specific protease TRE17/USP6. *The Journal of biological chemistry* **280**, 35967-73 (2005).

88. Popov, N., Wanzel, M., Madiredjo, M. & Zhang, D. The ubiquitin-specific protease USP28 is required for MYC stability. *Nature cell* **9**, 765-774 (2007).

89. Huang, T., Nijman, S. & Mirchandani, K. Regulation of monoubiquitinated PCNA by DUB autocleavage. *Nature cell* **8**, 339-347 (2006).

90. Nicassio, F. et al. Human USP3 is a chromatin modifier required for S phase progression and genome stability. *Current biology : CB* **17**, 1972-7 (2007).

91. Zhang, D., Zaugg, K. & Mak, T. A role for the deubiquitinating enzyme USP28 in control of the DNA-damage response. *Cell* **126**, 529-542 (2006).

92. Hu, M. et al. Structure and mechanisms of the proteasome-associated deubiquitinating enzyme USP14. *The EMBO journal* **24**, 3747-56 (2005).

93. Hetfeld, B.K.J. et al. The zinc finger of the CSN-associated deubiquitinating enzyme USP15 is essential to rescue the E3 ligase Rbx1. *Current biology : CB* **15**, 1217-21 (2005).

94. Cooper, E.M. et al. K63-specific deubiquitination by two JAMM/MPN+ complexes: BRISC-associated Brcc36 and proteasomal Poh1. *The EMBO journal* **28**, 621-31 (2009).

95. Brummelkamp, T.R., Nijman, S.M.B., Dirac, A.M.G. & Bernards, R. Loss of the cylindromatosis tumour suppressor inhibits apoptosis by activating NF-kappaB. *Nature* **424**, 797-801 (2003).

96. Lin, C.-H., Chang, H.-S. & Yu, W.C.Y. USP11 stabilizes HPV-16E7 and further modulates the E7 biological activity. *The Journal of biological chemistry* **283**, 15681-8 (2008).

97. Vos, R.M., Altreuter, J., White, E. a & Howley, P.M. The ubiquitin-specific peptidase USP15 regulates human papillomavirus type 16 E6 protein stability. *Journal of virology* **83**, 8885-92 (2009).

98. Crosas, B. et al. Ubiquitin chains are remodeled at the proteasome by opposing ubiquitin ligase and deubiquitinating activities. *Cell* **127**, 1401-13 (2006).

99. Yao, T. et al. Distinct modes of regulation of the Uch37 deubiquitinating enzyme in the proteasome and in the Ino80 chromatin-remodeling complex. *Molecular cell* **31**, 909-17 (2008).

100. Yoshida, H., Jono, H., Kai, H. & Li, J.-D. The tumor suppressor cylindromatosis (CYLD) acts as a negative regulator for toll-like receptor 2 signaling via negative cross-talk with TRAF6 AND TRAF7. *The Journal of biological chemistry* **280**, 41111-21 (2005).

101. Matsuoka, S. et al. ATM and ATR substrate analysis reveals extensive protein networks responsive to DNA damage. *Science (New York, N.Y.)* **316**, 1160-6 (2007).

102. Todi, S.V. et al. Ubiquitination directly enhances activity of the deubiquitinating enzyme ataxin-3. *The EMBO journal* **28**, 372-82 (2009).

103. Meulmeester, E., Kunze, M., Hsiao, H.H., Urlaub, H. & Melchior, F. Mechanism and consequences for paralog-specific sumoylation of ubiquitin-specific protease 25. *Molecular cell* **30**, 610-9 (2008).

104. Komander, D. et al. Molecular discrimination of structurally equivalent Lys 63-linked and linear polyubiquitin chains. *EMBO reports* **10**, 466-73 (2009).

105. Gupta, S.P. Quantitative structure-activity relationship studies on zinc-containing metalloproteinase inhibitors. *Chemical reviews* **107**, 3042–3087 (2007).

106. Sato, Y. et al. Structural basis for specific cleavage of Lys 63-linked polyubiquitin chains. *Nature* **455**, 358-62 (2008).

107. Turner, G.C. Detecting and Measuring Cotranslational Protein Degradation in Vivo. *Science* **289**, 2117-2120 (2000).

108. Boudreaux, D.A., Maiti, T.K., Davies, C.W. & Das, C. Ubiquitin vinyl methyl ester binding orients the misaligned active site of the ubiquitin hydrolase UCHL1 into productive conformation. *Proceedings of the National Academy of Sciences* **107**, 9117 (2010).

109. Hu, M. et al. Crystal structure of a UBP-family deubiquitinating enzyme in isolation and in complex with ubiquitin aldehyde. *Cell* **111**, 1041–1054 (2002).

110. Kovalenko, A. et al. The tumour suppressor CYLD negatively regulates NF-kappaB signalling by deubiquitination. *Nature* **424**, 801-805 (2003).

111. Overstreet, E., Fitch, E. & Fischer, J.A. Fat facets and Liquid facets promote Delta endocytosis and Delta signaling in the signaling cells. *Development Cambridge England* **131**, 5355-5366 (2004).

112. Reyes-Turcu, F.E., Ventii, K.H. & Wilkinson, K.D. Regulation and cellular roles of ubiquitin-specific deubiquitinating enzymes. *Annual review of biochemistry* **78**, 363-97 (2009).

113. Winborn, B.J. et al. The deubiquitinating enzyme ataxin-3, a polyglutamine disease protein, edits Lys63 linkages in mixed linkage ubiquitin chains. *Journal of Biological Chemistry* **283**, 26436 (2008).

114. Yao, T. A cryptic protease couples deubiquitination and degradation by the proteasome. *Nature* **419**, 403-407 (2002).

115. McCullough, J. et al. Activation of the endosome-associated ubiquitin isopeptidase AMSH by STAM, a component of the multivesicular body-sorting machinery. *Current biology : CB* **16**, 160-5 (2006).

116. Shao, G. et al. The Rap80-BRCC36 de-ubiquitinating enzyme complex antagonizes RNF8-Ubc13-dependent ubiquitination events at DNA double strand breaks. *Proceedings of the National Academy of Sciences of the United States of America* **106**, 3166-3171 (2009).

117. McCullough, J. et al. Activation of the endosome-associated ubiquitin isopeptidase AMSH by STAM, a component of the multivesicular body-sorting machinery. *Current Biology* **16**, 160-165 (2006).

118. Makarova, K.S., Aravind, L. & Koonin, E.V. A novel superfamily of predicted cysteine proteases from eukaryotes, viruses and Chlamydia pneumoniae. *Trends in Biochemical Sciences* **25**, 50-52 (2000).

119. Goodrich, J.S., Clouse, K.N. & Schüpbach, T. Hrb27C, Sqd and Otu cooperatively regulate gurken RNA localization and mediate nurse cell chromosome dispersion in Drosophila oogenesis. *Development (Cambridge, England)* **131**, 1949-58 (2004).

120. Juris, S.J., Shah, K., Shokat, K., Dixon, J.E. & Vacratsis, P.O. Identification of otubain 1 as a novel substrate for the Yersinia protein kinase using chemical genetics and mass spectrometry. *FEBS letters* **580**, 179-83 (2006).

121. Soares, L. et al. Two isoforms of otubain 1 regulate T cell anergy via GRAIL. *Nature immunology* **5**, 45-54 (2004).

122. Cravatt, B.F., Wright, A.T. & Kozarich, J.W. Activity-Based Protein Profiling : From Enzyme Chemistry to Proteomic Chemistry. *Annual Review of Biochemistry* (2008).

123. Dang, T.H.T. et al. Chemical probes of surface layer biogenesis in Clostridium difficile. *ACS Chemical Biology* **5**, 279–285 (2010).

124. Haedke, U., Götz, M., Baer, P. & Verhelst, S.H.L. Alkyne derivatives of isocoumarins as clickable activity-based probes for serine proteases. *Bioorganic & medicinal chemistry* 1-8 (2011).

125. Meldal, M. & Tornøe, C.W. Cu-catalyzed azide- alkyne cycloaddition. *Chemical reviews* **108**, 2952–3015 (2008).

126. Muralidharan, V. & Muir, T.W. Protein ligation: an enabling technology for the biophysical analysis of proteins. *Nature methods* **3**, 429–438 (2006).

127. Wilkinson, K., Cox, M. & Mayer, A. Synthesis and characterization of ubiquitin ethyl ester, a new substrate for ubiquitin carboxyl-terminal hydrolase. *Biochemistry* **25**, 6644-9 (1986).

128. Borodovsky, A. et al. Chemistry-based functional proteomics reveals novel members of the deubiquitinating enzyme family. *Chemistry & biology* **9**, 1149-59 (2002).

129. Bradford, M. RAPID AND SENSITIVE METHOD FOR QUANTITATION OF MICROGRAM QUANTITIES OF PROTEIN UTILIZING PRINCIPLE OF PROTEIN-DYE BINDING. *Analytical Biochemistry* **72**, 248-254 (1976).

130. Hemelaar, J., Borodovsky, A. & Kessler, B. Specific and covalent targeting of conjugating and deconjugating enzymes of ubiquitin-like proteins. *and cellular biology* **24**, 84-95 (2004).

131. Borodovsky, A. et al. Small-molecule inhibitors and probes for ubiquitin- and ubiquitin-like-specific proteases. *Chembiochem : a European journal of chemical biology* **6**, 287-91 (2005).

132. Heal, W.P., Dang, T.H.T. & Tate, E.W. Activity-based probes: discovering new biology and new drug targets. *Chemical Society reviews* **40**, 246-57 (2011).

133. Hillaert, U. et al. Receptor-mediated targeting of cathepsins in professional antigen presenting cells. *Angewandte Chemie (International ed. in English)* **48**, 1629-32 (2009).

134. Barglow, K.T. & Cravatt, B.F. Activity-based protein profiling for the functional annotation of enzymes. *Nature Methods* **4**, 822–827 (2007).

135. Larkin, M.A. et al. Clustal W and Clustal X version 2.0. *Bioinformatics* **23**, 2947-2948 (2007).

136. Huson, D.H. et al. Dendroscope: An interactive viewer for large phylogenetic trees. *BMC Bioinformatics* **8**, 460 (2007).

137. de Hoon, M.J.L., Imoto, S., Nolan, J. & Miyano, S. Open source clustering software. *Bioinformatics (Oxford, England)* **20**, 1453-4 (2004).

138. Saldanha, A.J. Java Treeview -- extensible visualization of microarray data. *Bioinformatics* **20**, (2004).

139. Shabek, N., Iwai, K. & Ciechanover, A. Ubiquitin is degraded by the ubiquitin system as a monomer and as part of its conjugated target. *Biochemical and biophysical research communications* **363**, 425-31 (2007).

140. Verhoef, L.G.G.C. et al. Minimal length requirement for proteasomal degradation of ubiquitin-dependent substrates. *The FASEB journal : official publication of the Federation of American Societies for Experimental Biology* **23**, 123-33 (2009).

141. Drag, M. et al. Positional-scanning fluorigenic substrate libraries reveal unexpected specificity determinants of DUBs (deubiquitinating enzymes). *The Biochemical journal* **415**, 367-75 (2008).

142. Komander, D. Conjugation and Deconjugation of Ubiquitin Family Modifiers: Mechanism, Specificity And Structure Of The Deubiquitinases. *Subcellular Biochemistry* **54**, 69-87 (2010).

143. Love, K.R., Pandya, R.K., Spooner, E. & Ploegh, H.L. Ubiquitin C-terminal electrophiles are activity-based probes for identification and mechanistic study of ubiquitin conjugating machinery. *ACS chemical biology* **4**, 275–287 (2009).

144. Schlieker, C., Korbel, G.A., Kattenhorn, L.M. & Ploegh, H.L. A Deubiquitinating Activity Is Conserved in the Large Tegument Protein of the Herpesviridae. *Society* **79**, 15582-15585 (2005).

145. Müller, K., Faeh, C. & Diederich, F. Fluorine in pharmaceuticals: looking beyond intuition. *Science (New York, N.Y.)* **317**, 1881-6 (2007).

146. Wu, C. et al. BioGPS: an extensible and customizable portal for querying and organizing gene annotation resources. *Genome biology* **10**, R130 (2009).

147. Shankavaram, U.T. et al. Transcript and protein expression profiles of the NCI-60 cancer cell panel: an integromic microarray study. *Molecular cancer therapeutics* **6**, 820-32 (2007).

148. Lee, H.-J. et al. The expression patterns of deubiquitinating enzymes, USP22 and Usp22. *Gene expression patterns : GEP* **6**, 277-84 (2006).

149. Zhang, Y. et al. Elevated expression of USP22 in correlation with poor prognosis in patients with invasive breast cancer. *Journal of cancer research and clinical oncology* **137**, 1245-53 (2011).

150. Pijnappel, W.W.M.P. & Timmers, H.T.M. Dubbing SAGA unveils new epigenetic crosstalk. *Molecular cell* **29**, 152-4 (2008).

151. Luna-Vargas, M.P. a et al. Ubiquitin-specific protease 4 is inhibited by its ubiquitin-like domain. *EMBO reports* **12**, 365-72 (2011).

152. Su, A.I. et al. A gene atlas of the mouse and human protein-encoding transcriptomes. *Proceedings of the National Academy of Sciences of the United States of America* **101**, 6062 (2004).

153. Parsons JL., et al., USP47 is a deubiquitylating enzyme that regulates base excision repair by controlling steady-state levels of DNA polymerase β, Molecular Cell, Volume 41, Issue 5, 609-615 (2011).

154. Williams, S.A. et al. USP1 Deubiquitinates ID Proteins to Preserve a Mesenchymal Stem Cell Program in Osteosarcoma. *Cell* **146**, 918-930 (2011).

155. Todi, S.V. et al. Activity and cellular functions of the deubiquitinating enzyme and polyglutamine disease protein ataxin-3 are regulated by ubiquitination at lysine 117. *The Journal of Biological Chemistry* **285**, 39303-39313 (2010).

156. Edelmann, M.J., Kramer, H.B., Altun, M. & Kessler, B.M. Post-translational modification of the deubiquitinating enzyme otubain 1 modulates active RhoA levels and susceptibility to Yersinia invasion. *The FEBS journal* **277**, 2515-2530 (2010).

157. Johnston, S.C., Larsen, C.N., Cook, W.J., Wilkinson, K.D. & Hill, C.P. Crystal structure of a deubiquitinating enzyme (human UCH-L3) at 1.8 A resolution. *the The European Molecular Biology Organization Journal* **16**, 3787-3796 (1997).

158. Ovaa, H. Active-site directed probes to report enzymatic action in the ubiquitin proteasome system. *Nature reviews. Cancer* **7**, 613-20 (2007).

159. Coleman, J. Zinc enzymes. *Current opinion in chemical biology* **2**, 222-34 (1998).

160. Kim, D.H. & Mobashery, S. Mechanism-based inhibition of zinc proteases. *Current medicinal chemistry* **8**, 959-65 (2001).

161. Li, Y.M. et al. Photoactivated gamma-secretase inhibitors directed to the active site covalently label presenilin 1. *Nature* **405**, 689-94 (2000).

162. Hagenstein, M.C. et al. Affinity-based tagging of protein families with reversible inhibitors: a concept for functional proteomics. *Angewandte Chemie (International ed. in English)* **42**, 5635-8 (2003).

163. Saghatelian, A., Jessani, N., Joseph, A., Humphrey, M. & Cravatt, B.F. Activity-based probes for the proteomic profiling of metalloproteases. *Proceedings of the National Academy of Sciences of the United States of America* **101**, 10000 (2004).

164. Catic, A. et al. Screen for ISG15-crossreactive deubiquitinases. *PloS one* **2**, e679 (2007).

165. Gredmark, S., Schlieker, C., Quesada, V., Spooner, E. & Ploegh, H.L. A functional ubiquitin-specific protease embedded in the large tegument protein (ORF64) of murine gammaherpesvirus 68 is active during the course of infection. *Journal of virology* **81**, 10300-9 (2007).

166. Love, K.R., Pandya, R.K., Spooner, E. & Ploegh, H.L. Ubiquitin C-Terminal Electrophiles Are Activity-Based Probes for Identification and Mechanistic Study of Ubiquitin Conjugating Machinery. *ACS Chemical Biology* **4**, 275-287 (2009).

167. Ovaa, H. et al. Activity-based ubiquitin-specific protease (USP) profiling of virus-infected and malignant human cells. *Proceedings of the National Academy of Sciences of the United States of America* **101**, 2253 (2004).

168. Rolén, U. et al. Activity profiling of deubiquitinating enzymes in cervical carcinoma biopsies and cell lines. *Molecular carcinogenesis* **45**, 260–269 (2006).

169. Gan-Erdene, T. et al. Identification and characterization of DEN1, a deneddylase of the ULP family. *The Journal of biological chemistry* **278**, 28892-900 (2003).

170. El Oualid, F. et al. Chemical Synthesis of Ubiquitin, Ubiquitin-Based Probes, and Diubiquitin. *Angewandte Chemie International Edition* **49**, 10149–10153 (2010).

171. Setsuie, R., Sakurai, M., Sakaguchi, Y. & Wada, K. Ubiquitin dimers control the hydrolase activity of UCH-L3. *Neurochemistry International* **54**, 314-321 (2009).

172. Misaghi, S. et al. Structure of the ubiquitin hydrolase UCH-L3 complexed with a suicide substrate. *The Journal of biological chemistry* **280**, 1512-20 (2005).

173. Nicastro, G. et al. Understanding the Role of the Josephin Domain in the PolyUb Binding and Cleavage Properties of Ataxin-3. *PloS one* **5**, e12430 (2010).

174. Chai, Y., Berke, S.S., Cohen, R.E. & Paulson, H.L. Poly-ubiquitin binding by the polyglutamine disease protein ataxin-3 links its normal function to protein surveillance pathways. *Journal of Biological Chemistry* **279**, 3605 (2004).

175. Weeks, S.D., Grasty, K.C., Hernandez-Cuebas, L. & Loll, P.J. Crystal structure of a Josephin-ubiquitin complex: evolutionary restraints on ataxin-3 deubiquitinating activity. *The Journal of biological chemistry* **286**, 4555-65 (2011).

176. Komander, D. et al. The structure of the CYLD USP domain explains its specificity for Lys63-linked polyubiquitin and reveals a B box module. *Molecular cell* **29**, 451-64 (2008).

177. Markin, C.J., Xiao, W. & Spyracopoulos, L. Mechanism for Recognition of Polyubiquitin Chains: Balancing Affinity through Interplay between Multivalent Binding and Dynamics. *Journal of the American Chemical Society* **132**, 11247-58 (2010).

178. Reyes-Turcu, F.E. et al. The ubiquitin binding domain ZnF UBP recognizes the C-terminal diglycine motif of unanchored ubiquitin. *Cell* **124**, 1197–1208 (2006).

179. Faesen, A.C. et al. Mechanism of USP7/HAUSP Activation by Its C-Terminal Ubiquitin-like Domain and Allosteric Regulation by GMP-Synthetase. *Molecular cell* **44**, 147-59 (2011).

180. Ye, Y. et al. Polyubiquitin binding and cross-reactivity in the USP domain deubiquitinase USP21. *EMBO reports* **12**, 350-7 (2011).

181. Chen, Z. et al. Prediction of Ubiquitination Sites by Using the Composition of k-Spaced Amino Acid Pairs. *PLoS ONE* **6**, e22930 (2011).

182. Hassink, G.C. et al. The ER-resident ubiquitin-specific protease 19 participates in the UPR and rescues ERAD substrates. *EMBO reports* **10**, 755-61 (2009).

183. Li, M. et al. Deubiquitination of p53 by HAUSP is an important pathway for p53 stabilization. *Nature* **416**, 648–653 (2002).

184. Saridakis, V. et al. Structure of the p53 binding domain of HAUSP/USP7 bound to Epstein-Barr nuclear antigen 1 implications for EBV-mediated immortalization. *Molecular cell* **18**, 25-36 (2005).

185. Sundaram, P., Pang, Z., Miao, M., Yu, L. & Wing, S.S. USP19-deubiquitinating enzyme regulates levels of major myofibrillar proteins in L6 muscle cells. *American journal of physiology. Endocrinology and metabolism* **297**, E1283-90 (2009).

186. Lauwers, E., Jacob, C. & André, B. K63-linked ubiquitin chains as a specific signal for protein sorting into the multivesicular body pathway. *The Journal of cell biology* **185**, 493-502 (2009).

187. Tan, J.M.M. et al. Lysine 63-linked ubiquitination promotes the formation and autophagic clearance of protein inclusions associated with neurodegenerative diseases. *Human molecular genetics* **17**, 431-9 (2008).

188. Gumbiner, B.M. Regulation of Cadherin Adhesive Activity. *Cell* **148**, 399-403 (2000).

189. Bonazzi, M., Veiga, E., Pizarro-Cerdá, J. & Cossart, P. Successive post-translational modifications of E-cadherin are required for InlA-mediated internalization of Listeria monocytogenes. *Cellular microbiology* **10**, 2208-22 (2008).

190. Buus, R., Faronato, M., Hammond, D.E., Urbé, S. & Clague, M.J. Deubiquitinase activities required for hepatocyte growth factor-induced scattering of epithelial cells. *Current Biology* **19**, 1463–1466 (2009).

191. Yee, M.-C., Fas, S.C., Stohlmeyer, M.M., Wandless, T.J. & Cimprich, K. a A cell-permeable, activity-based probe for protein and lipid kinases. *The Journal of biological chemistry* **280**, 29053-9 (2005).

192. Borodovsky, A., Ovaa, H. & Kessler, B. Applications for Chemical Probes of Proteolytic Activity. *Protein Science* 1-35 (2004).

193. Olson, E.S. et al. Activatable cell penetrating peptides linked to nanoparticles as dual probes for in vivo fluorescence and MR imaging of proteases. *Proceedings of the National Academy of Sciences of the United States of America* **107**, 4311-6 (2010).

194. Jing, C. & Cornish, V.W. Chemical Tags for Labeling Proteins Inside Living Cells. *Accounts of Chemical Research* **44**, (2011).

195. Rotili, D. et al. Photoactivable peptides for identifying enzyme-substrate and protein-protein interactions. *Chemical communications (Cambridge, England)* **47**, 1488-90 (2011).

196. Wright, A.T., Song, J.D. & Cravatt, B.F. A suite of activity-based probes for human cytochrome P450 enzymes. *Journal of the American Chemical Society* **131**, 10692–10700 (2009).

197. Jiang, H. et al. Mechanism-based small molecule probes for labeling CD38 on live cells. *Journal of the American Chemical Society* **131**, 1658–1659 (2009).

198. Tantama, M., Lin, W.-C. & Licht, S. An activity-based protein profiling probe for the nicotinic acetylcholine receptor. *Journal of the American Chemical Society* **130**, 15766-7 (2008).

199. Chiang, K.P., Niessen, S., Saghatelian, A. & Cravatt, B.F. An enzyme that regulates ether lipid signaling pathways in cancer annotated by multidimensional profiling. *Chemistry & biology* **13**, 1041-50 (2006).

200. Böttcher, T. & Sieber, S. a Beta-lactones as privileged structures for the active-site labeling of versatile bacterial enzyme classes. *Angewandte Chemie (International ed. in English)* **47**, 4600-3 (2008).

201. Bo ttcher, T. & Sieber, S.A. Showdomycin as a versatile chemical tool for the detection of pathogenesis-associated enzymes in bacteria. *Journal of the American Chemical Society* **132**, 6964–6972 (2010).

202. Ovaa, H. et al. Activity-based ubiquitin-specific protease (USP) profiling of virus-infected and malignant human cells. *Proceedings of the National Academy of Sciences of the United States of America* **101**, 2253 (2004).

203. Love, K.R., Pandya, R.K., Spooner, E. & Ploegh, H.L. Ubiquitin C-terminal electrophiles are activity-based probes for identification and mechanistic study of ubiquitin conjugating machinery. *ACS chemical biology* **4**, 275–287 (2009).

9 Acknowledgements

Prof. Dr. Lothar Jänsch danke ich herzlich für die Betreuung meiner Arbeit und die wunderbare Zeit in seiner Arbeitsgruppe, die ich sehr vermissen werde. Die hervorragenden Arbeitsbedingungen, sein Interesse an meinem Thema, die ständige Diskussionsbereitschaft und seine Bereitschaft auf persönliche Bedürfnisse einzugehen, weiß ich sehr zu schätzen. Desweitern möchte ich mich dafür bedanken, dass ich an internationalen Konferenzen teilnehmen durfte und damit meinen wissenschaftlichen Horizont erheblich erweitern konnte.

Prof. Dr. Michael Steinert danke ich sehr herzlich für die bereitwillige Übernahme des Zweitgutachtens.

Ebenso möchte ich mich für die Übernahme des Prüfungsvorsitzes bei Prof. Dr. Stefan Dübel bedanken.

Bei Dr. Raimo Franke möchte ich mich für die ausgezeichnete Kooperation, herzliche Unterstützung und kontinuierliche Diskussionsbereitschaft bedanken. Die gute Zusammenarbeit hat einen wichtigen Beitrag zum Gelingen der Arbeit geleistet.

Bei Kathrin Goltz und Undine Felgenträger möchte ich mich herzlichst für ihre wertvolle Hilfe, dauernden motivierten Einsatz, ständige Unterstützung und die unglaublich schöne Arbeitsatmosphäre bedanken.

Meiner Masterstudentin Anne Kummer möchte ich ebenfalls einen großen Dank für ihr großes Engagement im Labor, die tolle Zusammenarbeit und tatkräftige Unterstützung aussprechen.

Bei Dr. Manfred Nimtz möchte ich mich für seine Einführung in die Massenspectrometrie und die ständige Hilfsbereitschaft beim Auswerten der Spektren bedanken.

Ein sehr herzlicher Dank für die gute Arbeitsatmosphäre, wertvolle Unterstützungen und Diskussionen und für die schöne gemeinsame Zeit gilt auch meinen Mädels, Susanne Freund, Evelin Berger und Kirstin Jurrat.

Kirsten Minkhart, Anja Meier und Andrea Abrahamik danke ich für die wertvolle technische Unterstützung während der Massenspectrometrie Messungen.

Ein herzliches Dankeschön geht an Dr. Uwe Kärst für die wichtigen „up to date“ Literaturhinweise und seine ständige Hilfsbereitschaft. Außerdem möchte ihm und Amanda Mühlmann auch noch für das Korrekturlesen danken.

Desweiteren geht mein Dank auch an die Strukturbiologen Dr. Jörn Krauße, Dr. Joachim Reichelt und Dr. Peer Lukat, die mich beim Modulieren des UIPP Konstrukts unterstüzt haben und natürlich auch an die restlichen Gruppemitgliedern, die mir bei der Proteinaufreinigung mit Rat und Tat zur Seite gestanden haben.
Dr. Joop van den Heuvel und Daniela Gebauer danke ich für die Unterstützung bei der Fermentation des HAUb-Konstrukts.

Der ganzen CPRO Gruppe gilt mein tiefster Dank für das wunderbare Arbeitsklima, die schönen Ausflüge, die schönen Kaffeepausen und den vielen kleinen und großen Unterstützungen, die hier leider nicht alle erwähnt werden können.

Liebe Nadine, dir danke ich herzlichst für deine Geduld, Verständnis und die liebevolle Versorgung gerade in den letzten stressigen Monaten meiner Doktorarbeit. Dafür, und für die Liebe, die du mir entgegenbringst, bin ich froh, dass ich dich habe.

Zu guter Letzt danke ich herzlichst meiner Familie für die grenzenlose Unterstützung während meiner gesamten akademischen Ausbildung. Ohne Euch wäre es nicht möglich gewesen, das Studium, die Auslandsaufenthalte und die Doktorarbeit mit Freude zu bewältigen.
Es lässt sich schwer bis gar nicht mit einer Danksagung alles auszudrücken, trotzdem versuche ich es hier: Vielen Dank für alles!

10 Supplement

10.1 Ubiquitin sequence

Ubiquitin amino acid sequences of two ubiquitin constructs used in this study.

1-pTyb2HAUb - was used for generating of HAUb-VME, HAUb-VEE, HAUb-MVEE, HAUb-VFEA, HAUb-VF3EA.

ATGGCTAGCTCGCGAGTCGACTACCCATACGATGTTCCAGATTACGCCGAATTC
ACCATGCAGATCTTCGTGAAGACTCTGACTGGTAAGACCATCACCCTCGAGGTT
GAGCCCAGTGACACCATTGAGAATGTCAAGGCAAAGATCCAAGATAAGGAAGG
CATCCCTCCTGACCAGCAGAGGCTGATCTTTGCTGGAAAACAGCTGGAAGATG
GGCGCACCCTGTCTGACTACAACATCCAGAAAGAGTCCACCCTGCACCTGGTA
CTCCGTCTCAGAGGGTGMASSRVDYPYDVPDYAEFTMQIFVKTLTGKTITLEVEPS
DTIENVKAKIQDKEGIPPDQQRLIFAGKQLEDGRTLSDYNIQKESTLHLVLRLRG

10716.1 MW

2-pTyb2HAUb –was used for generating of HAUb-K48-UIPP, HAUb-K63-UIPP.

ATGATCGATGCCTACCCATACGACGTACCAGACTACGCACATATGCAGATCTTC
GTCAAGACGTTAACCGGTAAAACCATAACTCTAGAAGTGGAACCGAGCGATACC
ATCGAAAACGTGAAAGCGAAAATCCAGGATAAAGAAGGCATCCCGCCGGATCA
GCAGCGTCTGATCTTTGCGGGCAAACAGCTGGAAGATGGCCGCACCCTGTCTG
ATTATAACATCCAGAAAGAGTCGACCCTGCATCTGGTCTTAAGACTGCGTGGGT
MIDAYPYDVPDYAHMQIFVKTLTGKTITLEVEPSDTIENVKAKIQDKEGIPPDQQRLIF
AGKQLEDGRTLSDYNIQKESTLHLVLRLRG

10159.6 MW

10.2 Synthesis details of C-terminal electrophilic Glycine Analogs

***N*-tert-butyloxycarbonyl (Boc)-glycinal (2).**

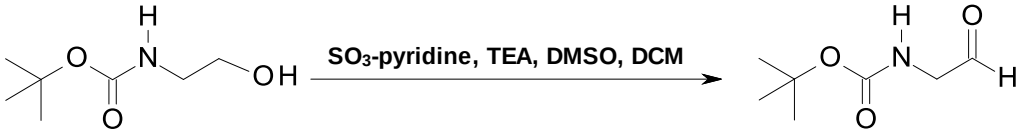

1 **2**

Primary and secondary alcohols are rapidly oxidized by SO_3-pyridine complex in DMSO in the presence of triethylamine[1]. Triethylamine (7.8 ml, 55.8 mmol) was added to a solution of *N*-Boc-glycinol (3 g, 18.6 mmol) in dichloromethane (60 ml) at 0°C. SO_3-pyridine (8,9 g, 55,8 mmol) was first dissolved in DMSO and pyridine (0.24 ml, 2.97 mmol) was added. After 10 minutes the SO_3-pyridine in DMSO was added dropwise to the *N*-Boc-glycinol solution at 0°C, upon which the solution turned from clear to yellow. The ice bath was removed and the solution stirred for a further 30 min at room temperature. The reaction mixture was poured into 180 ml ice cold brine. After removal of the dichloromethane layer, the aqueous layer was extracted with diethyl ether (3x120 ml). The combined organic layers were washed with ice cold $NaHSO_4$ solution (1 M, 1 x 42 ml) and with ice cold brine (2 x 42 ml). The organic layer was dried over $MgSO_4$ anhydrous, filtered and concentrated under vacuum. A silica gel column was used to purify the product. The aldehyde was eluted with 20% ethyl acetate in dichloromethane and isolated with 68% yield (2.0 g, 12.6 mmol). The aldehyde was either used immediately in the following reaction or stored at -70°C.

***N*-tert-butyloxycarbonyl-(E)-4-amino-2-butenoic acid methylester (VME, 3).**

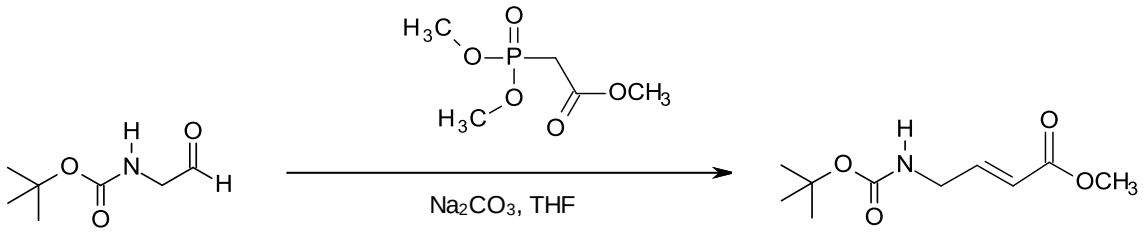

2 **3**

K_2CO_3 (651 mg, 4.71 mmol) was suspended in THF (10 ml). Trimethyl phosphonoacetate (858 mg, 4.71 mmol) was dissolved in THF (1 ml) and added dropwise to the K_2CO_3 slurry at room temperature. The solution was stirred for 60 min at room temperature. 500 mg (3.14 mmol) *N*-tert-butyloxycarbonyl (Boc)-glycinal (**2**) was dissolved in THF (2 ml) and added dropwise to the solution at room temperature. After stirring overnight at room temperature, water (10 ml) was added to the solution. After removal of the THF with a rotary evaporator, dichloromethane (15 ml) was added. The organic layer was separated and washed with 2% HCl, 10% $NaHCO_3$ and dried over $MgSO_4$ anhydrous, filtered and concentrated to yield **3**, which was further purified using silica gel chromatography. Compound **3** was eluted with 10% ethyl acetate in dichloromethane to yield 550 mg (2.56 mmol, 82%) of the purified compound.

***N*-tert-butyloxycarbonyl-(E)-4-amino-2-butenoic acid ethylester (VEE, 4).**

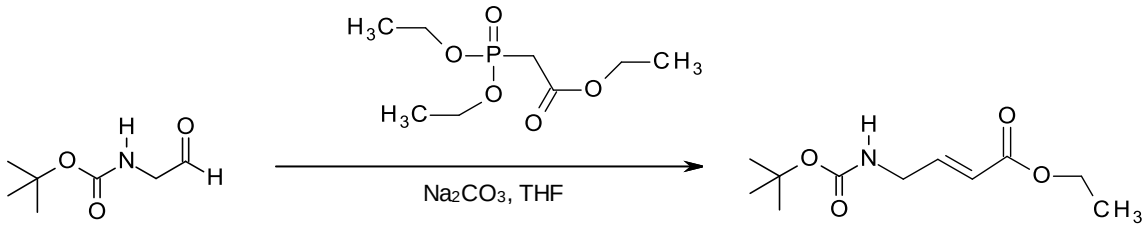

2 **4**

K_2CO_3 (390 mg, 2.82 mmol) was suspended in THF (10 ml). Triethyl phosphonoacetate (632 mg, 2.82 mmol) was dissolved in THF (1 ml) and added dropwise to the K_2CO_3 slurry at room temperature. The solution was stirred for 60 min at room temperature. 300 mg (1.88 mmol) *N*-tert-butyloxycarbonyl (Boc)-glycinal (**2**) was dissolved in THF (2 ml) and added dropwise to the solution at room temperature. After stirring overnight at room temperature, water (10 ml) was added to the solution. After removal of the THF with a rotary evaporator, dichloromethane (15

ml) was added. The organic layer was separated and washed with 2% HCl, 10% $NaHCO_3$ and dried over $MgSO_4$ anhydrous, filtered and concentrated to yield **4**, which was further purified using silica gel chromatography. Compound **4** was eluted with 10% ethyl acetate in dichloromethane to yield 268 mg (1.17 mmol, 62%) of the purified compound.

_N_-tert-butyloxycarbonyl-(E)-4-amino-3-methyl-2-butenoic acid ethylester (MVEE, 5).

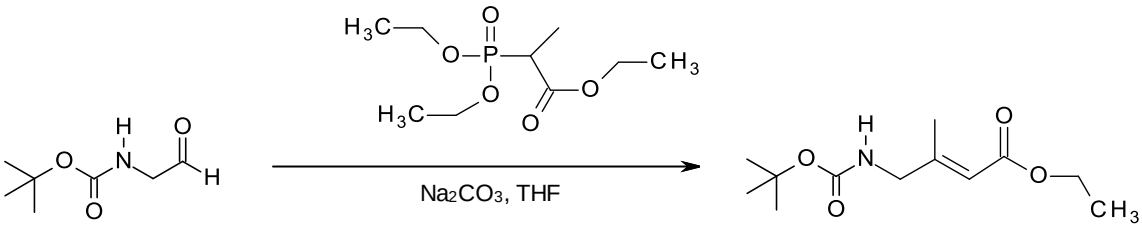

2 **5**

K_2CO_3 (390 mg, 2.82 mmol) was suspended in THF (10 ml). Triethyl-2-phosphonopropionate (672 mg, 2.82 mmol) was dissolved in THF (1 ml) and added dropwise to the K_2CO_3 slurry at room temperature. The solution was stirred for 60 min at room temperature. 300 mg (1.88 mmol) *N*-tert-butyloxycarbonyl (Boc)-glycinal (*2*) was dissolved in THF (2 ml) and added dropwise to the solution at room temperature. After stirring overnight at room temperature, water (10 ml) was added to the solution. After removal of the THF with a rotary evaporator, dichloromethane (15 ml) was added. The organic layer was separated and washed with 2% HCl, 10% $NaHCO_3$ and dried over $MgSO_4$ anhydrous, filtered and concentrated to yield **5**, which was further purified using silica gel chromatography. Compound **5** was eluted with 5% ethyl acetate in dichloromethane to yield 140 mg (0.575 mmol, 31%) of the E-/Z-mixture of **5**. Preparative HPLC was used to separate the E- and Z-isomers (Nucleodur C18, 5µm, 250x21 mm column, isochratic flow of 55/45 acetonitrile/water at 12ml/min. The E-isomer had a retention time of 17 min and the Z-isomer of 21 min. 93mg (0.382 mmol, 20%) of the purified E-isomer of **5** were isolated.

***N*-tert-butyloxycarbonyl-(E)-4-amino-2-butenoic acid (VA, 6).**

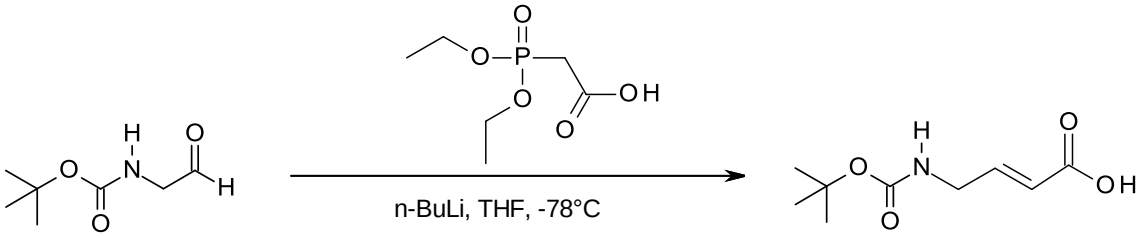

2 **6**

n-Buthyllithium (4.8 ml, 1.6 M in hexane, 7.54 mmol) was dissolved in THF (12 ml) at -78°C. Diethyl phosphonoacetic acid was dissolved in THF (5 ml) and added dropwise to the nBuLi solution at -78°C. The solution turned slightly yellow and was stirred for 30 min at -78°. *N*-tert-butyloxycarbonyl (Boc)-glycinal (**2**) was dissolved in THF (3 ml) and added dropwise to the solution at -78°C. After stirring for 3h at room temperature water (12 ml) was added to the solution. The organic layer was separated and washed with 10% $NaHCO_3$ (2 x 10 ml), the combined aqueous layers were then acidified to pH 3.5 with conc. HCl and extracted with diethyl ether (3 x 18 ml). The combined organic layers were dried over $MgSO_4$ anhydrous, filtered and concentrated to yield **6**, which was further purified using silica gel chromatography. Compound **6** was eluted with 20% ethyl acetate in dichloromethane containing 1% acetic acid to yield 389 mg (1.93 mmol, 51%) of the purified compound.

***N*-tert-butyloxycarbonyl-(E)-4-amino-2-butenoic acid fluoroethylester (VFEA, 7).**

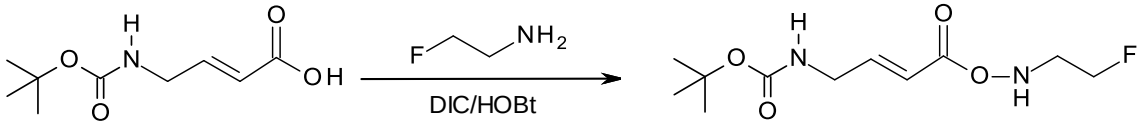

6 **7**

50 mg (0.248 mmol) of **6** were dissolved in DMF abs., activated with DIPEA (130 µl, 0.745 mmol), EDC (71.5 mg, 0.375mmol) and HOBt anh. (50.4 mg, 0.375 mmol). 2-fluoroethylamine hydrochloride (37.1 mg, 0.375 mmol) were added and the solution was stirred overnight at room temperature. The reaction was quenched by adding phosphate buffer (pH7). After addition of saturated NH_4Cl solution, the solution was extracted with ethyl acetate (3x5 ml). The combined ethyl acetate layers were washed with a saturated NaCl solution and dried over $MgSO_4$ anhydrous, filtered and

concentrated to yield **7**, which was further purified using silica gel chromatography. Compound **7** was eluted with 50% ethyl acetate in dichloromethane to yield 56.7 mg (0.23 mmol, 93%) of the purified compound.

_N_-tert-butyloxycarbonyl-(E)-4-amino-2-butenoic acid trifluoroethylester (VF3EA, 8).

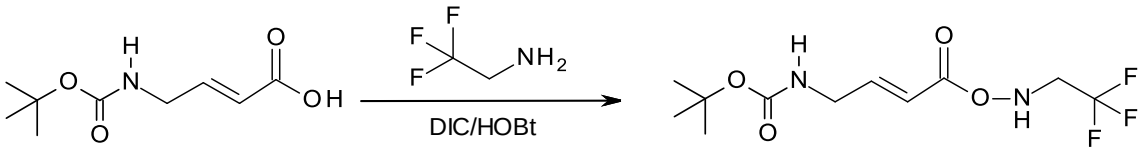

6 **8**

50 mg (0.248 mmol) of **6** were dissolved in DMF abs. (2.4ml), activated with DIPEA (130 µl, 0.745 mmol), EDC (71.5 mg, 0.375mmol) and HOBt anh. (50.4 mg, 0.375 mmol). 2,2,2-Trifluoroethylamine hydrochloride (29µl mg, 0.373 mmol) were added and the solution was stirred overnight at room temperature. The reaction was quenched by adding phosphate buffer (pH7). After addition of saturated NH_4Cl solution, the solution was extracted with ethyl acetate (3x5ml). The combined ethyl acetate layers were washed with a saturated NaCl solution and dried over $MgSO_4$ anhydrous, filtered and concentrated to yield **8**, which was further purified using silica gel chromatography. Compound **8** was eluted with 50% ethyl acetate in dichloromethane to yield 44.3 mg (0.157 mmol, 63%) of the purified compound.

Peptide synthesis of Ac-seq1-X-seq2 (9).

Peptides were synthesized on a 25 µmol scale using an automated multiple peptide synthesizer (Syro I from MultiSynTech, Witten, Germany). The sequences were assembled as C-terminal amide on polyoxyethylene-grafted polystyrene resin, to which the Rink amide linker was attached (TentaGel S RAM resin, 100 mg, 0.25 mmol g^{-1}). Five equivalents of Fmoc-amino acid/DIC/HOBt (0.36 M in DMF) were coupled (2 × 1 h + capping with acetic anhydride/pyridine/DMF 1:2:3) for each coupling cycle. Lysine was incorporated with a Mtt-protecting group for the ε-amino group in its side chain. The N-terminus was acetylated using acetic anhydride/pyridine/DMF (1:2:3, 30min).

Mtt group cleavage and coupling of (E)-4-amino-2-butenoic (6) acid and isolation of (10).

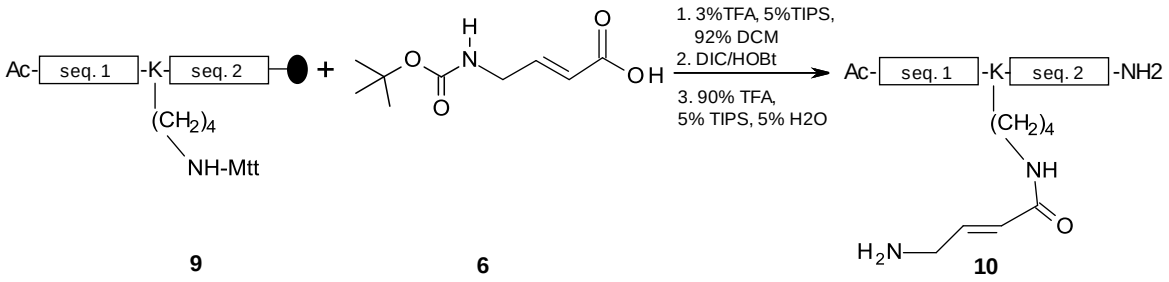

9 **6** **10**

For Mtt group cleavage from the ε-amino group of lysine resins were swollen in DCM and treated with 3% TFA, 5% TIPS, 92% DCM (1 ml, 8 x 20 min). The resin was then washed with DCM (1 ml), 5% DIPEA/DCM (1ml), DCM (1 ml) and DMF anhydrous (1ml). 5 eq. of *N*-tert-butyloxycarbonyl-(E)-4-amino-2-butenoic acid (3) (relative to the loading of the resin: 125 µmol, 25.2 mg) were pre-activated for 1h with DIC (5 eq., 125 µmol, 19.4 µl) and HOBt anhydrous (5.5 eq., 137.5 µmol, 18.6 mg) in 0.5 ml DMF anhydrous. The solution was added to the resin and shaken for 5d. Peptides were cleaved from the resin as C-terminal amides using a mixture of TFA, DCM, water, and triisopropylsilane (70:20:5:5) for four hours, precipitated in a cold 1:1 mixture of tert-butylmethyl ether and cyclohexane, extracted with water, and lyophilized. Crude peptides were purified by preparative HPLC on a 250 × 10 mm NUCLEOSIL RP18 column and characterized by LC-MS.

Peptide Sequences and HPLC/ESI-MS

<u>K48-isopeptide thiol reactive trap:</u>

Ub(42-54): Ac-RLIFAG-**K_{48}(VA)**-QLEDGR-NH2

ESI-MS (*m/z*): $[M+2H]^{2+}$ calc.: 813.98, found: 814.0

<u>K63-isopeptide thiol reactive trap:</u>

Ub(54-72): Ac-RTLSDYNIQ-**K_{63}(VA)**-ESTLHLVLR-NH2

ESI-MS (*m/z*): $[M+2H]^{2+}$ calc.: 1205.69, found: 1205.8

10.3 Identified DUBs using modulated active site directed probes (4.1.1)

Unique spectral counts of DUBs after an overnight α-HA immunoprecipitation using indicated HAUb derived probes.

Accession Number	HAUb-VME	HAUb- VEE	HAUb-MVEE
USP5	64	57	39
USP4	15	26	15
USP47	21	28	25
USP7	19	27	10
USP14	25	36	13
USP9X	2	9	2
USP15	13	24	9
USP16	6	6	6
UCHL3	15	38	15
UCHL5	11	18	3
USP8	2	5	
USP19	1	3	2
OTUB1	6	16	10
UCHL1	20	12	
EIF3F	8	16	8
EIF3H	5	13	5
PSD7	8	8	16

10.4 Identified DUBs of profiling experiment using new active site directed probe HAUb-VFEA

Accession Number	MW	A549	EL-4	HeLa	Jurkat	MCF-7
ATXN3	42	2	4	5	8	7
BAP1	80	17	5	24	15	19
CSN5	38		1	2	4	
CYLD	107	4	20	7	12	6
EIF3F	38				3	
EIF3H	40	1	1	1	1	1
JOS1	23			1	2	
JOS2	23					2
OTU6B	34	8	5	10	9	6
OTU7A	101		1	5		
OTU7B	93	19	13	37	14	39
OTUB1	31		6	1		8
OTUB2	27	2	2		6	3
OTUD3	20			1		
OTUD4	123		3			
OTUD5	61			2		
PRO8	274	7	6	5	31	9
PSMD14	35	1	3		2	1
PSMD7	37		1	2	1	
UCHL1	25	15	5			
UCHL3	26	8	13	11	15	10
UCHL5	38	26	6	27	25	26
USP1	88			14	2	3
US14	56	38	15	41	40	43
USP10	87	19	7	26	18	27
USP11	110	28		30	52	39
USP12	43	6		5	3	6
USP15	112	48	14	56	46	60
USP16	94	20	3	29	24	30
USP17L2	88		9	14	2	3
USP19	146	31	23	52	42	44
USP2	68			1	1	1
USP20	102	4	1	13	17	25

Accession Number	MW	A549	EL-4	HeLa	Jurkat	MCF-7
USP21	63				4	
USP22	60	15		7	13	6
USP24	294	35	11	89	78	49
USP25	122	34	17	39	21	32
USP27	50	1			1	
USP28	122	34	2	50	17	33
USP29	98		1			
USP3	59	1		9	3	4
USP30	59	2		6	11	9
USP31	147	2			1	6
USP32	182	13	1	28	20	63
USP33	107	30	5	39	8	14
USP34	404	12	1	40	15	11
USP35	113		1	4	2	24
USP36	123	4		3	15	
USP37	110	1		11	11	6
USP38	117	6	22	6	9	8
USP39	65				1	
USP4	109	16	26	33	47	45
USP40	140	4		7		25
USP42	145	4		3	7	6
USP43	123	1		1		6
USP45	90				2	
USP46	42	7	7	9	9	9
USP47	157	36	30	79	71	68
USP48	119	35	4	48	45	48
USP5	96	44	37	58	44	57
USP54	177	1				
USP7	128	74	65	96	86	86
USP8	128	43	27	54	26	54
USP9X	297	108	19	128	104	116
USP9Y	291				3	2
VCIP1	134	8	1	20	14	1
ZRANB1	81			1	1	1

10.5 Comparison of identified DUBs using HAUb-VME or HAUb-VFEA

VME	HAUb-VME & HAUb-VFEA	HAUb-VFEA	Reference
USP13			[128]
A20			[165]
	USP2		[164]
	USP3		[164]
	USP4		[128]
	USP5		[128]
	USP7		[128]
	USP8		[128]
	USP9X		[128]
	USP10		[128]
	USP11		[128]
	USP12		[128]
	USP14		[128]
	USP15		[128]
	USP16		[128]
	USP19		[128]
	USP20		[165]
	USP22		[202]
	USP24		[128]
	USP25		[128]
	USP28		[128]
	USP29		[203]
	USP30		[165]
	USP32		[165]
	USP36		[164]
	USP37		[164]
	USP38		[165]
	USP40		[165]
	USP46		[165]
	USP47		[203]
	USP48		[165]
	CYLD		[128]
	UCHL1		[128]

VME	HAUb-VME & HAUb-VFEA	HAUb-VFEA	Reference
	UCHL3		[128]
	UCHL5		[128]
	OTUB1		[128]
	OTUB2		[165]
	OTUD4		[203]
	OTUD5		[203]
	OTU6B		[203]
	OTU7A		[203]
	OTU7B		[203]
	VCIP135		[203]
	JOS1		[203]
	JOS2		[203]
		USP1	
		USP9Y	
		USP17L2	
		USP21	
		USP27	
		USP31	
		USP33	
		USP34	
		USP35	
		USP42	
		USP43	
		USP45	
		BAP1	
		OTUD3	
		ZRANB1	
		Ataxin 3	
		USP39	
		USP54	
		CSN5	
		EIF3F	
		EIF3H	
		PRO8	
		PSMD14	
		PSMD7	

10.6 Deubiquitinating enzymes modified with branched Ubiquitin Isopeptide Probes (UIPPs) by applying functional proteomics

Modified proteins were immunoprecipitated and sequenced as described in the text. Peptide matches were assigned using the Mascot2 W2K3 2.3.02 (Matrix Science) the considered significance was determined as described in the text above. SwissProt accession numbers are for human sequences. Number of unique peptides gives the number of unique peptides identified for each protein. The greatest observed sequence coverage is given by Percentage sequence coverage. Spectral count numbers were normalized using Proteome-Software Scaffold 3.0 which are represented as Quantative values.

			No. of unique peptides			**Percentage sequence coverage [%]**			**Quantative value**		
Identified DUBs	Accession Number	MW [kDa]	UIPP-K48	UIPP-K63	VME	UIPP-K48	UIPP-K63	VME	UIPP-K48	UIPP-K63	VME
USP47	UBP47_HUMAN	157	21	20	27	19	18	22	48	56	34
USP7	UBP7_HUMAN	128	23	5	44	22	5.1	45	46	6	98
USP9X	USP9X_HUMAN	292	30	19	34	15	8.5	17	35	25	34
USP5	UBP5_HUMAN	96	18	5	25	26	8.5	31	33	8	62
USP11	UBP11_HUMAN	110	18	14	33	22	17	40	29	32	66
USP15	UBP15_HUMAN	112	14	17	18	18	20	21	28	46	30
UCHL5	UCHL5_HUMAN	38	12	8	16	45	28	59	26	15	32
USP19	UBP19_HUMAN	146	10	14	15	9,6	15	15	22	39	19
UCHL3	UCHL3_HUMAN	26	6	4	10	32	23	46	20	16	26

Identified DUBs	Accession Number	MW [kDa]	UIPP-K48	UIPP-K63	VME	UIPP-K48	UIPP-K63	VME	UIPP-K48	UIPP-K63	VME
USP4	UBP4_HUMAN	109	9	8	23	12	11	38	16	20	33
USP14	UBP14_HUMAN	56	11	9	27	30	25	55	13	13	96
USP8	UBP8_HUMAN	128	6	6	14	7	7	16	11	13	21
USP24	UBP24_HUMAN	294	8	6	26	3.90	2.9	14	8	8	23
USP16	UBP16_HUMAN	94	5	5	6	6.60	8.3	9,7	6	9	7
USP38	UBP38_HUMAN	117	5	12	12	5	12	13	5	15	9
USP36	UBP36_HUMAN	123	4	5	3	3.70	4.5	3.4	4	6	3
USP42	UBP42_HUMAN	146	3	1	4	2.30	0.75	4.2	4	3	4
USP10	UBP10_HUMAN	87	2	1	8	3.30	1.5	11	3	1	16
USP20	UBP20_HUMAN	102	2	2	2	3.40	3.4	3.1	3	4	2
BAP1	BAP1_HUMAN	80	2	3	5	2.70	4.1	7.7	2	5	4
EIF3F	EIF3F_HUMAN	38	4	2	3	13	7	9	4	3	2
PRPF8	PRP8_HUMAN	274	11	9	9	4.8	4.4	4.4	12	11	7
USP28	UBP28_HUMAN	122	2		8	2.2		8.9	2		9
USP12	UBP12_HUMAN	43	1		6	2.2		20	1		5
USP22	UBP22_HUMAN	60	1		2	1.5		5.3	1		2
USP48	UBP48_HUMAN	119			23			24			23
VCPIP1	VCIP1_HUMAN	134			12			14			12
CYLD	CYLD_HUMAN	107			7			9.6			6
USP25	UBP25_HUMAN	122			9			9.3			7
USP32	UBP32_HUMAN	182			7			4.8			9

Identified DUBs	Accession Number	MW [kDa]	UIPP-K48	UIPP-K63	VME	UIPP-K48	UIPP-K63	VME	UIPP-K48	UIPP-K63	VME
USP37	UBP37_HUMAN	110			4			5.5			3
USP46	UBP46_HUMAN	42			2			19			5
USP34	UBP34_HUMAN	404			2			0.79			2
USP3	UBP3_HUMAN	59			2			5.6			2
Ataxin-3	ATX3_HUMAN	42			5			19			9
Josephin-1	JOS1_HUMAN	23			2			10			2
OTU6B	OTU6B_HUMAN	34			6			19			9

10.7 Represantative example of the fraction analysis using mass spectrometry (MALDI-TOF)